

UNIVERSIDADE FEDERAL DO RIO GRANDE DO SUL  
INSTITUTO DE GEOCIÊNCIAS  
PROGRAMA DE PÓS-GRADUAÇÃO EM GEOCIÊNCIAS

**PETROGÊNESE DA CAMADA DE CROMITITO MACIÇO DO  
COMPLEXO JACURICI, BAHIA, BRASIL:  
EVIDÊNCIAS DE INCLUSÕES EM CROMITA**

BETINA MARIA FRIEDRICH

ORIENTADORA: Prof<sup>a</sup>. Dr<sup>a</sup>. Juliana Charão Marques

COORIENTADOR: Prof. Dr. José Carlos Frantz

Porto Alegre – 2018

UNIVERSIDADE FEDERAL DO RIO GRANDE DO SUL  
INSTITUTO DE GEOCIÊNCIAS  
PROGRAMA DE PÓS-GRADUAÇÃO EM GEOCIÊNCIAS

**PETROGÊNESE DA CAMADA DE CROMITITO MACIÇO DO  
COMPLEXO JACURICI, BAHIA, BRASIL:  
EVIDÊNCIAS DE INCLUSÕES EM CROMITA**

BETINA MARIA FRIEDRICH

ORIENTADORA: Prof<sup>a</sup>. Dr<sup>a</sup>. Juliana Charão Marques

COORIENTADOR: Prof. Dr. José Carlos Frantz

BANCA EXAMINADORA

Prof. Dr. Rommulo Vieira Conceição - Universidade Federal do Rio Grande do Sul

Prof. Dr. César Fonseca Ferreira Filho - Universidade de Brasília

Prof. Dr. Nilson Francisquini Botelho - Universidade de Brasília

Dissertação de Mestrado apresentada  
como requisito parcial para a obtenção  
do Título de Mestre em Geociências

Porto Alegre – 2018

## CIP - Catalogação na Publicação

FRIEDRICH, BETINA MARIA  
PETROGÊNESE DA CAMADA DE CROMITITO MACIÇO DO  
COMPLEXO JACURICI, BAHIA, BRASIL: EVIDÊNCIAS DE  
INCLUSÕES EM CROMITA / BETINA MARIA FRIEDRICH. --  
2018.

94 f.

Orientador: Juliana Charão Marques.

Coorientador: José Carlos Frantz.

Dissertação (Mestrado) -- Universidade Federal do  
Rio Grande do Sul, Instituto de Geociências, Programa  
de Pós-Graduação em Geociências, Porto Alegre, BR-RS,  
2018.

1. Depósito de cromita. 2. formação de cromitito.  
3. inclusões hidratadas em cromita. 4. inclusões de  
carbonato em cromita. 5. lama cromitífera. I. Marques,  
Juliana Charão, orient. II. Frantz, José Carlos,  
coorient. III. Título.

## AGRADECIMENTOS

Ao CNPq, pelo financiamento desta pesquisa através do projeto nº 131133/2016-0.

À Companhia de Ferro Ligas da Bahia – FERBASA, pelo suporte financeiro e técnico fornecido para a realização do trabalho de campo e por permitir acesso e amostragem dos testemunhos de sondagem.

Ao Programa de Pós-graduação em Geociências (PPGGeo) da Universidade Federal do Rio Grande do Sul, pela estrutura oferecida para que os alunos tenham acesso à pós-graduação pública e de qualidade, e pelo auxílio financeiro concedido para revisão de inglês do artigo científico, parte integrante desta Dissertação.

À Universidade Federal do Rio Grande do Sul, pelo auxílios financeiros concedidos que viabilizaram a participação da aluna em eventos de âmbito nacional e internacional para apresentação e discussão dos resultados parciais desta pesquisa.

Aos orientadores, que me proporcionaram suporte muito além dos ensinamentos técnicos; especialmente à Juliana, por acreditar no meu potencial e me ajudar a acreditar em mim mesma.

Aos colegas de pesquisa e de sala ao longo desta caminhada, Gabriel, Renan, Luiz, Natanael, Jhenifer, Bruna, João Rodrigo, Carlos e Daianne, pelas discussões geológicas, cafés e risadas compartilhadas.

Aos amigos do SEG UFRGS Student Chapter, por todos momentos e aprendizados compartilhados. Meu tempo de mestrado não seria tão rico sem vocês.

Ao Prof. Vitor Pereira, pelos cafés regados a divagações geológicas.

À minha família, Beatriz, Renato, Leonardo e Monique, que jamais pouparam esforços pra me ajudar, e entenderam com paciência os momentos de ausência. Especialmente à minha mãe, que sofreu comigo cada angústia e vibrou comigo cada vitória.

Aos meus amigos e amigas, especialmente à Elis, à Franciele, ao Alberto, ao Jonatas, à Michele e à Fernanda, que sempre foram ouvidos e abraços nos momentos de ansiedade, e alegria e parceria nos momentos de comemoração

*“Foi o tempo que dedicaste à tua rosa que fez tua  
rosa tão importante”*

Antoine de Saint-Exupéry

## RESUMO

O Complexo Jacurici abriga o maior depósito de cromo no Brasil, representado por uma camada de cromitito de até 8 m de espessura em uma intrusão de 300 m de espessura tectonicamente segmentada. O minério foi interpretado como resultado de cristalização causada contaminação crustal em um conduto magmático. Este estudo aborda as relações estratigráficas, mineralógicas e texturais, assim como a química mineral do Segmento Monte Alegre Sul, com foco nas inclusões hospedadas em cromita da Camada de Cromitito Principal, com objetivo de aprofundar o conhecimento acerca do papel dos voláteis na gênese do cromitito maciço. Inclusões de silicatos (enstatita, flogopita, magnesiohornblenda, diopsídio e olivina) são comumente monominerálicas e sub- a euédricas, e suas composições sugerem que elas cristalizaram antes ou contemporaneamente ao estágio principal de cristalização da cromita. As inclusões de carbonato (dolomita e magnesita) tem formas irregulares ou de cristal negativo, sugerindo aprisionamento como gotas de magma carbonático. Inclusões de sulfeto (pentlandita, millerita, heazlewoodita, polidimita, pirita e calcopirita) são frequentemente poliminerálicas, com formas irregulares ou hexagonais, sugerindo aprisionamento na forma de *melt* e *monosulfide solid solution*. Coletivamente, essas inclusões indicam um magma residente saturado em H<sub>2</sub>O e S, contendo gotículas imiscíveis de carbonato durante a cristalização da cromita. Cristais de cromita com e sem inclusões ocorrem juntos, apresentam química semelhante e são considerados formadas a partir do mesmo magma em resposta a variações no grau de saturação de Cr. O magma primitivo pode ter aquecido e introduzido CO<sub>2</sub> e provavelmente água das rochas carbonáticas encaixantes desvolatilizadas e assimiladas, aumentando a *fO*<sub>2</sub> e desencadeando a cristalização da cromita. Propõe-se um modelo no qual o intervalo basal seja o resultado da cristalização *in situ* com material adicionado por deslizamentos de lama cromítífera remobilizada localmente, processo facilitado pela presença de voláteis.

**PALAVRAS-CHAVE:** Depósito de cromita; formação de cromitito; inclusões hidratadas em cromita; inclusões de carbonato em cromita; lama cromítífera.

## ABSTRACT

The Jacurici Complex hosts the largest chromium deposit in Brazil in an up to 8 m thick chromitite layer within a tectonically-segmented 300 m thick intrusion. The ore has been interpreted as the result of crustal contamination-driven crystallization in a magma conduit. This study addresses the stratigraphy, mineralogical and textural relationships and mineral chemistry of the Monte Alegre Sul Segment focusing on chromite-hosted inclusions from the Main Chromitite Layer to further the understanding of the role of volatiles in the genesis of the massive chromitite. Silicate inclusions (enstatite, phlogopite, magnesiohornblende, diopside and olivine) are commonly monomineralic and sub- to euhedral, and crystallized prior to, or coeval with, the chromite crystallization. Carbonate inclusions (dolomite and magnesite) are irregular or negative-crystal shaped, suggesting entrapment as melt droplets. Sulfides (pentlandite, millerite, heazlewoodite, polydymite, pyrite and chalcopyrite) are often polymimetic, irregular or hexagonal-shaped, indicating entrapment as sulfide melt and as monosulfide solid solution. The inclusions indicate an H<sub>2</sub>O- and S-saturated resident magma with immiscible droplets of carbonate melt during chromite crystallization. Inclusion-rich and inclusion-free chromites occur together, have similar chemistries and are considered to have formed from the same magma in response to variations in the degree of Cr saturation. Hot primitive magma might have heated and introduced CO<sub>2</sub> and probably water from devolatilized and assimilated carbonate wall-rocks, increasing  $fO_2$  and triggering chromite crystallization. It is proposed that the basal interval is the result of in situ crystallization with additional material added by slumping of locally remobilized chromite slurries, facilitated by the presence of volatiles.

**KEY WORDS:** Chromite deposit; origin of chromitite; hydrated inclusions in chromite; carbonate inclusions in chromite; chromite slurry.

## SUMÁRIO

Sobre a estrutura desta dissertação .....	4
<b>CAPÍTULO 1</b>	
1. INTRODUÇÃO .....	5
1.1 Objetivos .....	5
1.2 Localização e vias de acesso .....	5
1.3 Estado da Arte .....	6
1.3.1 Contexto geológico regional .....	6
1.3.2 Modelos de formação de cromita em complexos máfico-ultramáficos .....	8
1.3.3 Inclusões hospedadas em cromita .....	14
1.3.4 Geologia e gênese do Complexo Jacurici .....	16
<b>CAPÍTULO 2</b>	
2. MATERIAIS E MÉTODOS .....	21
REFERÊNCIAS.....	23
<b>CAPÍTULO 3</b>	
3. ARTIGO CIENTÍFICO .....	27
<b>CAPÍTULO 4</b>	
4. ANEXOS .....	76
4.1 Resumos e resumos expandidos de autoria da pós-graduanda publicados em anais de eventos durante o período de Mestrado .....	76
4.1.1 13th International Platinum Symposium (IPS) .....	76
4.1.2 VIII Simpósio Brasileiro de Exploração Mineral (SIMEXMIN) / I Encontro Nacional dos Estudantes de Geologia Econômica (ENAGE).....	78
4.1.3 14th SGA Biennial Meeting.....	79
4.1.4 48º Congresso Brasileiro de Geologia (CBG).....	84
4.2 Artigo científico de coautoria da pós-graduanda publicado durante o período de Mestrado.....	85
4.3 Histórico Escolar .....	86
4.4 Pareceres da Banca Examinadora .....	87

## SOBRE A ESTRUTURA DESTA DISSERTAÇÃO

Esta Dissertação de Mestrado está estruturada em torno de artigo submetido à publicação na revista Mineralium Deposita. Sua organização compreende os seguintes capítulos:

CAPÍTULO I: Introdução: “objetivos”, “localização e vias de acesso” e “estado da arte”, este contendo uma revisão sobre o contexto geológico regional, modelos de formação de cromita em complexos máfico-ultramáficos acamados, inclusões hospedadas em cromita e geologia e gênese do Complexo Jacurici;

CAPÍTULO II: “Materiais e Métodos” empregados;

CAPÍTULO III: “Artigo científico” intitulado “Petrogenesis of the massive chromitite layer from the Jacurici Complex, Brazil: evidence from inclusions in chromite”

CAPÍTULO IV: “Anexos”, compreendendo publicações relevantes nas quais a pós-graduanda é autora e coautora, como produto de pesquisas nas quais esteve envolvida durante o período de Mestrado, assim como documentação pertinente (Histórico Escolar e Pareceres da Banca Examinadora).

## 1. INTRODUÇÃO

### 1.1 Objetivos

Os mecanismos de formação de cromititos, especialmente de cromititos espessos, como é o caso do Complexo Jacurici, permanecem pouco compreendidos. Neste estudo, detalhou-se com petrografia e química mineral a estratigrafia recuperada do furo MAS-105-65° do corpo Monte Alegre Sul, um dos segmentos do Complexo Jacurici. Atenção especial foi dedicada à camada de minério, onde inclusões minerais em cromita foram detalhadas quanto às texturas e caracterização mineralógica e química. O trabalho teve por objetivo avançar nos conhecimentos acerca dos processos petrogenéticos responsáveis pela formação do depósito.

### 1.2 Localização e vias de acesso

O corpo Monte Alegre Sul está localizado no município de Monte Santo, norte do estado da Bahia, cerca de 440 km de Salvador e 170 km de Petrolina, no estado de Pernambuco. A área situa-se entre as coordenadas geográficas 10°7'8.58"S a 10°7'38.95"S e 39°43'15.75"W a 39°43'53.48"W (Fig. 1).

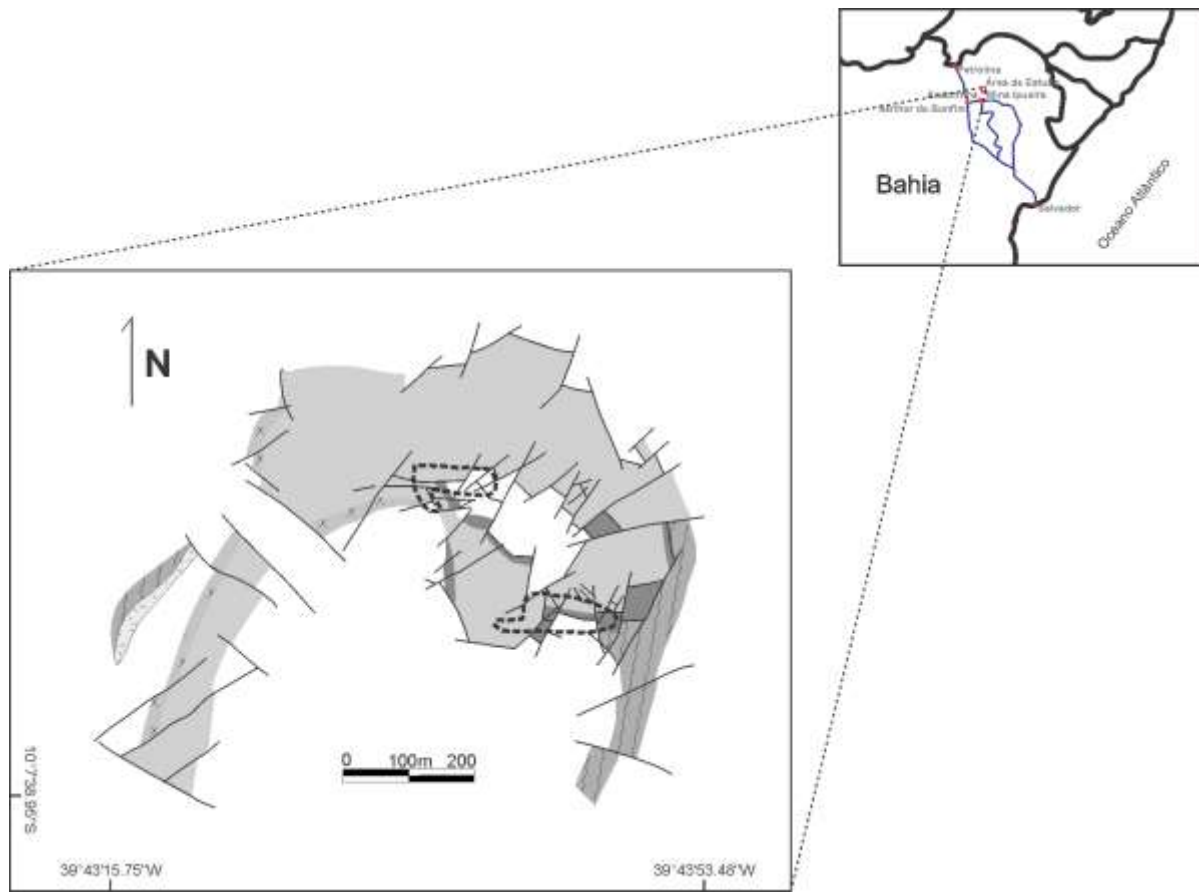


Figura 1: Mapa de localização e vias de acesso

O acesso rodoviário a partir de Salvador é feito pela BR324 até o município de Capim Grosso, onde segue-se a norte, pela BR407 até o município de Senhor do Bonfim, onde toma-se a BA220 até o município de Andorinha. A partir de Andorinha segue-se por 8km pela estrada não-pavimentada Rua Antônio Laurindo até as instalações da FERBASA na Mina Ipueira. De Petrolina, segue-se para sudeste pela BR407 até Senhor do Bonfim, a partir de onde segue-se o mesmo trajeto até o município de Andorinha e até as operações da Mina Ipueira. Das instalações da FERBASA segue-se 25 km para norte, por estrada secundária não pavimentada.

### 1.3 Estado da Arte

#### 1.3.1 Contexto geológico regional

O Complexo Jacurici contém o maior depósito de cromo do Brasil, sendo composto por 22 corpos máfico-ultramáficos, em sua maioria orientados N-S, que ocorrem ao longo de uma faixa de mais de 70 km de extensão por 20 km de largura na porção NE do Cráton São Francisco (Fig. 2). Os corpos são mineralizados com uma espessa camada de cromita que vem sendo explorada desde a década de 1970 pela Companhia de Ferro Ligas da Bahia – FERBASA. Inicialmente, a mineração era realizada por lavra a céu aberto e atualmente a produção é obtida a partir da mina subterrânea de Ipueira, onde o processo de extração é realizado pelos métodos de *sublevel caving* e *sublevel open stoping*.

De acordo com o trabalho clássico de Jardim de Sá (1984), o Complexo Jacurici é intrusivo em uma sequência supracrustal de grande variabilidade litológica. O litotipo predominante é um gnaiss leucocrático granodiorítico a tonalítico, contendo intercalações de anfibolitos, formações ferríferas, olivina-mármores, calcisilicáticas ricas em diopsídio, quartzitos, gnaisses granadiníferos e metacherts (Marinho et al. 1986). Na região do Vale do Jacurici ortognaisses são litotipos abundantes e foram considerados por Jardim de Sá (1984) e Marinho et al. (1986) como intrusões posteriores às rochas ultramáficas do Complexo Jacurici. Já os trabalhos realizados pela FERBASA consideram o complexo como intrusivo em basicamente três grandes conjuntos litológicos: um conjunto de migmatitos e gnaises muito deformados, de ocorrência restrita, um conjunto de paragnaisses e um conjunto de ortognaisses (Silveira et al., 2015). O conjunto denominado de paragnaisses inclui as lentes intercaladas de metassedimentares citadas. Silveira et al. (2015) realizaram estudos geocronológicos na área e demonstraram que os ortognaisses são, pelo menos parte, mais antigos que os paragnaisses. Trabalho recente de Marques et al. (2017) considera o complexo intrusivo no contato entre ortognaisses e sequências metassedimentares.

O complexo Jacurici é datado de  $2085 \pm 5$  Ma (Oliveira et al., 2004), similar à idade de pico metamórfico de 2.1-2.0 Ga na região (Barbosa, 1997; Barbosa e Sabaté, 2002, 2003). O trabalho de Silveira et al. (2015) revelou que um dos corpos anfibolíticos considerados de origem sedimentar se trata de um metagabronorito de idade similar às rochas do complexo ( $2102 \pm 5$  Ma), podendo representar os primeiros pulsos do evento magmático. A partir deste dado, Marques et al. (2017) sugeriram que pelo menos parte das lentes anfibolíticas até então julgadas pertencer ao embasamento trata-se, na verdade, de intrusões cogenéticas ao Complexo Jacurici, implicando um magmatismo de proporções maiores do que previamente acreditado.

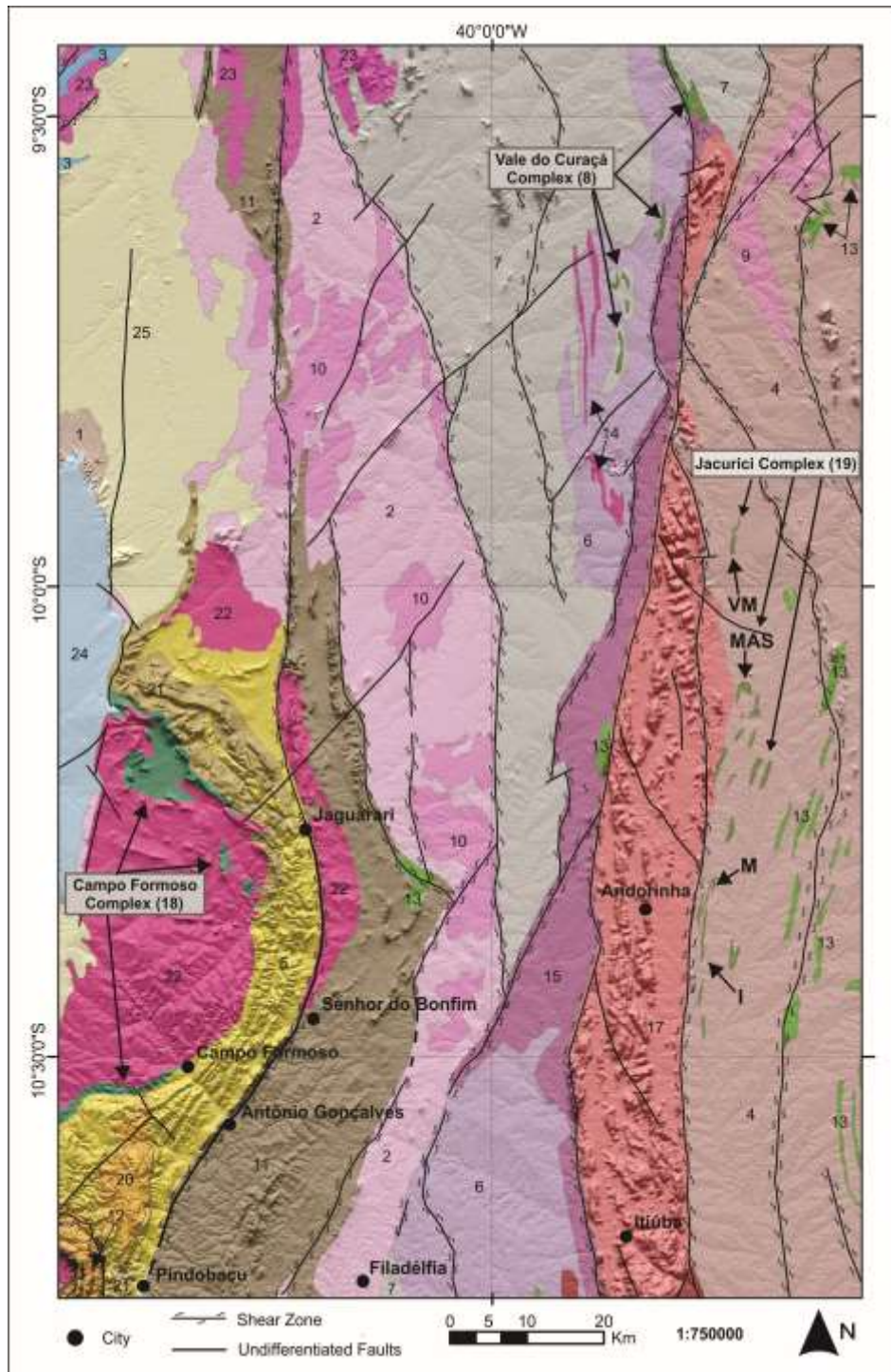


Figura 2: Contexto geológico regional do Complexo Jacurici. A localização dos segmentos Ipueira (I), Medrado (M), Monte Alegre Sul (MAS) e Várzea do Macaco (VM) é indicada. Unidades litoestratigráficas: Paleoárqueano - (1) Rochas do embasamento; Mesoárqueano - (2) Complexo de Santa Luz; Neoárqueano - (3) Complexo Itapicuru; (4) Complexo Caraíba; (5) Complexo Tanque Novo-Ipirá; (6) Complexo Vale do Curaçá; (7) granitóides indiferenciados; Paleoproterozóico - (8) Complexo Saúde; (9) corpos máfico-ultramáficos indiferenciados; (10) Granitoide do Riacho da Onça; (11) Sienito Itiúba; (12) Complexo Campo Formoso; (13) Complexo Jacurici; (14) Grupo Jacobina; (15) granitóides da região de Campo Formoso e Jaguari; Neoproterozóico - (16) Formação Salitre; Cenozóico - (17) Cobertura sedimentar. Extraído de Marques et al. (2017).

O posicionamento do Complexo Jacurici no limite entre o Bloco Serrinha e o Orógeno Itabuna-Salvador-Curaçá, aliado à complexidade geológica da área, traz inconsistências a respeito de sua colocação geotectônica. Esta discussão é abordada por Silveira et al. (2015), que sugerem que a intrusão do complexo se tenha dado após a colisão e, que, portanto, as rochas do Complexo Jacurici possam ocorrer em ambos os segmentos crustais.

### 1.3.2 Modelos de formação de cromita em complexos máfico-ultramáficos

Cromita (cromoespínélio) é a única fonte primária para o elemento metálico cromo, utilizado na indústria metalúrgica, química e de materiais refratários (Kropschot e Doebrich 2010). Os depósitos magmáticos de cromita são classificados em três tipos principais: estratiformes (formados em intrusões máfico-ultramáficas acamadas), podiformes (hospedados em ofiolitos), e cromititos relacionados a complexos máfico-ultramáficos zonados, também conhecidos como complexos do tipo alasquiano-uraliano. Muito se avançou no conhecimento e nos modelos a respeito da formação de cromititos, mas sua origem permanece controversa e é combustível para inflamados debates. Esta seção apresenta uma revisão das principais ideias sobre a gênese de cromititos em complexos acamados.

Durante várias décadas, a maioria dos modelos consideravam a formação de cromititos *in situ*, ou “*on stage*”, ou seja, a cromita cristaliza e acumula dentro da câmara magmática, sem remobilização significativa. Ideias que consideram a formação de cromititos a partir da remobilização de cromita previamente cristalizada, os assim chamados modelos “*off stage*”, se tornaram mais populares a partir dos anos 2000.

#### Modelos *on stage*

Jackson (1961) propôs que as camadas de cromitito maciço do Complexo de Stillwater, nos Estados Unidos, representassem acumulações de cristais de cromita que cristalizaram próximo à base da câmara magmática, tendo se estabelecido em um magma relativamente estagnado sem transporte lateral importante. O mesmo autor, em 1963, publicou importantes variações na soma de ferro total ( $\text{Fe}^{2+} + \text{Fe}^{3+}$ ) entre as diferentes camadas de cromitito, e variações laterais na razão de oxidação ( $\text{Fe}^{3+}/(\text{Fe}^{2+} + \text{Fe}^{3+})$ ) ao longo de uma mesma camada (Jackson, 1963). Às variações laterais na razão de oxidação o autor atribuiu a existência de um gradiente lateral na  $f\text{O}_2$  do magma durante a formação da Zona Ultramáfica, o que poderia estar relacionado ao padrão de convecção na célula, ao posicionamento dos condutos alimentadores ou à extração de água dos sedimentos intrudidos, ao longo das margens da intrusão.

Irvine (1975) estudou o sistema  $\text{K}_2\text{O}-\text{MgO}-\text{Cr}_2\text{O}_3-\text{SiO}_2$  onde representou a curva cotética olivina-cromita. O autor concluiu que um incremento em  $\text{SiO}_2$  por vias de contaminação com encaixante granítica poderia causar uma mudança no sentido da cristalização, levando-a para o campo de cristalização exclusivo de cromita. Esse processo permitiria a formação *in situ* de camadas de cromita. Evidências de campo e composição de inclusões de *melt* hospedadas em cromita sustentaram seu modelo de contaminação crustal com adição de sílica. Dois anos depois o autor concluiu que sua ideia de contaminação talvez não fosse a mais adequada por considerar

que quantidades geologicamente improváveis de assimilação seriam necessárias para deslocar o sentido da cristalização para o campo exclusivo de cromita (Irvine 1977). O autor sugeriu, portanto, um novo modelo no qual o deslocamento do cotético seria causado pela mistura de um magma residente, mais evoluído, com um magma primitivo a adentrar a câmara magmática. Tal modelo de mistura entre magma residente e magma primitivo injetado na câmara magmática é também proposto por Eales et al. (1987), Scoon and Teigler (1994) e Naldrett et al. (2009) para explicar a formação de cromtititos (e elementos do grupo da platina - EGP associados) na Zona Crítica do Complexo de Bushveld.

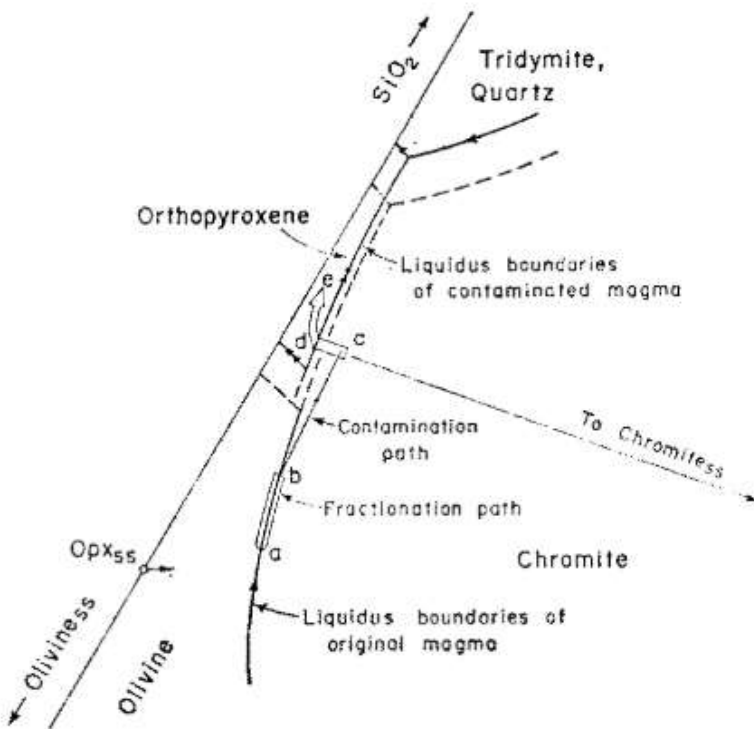


Figura 3: Modelo de diagrama de fases ilustrando a formação das partes inferiores das unidades cíclicas do Complexo de Muskox contendo camadas ricas em cromita por uma combinação de cristalização fracionada e contaminação. De acordo com o modelo, um líquido de composição “a” cristalizando olivina com cromita subordinadamente ao longo do cotético “a-b” sofre contaminação; a adição de sílica ao sistema desloca o sentido da cristalização, seguindo a curva “b-c”, ao longo da qual ocorre cristalização exclusiva de cromita. Extraído de Irvine (1975).

Kinnaird et al. (2002) observou que o plagioclásio intersticial à cromita nas camadas de cromitito da Zona Crítica do Complexo de Bushveld apresenta Sr<sub>i</sub> drasticamente mais elevado que os líquidos residentes das camadas imediatamente subjacentes. Considerando essa variação isotópica, os autores trouxeram novamente à tona o modelo de Irvine (1975), sugerindo contaminação com encaixante granítica. Segundo o modelo, enquanto o magma adentrando a câmara tivesse energia suficiente para atravessar a coluna de magma residente e interagir com as rochas do teto, haveria dominância de contaminação crustal; no entanto, a entrada de magma com tamanha energia não duraria por longos períodos, de modo que o processo dominante seria o de mistura do novo magma com o magma residente contaminado. Ambos os processos favorecendo a cristalização de cromita. A nuvem de cromita formada colapsaria para a base da câmara na forma

de uma lama (*slurry*) rica em cromita. Dessa forma, cada uma das importantes camadas de cromita no Complexo de Bushveld marcaria um evento de substancial influxo de magma na câmara magmática, sua interação com rochas encaixantes, mistura de magmas e fluxo turbidítico de lama cromitífera (Kinnaird et al., 2002). As investigações geoquímicas nos cromititos do grupo intermediário (*Middle Group chromitites*) de Kottke-Levin et al. (2009) sustentam o modelo de contaminação com rochas encaixantes e mistura magmas, tal qual sugerido por Kinnaird et al. (2002).

Cameron (1980), investigando a Zona Crítica inferior do Complexo de Bushveld, não encontrou evidências de contaminação ou mistura de magmas, assim como não detinha à época dados suficientes para avaliar a importância da  $fO_2$  e  $fS_2$  na evolução do intervalo estudado. Alternativamente, propôs que a origem dos cromititos intercalados aos bronzititos e harzburgitos esteja relacionada a flutuações na pressão total da câmara magmática: baseando-se nos dados experimentais de Osborn (1978), Cameron sugeriu que durante a maior parte da formação da Zona Crítica inferior, o magma estava nos campos da bronzita e da olivina no liquidus, mas sempre próximo ao limite da cromita; variações intermitentes da pressão deslocariam o sistema para o campo de estabilidade da cromita (Fig. 4), coprecipitando com bronzita ou olivina, ou ambos, ou mesmo precipitando sozinha, se o deslocamento do limite de fases fosse suficiente. O autor sugere que as variações de pressão poderiam ter origem em eventos de deformação tectônica na câmara magmática, aumento na altura da coluna de magma por adição de magma à câmara magmática, ruptura das paredes da câmara levando a escape lateral de magma ou, ainda, erupções vulcânicas, se considerar o Complexo de Bushveld como parte de um sistema subvulcânico.

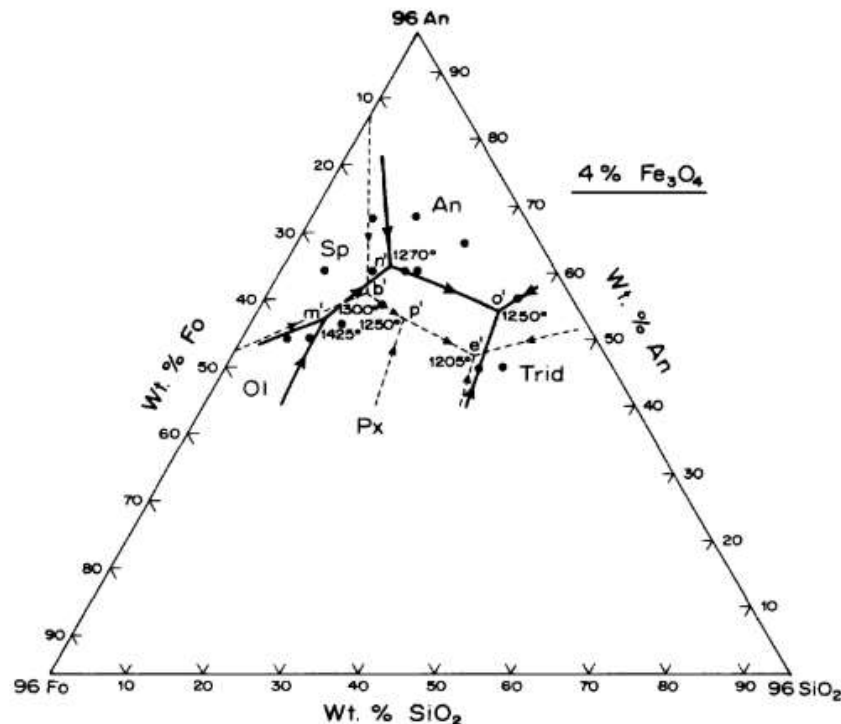


Figura 4: Relações de fases no sistema  $Mg_2SiO_4$ -óxido de ferro- $CaAl_2Si_2O_8$ - $SiO_2$ . As linhas tracejadas indicam as relações de fases a 1 atm e as linhas sólidas a 10 kbar. Extraído de Cameron (1980).

Lipin (1993) também considera flutuações na pressão total da câmara magmática fator fundamental na formação dos cromititos do Complexo de Stillwater. O autor sugere que durante eventos de influxos de magma a nucleação de bolhas de CO<sub>2</sub> e sua subsequente ascensão e expansão na câmara magmática seja a possível causa de sobrepressão, deslocando o sistema para o campo de cristalização da cromita. Diminuição da pressão por ruptura da câmara ou escape de magma deslocariam o sistema para o limite olivina-cromita, explicando os cromititos disseminados e textura em rede comumente observados acima dos cromititos maciços. Cawthorn (2005) propõe que o aumento de pressão causado por influxo de magma, afetando toda a extensão da câmara magmática de forma homogênea, seja uma explicação mais plausível para a formação do cromitito UG2 e do Merensky Reef no Complexo de Bushveld, com sua continuidade lateral, do que o modelo de mistura de magmas.

Modelamentos geoquímicos realizados por Naldrett et al. (2012) indicaram que contaminação de um magma com a composição da Zona crítica do Complexo de Bushveld com um magma felsico poderia induzir a imiscibilidade de S e formação de sulfetos, mas não causaria a precipitação de cromita. Igualmente, a cristalização de cromita antes de piroxênio não poderia ser desencadeada por aumento de pressão, mistura entre magma primitivo com evoluído, ou adição de H<sub>2</sub>O. Os modelamentos indicaram que a única forma de a cristalização de cromita preceder a de piroxênio é se a concentração inicial de Cr<sub>2</sub>O<sub>3</sub> no magma for maior que 0.2 % em massa. Os autores sugerem que a maior parte da cromita tenha cristalizado *in situ*, em uma câmara magmática estratificada e que, à medida que a cromita é extraída, a gradual diminuição da densidade do magma residual permite que ele misture lentamente com a camada de magma sobrejacente, explicando a variação química ao longo da estratigrafia dos cromititos. Apesar de os autores proporem um modelo em que a maior parte do sistema cromítífero tenha se formado *on stage*, eventuais influxos de magma trazendo uma carga de cristais de cromita suspensos são considerados.

### Modelos Off-Stage

Em contraste aos modelos de formação de cromititos *in situ*, Eales (2000) propôs que subjacente à câmara magmática que formou o Complexo de Bushveld existisse, à mesma época, uma outra câmara magmática contendo magma de composição mais magnesiana e mais rico em Cr. Nesta câmara subjacente, processos de cristalização fracionada e assentamento gravitacional de cristais estariam ocorrendo. O escape de líquido intercumulus da pilha acumulada poderia carregar consigo microfenocristais de cromita e periodicamente injetar magma contendo até 3% de cromita previamente cristalizada na câmara magmática de Bushveld. Este modelo explica o excesso de Cr na Zona Crítica (valor médio considerando todas as litologias presentes) sem a necessidade de se considerar escape de grande quantidade de magma da câmara magmática. A ideia de injeção de magma carregado com cristais de cromita suspensos, formados em uma câmara magmática subjacente, é também considerada por Mondal e Mathez (2007). Um modelo similar, que considera a cromita cristalizada previamente e injetada como lama cromítífera foi proposto por Voordouw et al. (2009). Nele, cromita seria formada ao longo de condutos alimentadores da câmara magmática, desencadeada pela mistura de magmas que por ali fluíram, e acumulada em

armadilhas estruturais. Os cristais de cromita acumulados ao longo dos condutos seriam remobilizados e injetados na câmara magmática na forma de sills de lama cromitífera contendo de 53 a 62% de cristais de cromita (Fig. 5).

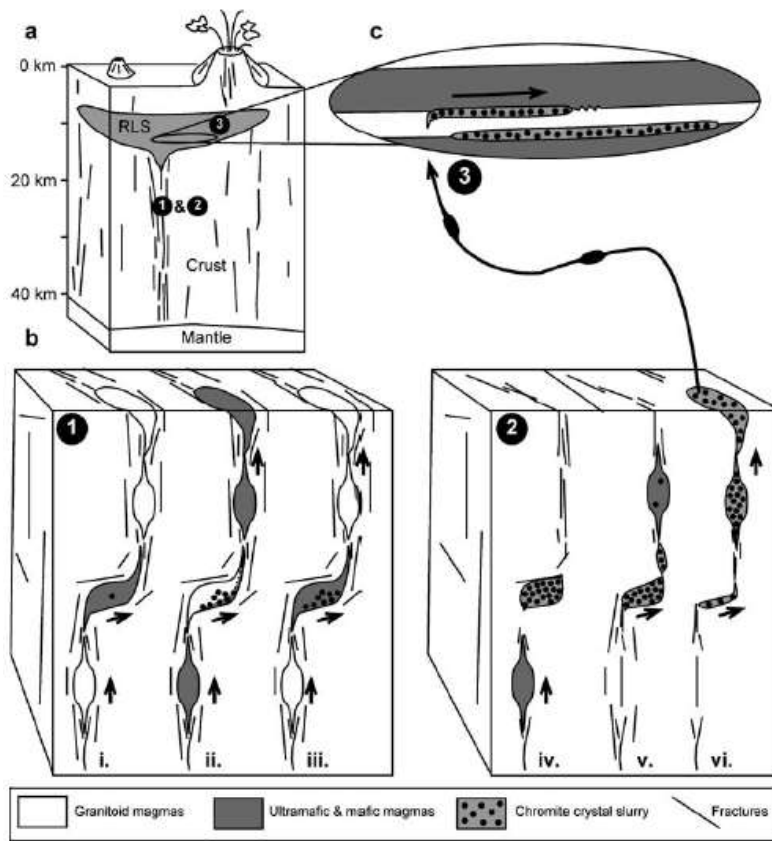


Figura 5: Modelo ilustrando uma origem intrusiva para camadas de cromitito. (a) Esboço da crosta terrestre, mostrando as localizações aproximadas das três etapas (RLS = Rustenburg Layered Suíte). (b) Etapas 1–3: (1) acumulação de lama cromitífera em uma armadilha estrutural; (2) remobilização da lama rica em cristais de cromita e ascensão através do conduto; (3) colocação da lama cromitífera ao longo de contatos litológicos na Suíte Acamada de Rustenburg. Extraído de Voordouw et al. (2009).

Uma variação dos modelos *off stage* de formação de cromititos considera a cristalização de cromita dentro da câmara magmática onde se encontra, mas tendo sofrido remobilização e concentração ainda em estágio magmático. Cameron e Desborough (1969) defendem que a ocorrência de cromititos contendo frequentes xenólitos na porção leste do Complexo de Bushveld argumenta contra o modelo de formação por assentamento gravitacional de cristais de cromita em uma câmara magmática calma. Pelo contrário, tais feições seriam indicativas de ambiente turbulento. Os autores sugerem que os cristais de cromita se tenham cristalizado ao longo do teto e das laterais da câmara magmática, sendo carregados e acumulados por correntes de convecção nas suas margens; a espessa pilha de cromita acumulada seria subsequentemente remobilizada na forma de correntes de turbidez de uma lama cromitífera, propagando-se rápida e uniformemente sobre o topo da pilha magmática. Cameron e Desborough (1969) sugeriram que a cristalização de cromita teria iniciado como resposta a um aumento na  $fO_2$  e terminado seguindo uma diminuição da mesma. Maier e Barnes (2008) sugeriram que a cromita teria se formado majoritariamente

disseminada dentro de suas rochas hospedeiras, e, durante um estágio tardi-magmático, a lama rica em cromita acumulada teria sido remobilizada em função de subsidência da parte central da câmara magmática de Bushveld. O processo de remobilização por deslizamento de cumulatos não totalmente cristalizados daria origem ao acamamento e concentração de cromita. A associação de sulfetos às camadas de cromita é explicada pelo fato de ambos (cromita e sulfetos) terem densidade similar, e serem, portanto, concentrados no mesmo intervalo. Este modelo de classificação gravitacional durante deslizamentos no Complexo de Bushveld foi reafirmado e detalhado por Maier et al. (2013). No Complexo de Uitkomst, África do Sul, Maier et al. (2018) sugerem que a cristalização de cromita tenha sido desencadeada por oxidação do magma devido à devolatilização de encaixantes carbonáticas ou por mistura entre magma primitivo e evoluído, tendo precipitado no topo da pilha cumulática. A continuidade da devolatilização e erosão do dolomito subjacente provoca subsidência da base do conduto, causando deslizamentos. Classificação hidrodinâmica por meio dos deslizamentos teria sido responsável pela remobilização e formação das camadas de cromitito e sulfeto maciços (Fig. 6).

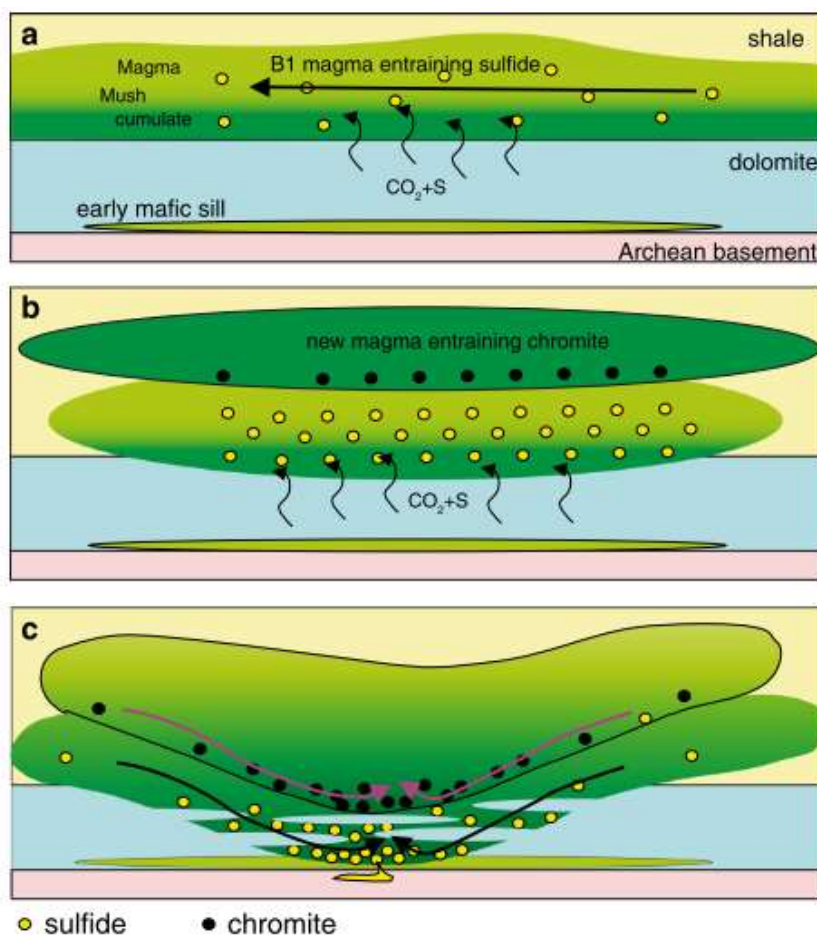


Figura 6: Modelo esquemático ilustrando o modelo de formação proposto para as camadas de sulfeto e cromita maciças no Complexo de Uitkomst. A: devolatilização de dolomitos e adição de S de xistos encaixantes. B: Influxo de novo magma, causando dilatação do sill. CO<sub>2</sub> proveniente da devolatilização causa oxidação do magma e supersaturação em cromita. C: A continuidade da devolatilização e erosão magnética do dolomito causa deslizamentos de lama magnética rica em cromita e em sulfetos para a base da câmara, sofrendo classificação hidrodinâmica. Extraído de Maier et al. (2018).

### 1.3.3 Inclusões hospedadas em cromita

Inclusões sólidas em Cr-espinélios tem sido descritas em cromititos maciços e disseminados tanto em complexos ofiolíticos quanto estratiformes. Já na década de 1960, McDonald (1965), estudando camadas de cromitito da Zona Crítica Inferior do Complexo de Bushveld, percebeu que as inclusões sólidas na cromita poderiam ser uma chave para o entendimento da formação do depósito. Desde então, diversas tentativas tem sido feitas para compreender os mecanismos de aprisionamento e a relação entre as inclusões em cromita com a origem de cromititos maciços. O estudo de inclusões em Cr-espinélio tem se mostrado uma importante ferramenta de acesso a informações magmáticas, uma vez que é comum Cr-espinélios aprisionarem inclusões quando de sua cristalização e estas não sofrem modificações significativas pós-aprisionamento comparadas às inclusões hospedadas em silicatos (Kamenetsky, 1996). Além disso, o Cr-espinélio é considerado um excelente “microcontainer” para inclusões, uma vez que é capaz de reter teores de água 4 a 5 vezes mais elevados em inclusões de *melt* do que a olivina, por exemplo (Shimizu et al., 2001). Ainda, devido a sua alta resistência à alteração, comparativamente aos silicatos junto aos quais costuma cristalizar, até mesmo o estudo de inclusões em espinélios detriticos são possíveis (Lenaz et al., 2000; Shimizu et al., 2009). A seguir é exposta uma revisão sobre os principais trabalhos envolvendo a investigação de inclusões em cromita e como elas contribuíram para a compreensão da gênese de cromititos.

McDonald (1965) propôs a formação de gotículas imiscíveis ricas em cromo que se aglutinariam e acumulariam no chão da câmara magmática. Tais gotículas iniciariam a cristalização das bordas para o núcleo, tornando-se enriquecidas na fase silicatada, até que houvesse a separação de uma fase silicatada imiscível que posteriormente cristalizaria formando uma inclusão de silicato. Por outro lado, o autor acredita que os cristais de cromita sem inclusões cristalizaram diretamente a partir do magma. A interpretação de McDonlad (1965) quanto à formação de cromita contendo inclusões silicáticas a partir de um líquido imiscível foi refutada por Jackson (1966), entre outras razões, por considerar improvável a formação de um líquido imiscível rico em cromo a partir de um magma basáltico, dada a alta temperatura necessária para formação de um líquido de tal natureza (1700 a 2100 °C, dependendo da composição da cromita).

Irvine (1975), estudando os cromititos da intrusão de Muskox, Canadá, propôs que os altos teores de sílica e álcalis medidos nas inclusões hospedadas em cromita poderiam representar vários graus de mistura entre o magma parental basáltico e um contaminante granítico. Para o autor, a ocorrência de rutilo como inclusões na cromita também sugere que o magma foi enriquecido em sílica antes que a cromita fosse precipitada. Talkington et al. (1983) consideram a presença de inclusões de silicatos hidratados (fogopita e pargasita) em cromita como indicativo de que a precipitação de cromita tenha se dado em resposta a flutuações de  $fO_2$  relacionadas a variações da  $pH_2O$  no Sill Bird River, Canadá.

Augé (1987) encontrou diferenças fundamentais nas proporções de silicatos inclusos e intersticiais à cromita no ofiolito de Omã. O autor sugere que o aprisionamento ocorreu após um período de desestabilização de auréolas de anfibólito cristalizadas sobre grãos de cromita e um estágio subsequente de crescimento de cromita. O autor observa ainda que, embora a presença de inclusões de silicatos hidratados (anfibólito, K-flogopita e Na-flogopita) ateste que o magma

estivesse hidratado quando a cromita cristalizou, “a concentração de cromita não parece estar relacionada à presença de água no sistema”, uma vez que estas inclusões também são observadas em espinélios disseminadas em dunito. Lorand e Ceuleneer (1989), também trabalhando no ofiolito de Omã, postularam que a mineralogia peculiar das inclusões seria resultado de uma complexa interação ocorrida dentro das inclusões entre cristais magmáticos precocemente cristalizados e um líquido contendo sódio e enxofre que foi injetado na câmara magmática em certos estágios de sua evolução.

Peng et al. (1995) sugeriram que o magma parental tenha coexistido com líquido aquoso alcalino de alta temperatura para formar as inclusões de silicatos hidratados como flogopita e pargasita descritas no ofiolito Hongguleleng, na China. Além disso, os autores sugeriram que a existência de K-flogopita e Na-flogopita em cromita não poderia ter se originado apenas do magma primário da seqüência ofiolítica; eles propuseram uma formação de flogopita a partir de misturas de um líquido aquoso rico em Na oriundo do magma primário com fluidos aquosos ricos em K provenientes da desidratação de placas oceânicas subductadas.

Spandler et al. (2005) conduziram experimentos de aquecimento para refundir inclusões silicatadas polifásicas, consideradas como representantes do magma parental aprisionadas pelas cromitas, no Complexo Stillwater. As composições analisadas nas inclusões reomogeneizadas não se assemelham a nenhum magma proposto como sendo o magma parental de nenhuma intrusão acamada. Os autores revivem o modelo proposto por Irvine (1975) para a intrusão de Muskox, sugerindo que as inclusões de *melt* representam assimilação localizada de rochas encaixantes pelo magma primitivo. Tal contaminação seria o gatilho para a supersaturação em cromita e, portanto, seria responsável pela formação do cromitito.

Borisova et al. (2012) recorrem a um modelo de três estágios para a petrogênese do cromitito da área de Maqsad, ofiolito de Omã. A primeira etapa, sustentada por algumas raras inclusões de serpentina e espinélio alterado, é caracterizada por metamorfismo retrógrado e alteração hidrotermal do manto harzburgítico, que constitui uma abundante fonte de cromo, por fluido de origem marinha; o segundo estágio envolve metamorfismo progressivo e desidratação de serpentinitos; no terceiro estágio, um magma do tipo MORB em ascensão (considerado consistente como um magma parental devido à química da cromita) assimila o manto harzburgítico serpentinizado, tornando-se enriquecido em água, S, Cl e Na, coerente com inclusões de pargasita e K- e Na- flogopita hospedadas em cromita.

Vukmanovic et al. (2013) investigaram as texturas de cromita dos cromititos de base e topo do Merensky Reef, no Complexo de Bushveld, utilizando difração por retroespalhamento de elétrons. A camada da base contém duas populações de cromita, cristais idiomórficos de granulometria fina e cristais de cromita ameboides contendo inclusões silicáticas, ao passo que a camada de topo contém apenas cristais idiomórficos de granulometria fina. Trabalhos anteriores haviam sugerido que os cristais ameboides contendo inclusões seriam produto de sinterização de cristais menores pré-existentes. O estudo de Vukmanovic et al. (2013) indicou que os cristais ameboides haviam se formado a partir de crescimento dendrítico, em um estágio inicial de cristalização. Os autores sugeriram que a textura teria se formado por super-resfriamento (*supercooling*) durante o posicionamento do magma que formou o Merensky Reef contra a camada

de anortosito mais fria subjacente. Já a camada de cromitito superior, contendo apenas cristais idiomórficos sem inclusões, teria se formado a partir de um influxo de magma subsequente sobre um substrato mais quente, não tendo sofrido efeito de super-resfriamento.

Prichard et al. (2015) realizaram tomografia computadorizada de raios X de alta resolução e difração por retroespalhamento de elétrons em nódulos de cromita do ofiolito de Troodos, no Chipre. Neste ofiolito, é recorrente a ocorrência de nódulos de cromita com núcleo esqueletal, contendo grande quantidade de inclusões de material silicático; o núcleo esqueletal é bordeado por uma margem “limpa”, sem inclusões. O estudo revelou que a porção central do nódulo é composto por um único grande cristal de cromita esqueletal, e a borda se trata de diversos grãos de granulometria fina, cristalizados ao redor do núcleo esqueletal. A formação destas feições foi interpretada como uma etapa inicial de supersaturação em Cr no magma, levando a uma rápida taxa de crescimento de cromita, e, à medida que o grau de supersaturação diminui, o crescimento esqueletal cessa e inicia a nucleação de novos cristais no entorno do núcleo formado.

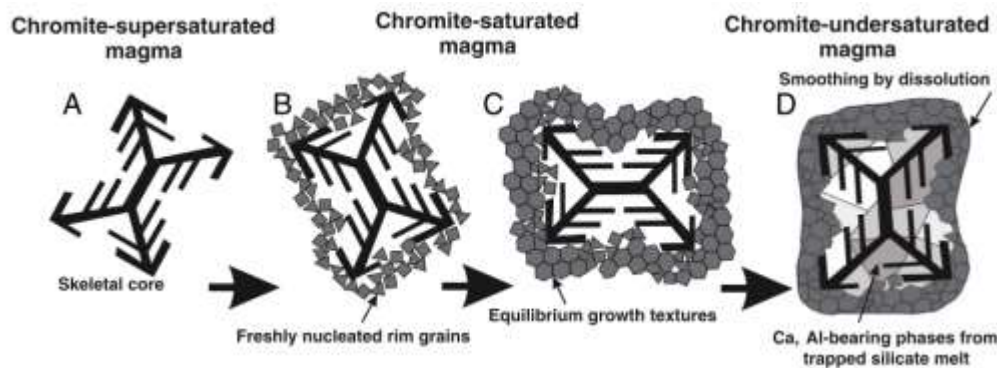


Figura 7: Modelo mostrando os estágios de crescimento dos nódulos com núcleos esqueletais do Complexo de Troodos. A: crescimento inicial rápido do cristal esquelético B: nucleação heterogênea de cromita granular ao redor das bordas do núcleo esqueletal parcialmente formado C: continuidade do crescimento de cromita granular, com crescimento *in situ* de cristais adacumulus produzindo equilíbrio textural D: dissolução do aro de cromita produzindo uma margem arredondada e lisa, e borda de grãos truncados. Extraído de Prichard et al. (2015).

Mansur e Ferreira Filho (2017) reportam a ocorrência de dois distintos padrões de tamanho e número de inclusões em cromita de duas camadas de cromitito no Complexo Luanga, Brasil. Um deles é caracterizado por uma única grande inclusão silicática, ao passo que o outro contém cromita com inclusões pequenas e abundantes. Os autores argumentam que a primeira (cromita com uma grande inclusão) é formada por taxa de cristalização mais baixa que a segunda (cromita com abundantes inclusões), permitindo a coalescência de inclusões. Em ambos os casos, no entanto, a taxa de cristalização é considerada alta.

### 1.3.4 Geologia e gênese do Complexo Jacurici

Os vários corpos máfico-ultramáficos que compõem o Complexo Jacurici são considerados segmentos de uma única intrusão que foram tectonicamente rompidos e deslocados ao longo de uma zona de cisalhamento. Os segmentos são delgados (<300 m de espessura) e hospedam camadas de cromitito, sendo a mais importante de até 8 m de espessura (Marques et al. 2017). O

corpo Monte Alegre Sul (MAS), foco desta investigação, está localizado na região central do Complexo, aproximadamente 20 km a norte da mina subterrânea de Ipueira (Fig. 2). Marques e Ferreira-Filho (2003) consideraram, baseados em cálculo de balanço de massa proposto por Campbell e Murck (1993), que uma coluna de magma de mais de 10.000 m de espessura fosse necessária para viabilizar a formação do cromitito. Tamanha quantidade de magma não está representada na forma de sequência silicática, o que levou Marques e Ferreira-Filho (2003) a conceber a ideia de que o Complexo tenha atuado como um conduto pelo qual uma imensa quantidade de magma passou, cristalizando a acumulando cromita. Os autores propuseram a seguinte divisão estratigráfica, da base para o topo, para os segmentos Ipueira-Medrado, localizados ao sul do Complexo: Zona Marginal, composta por gabro cisalhado e harzburgito rico em piroxênio; Zona Ultramáfica, subdividida em Unidade Ultramáfica Inferior (dunito com harzburgitos e cromititos com textura em rede associados), a Camada de Cromitito Principal (cromititos maciços e com textura em rede associados), e Unidade Ultramáfica Superior (principalmente harzburgitos, com cromititos com textura em rede e dunitos subordinados); Zona Máfica, consistindo em leuconoritos a melanoritos. Posteriormente, esta divisão estratigráfica foi também aplicada aos segmentos Monte Alegre Sul (localizado na porção intermediária do complexo) e Várzea do Macaco (na porção norte do complexo) (Marques et al. (2017) - Fig. 8).

Embora a mesma divisão estratigráfica possa ser aplicada aos quatro segmentos, algumas diferenças de sul para norte são observadas (Marques et al. 2017): as rochas da Zona Ultramáfica nos segmentos das porções central (MAS) e norte do complexo (VM) são enriquecidas em piroxênio comparadas aos segmentos na porção sul (I-M). Clinopiroxênio é mais frequente em MAS e VM, formando lherzolitos e websteritos com maior frequência nestes segmentos. O corpo VM apresenta sulfetos disseminados (1 a 15 %) ao longo de um intervalo que inicia 20 m abaixo e termina 15 m acima da CCP, compostos por pirrotita + pentlandita + calcopirita. Uma revisão completa sobre as relações mineralógicas e texturais das rochas do complexo é obtida em Marques et al. (2017).

Em todos os segmentos estudados, anfibólio intercumulus magmático ocorre tanto na UUI quanto na UUS, sendo mais abundante na UUS Marques et al. (2017). Marques et al. (2003) realizaram estudos isotópicos e observaram que embora todas as rochas tenham  $\epsilon_{\text{Nd}}$  fortemente negativo (média -4.4), os valores de  $\epsilon_{\text{Nd}}$  mais negativos (média -6.5) estavam associados às rochas da UUS mais ricas em anfibólio intercumulus. Além disso, concentrados de cromita UUI, da CCP e da UUS apresentam aumento nos valores de  $\gamma_{\text{Os}}$  ao longo da estratigrafia, variando de -4.6 a +3. Modelamentos indicaram que este comportamento isotópico seria consistente com contaminação crustal de um manto litosférico subcontinental Arqueano metassomaticamente enriquecido. Os autores sugeriram que a contaminação crustal, indicada pelos estudos isotópicos, com adição de fluidos, indicada pela abundância de anfibólio, teria desencadeado a cristalização de cromita. Ferreira Filho e Araújo (2009) sugeriram que a participação da contaminação crustal por rochas carbonáticas, indicadas pela ocorrência de xenólitos calci-silicáticos, como também pela associação das rochas do complexo com encaixantes carbonáticos tenha tido participação importante formação do cromitito.

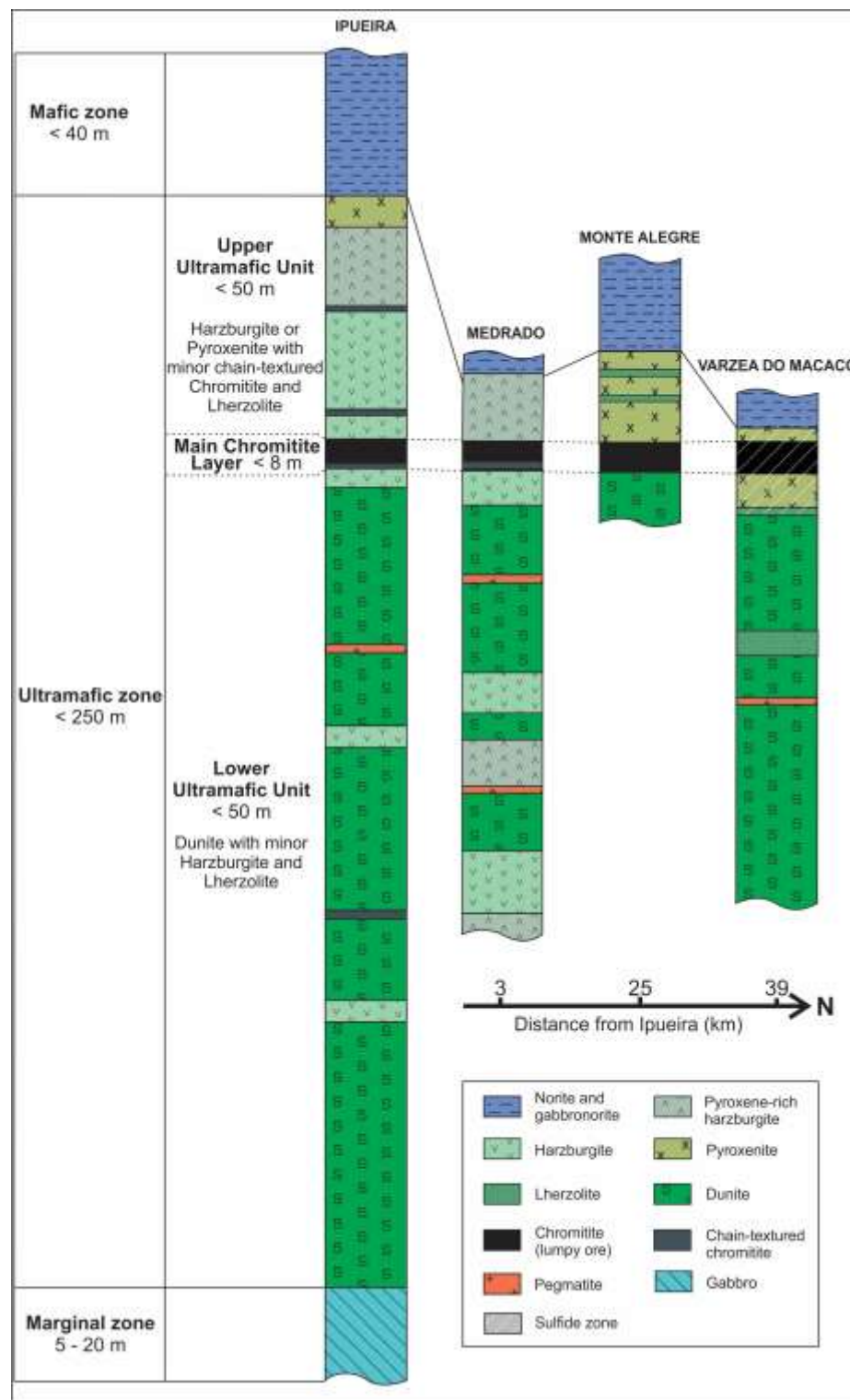


Figura 8: Seções representativas dos segmentos Ipueira, Medrado, Monte Alegre Sul e Várzea do Macaco, mostrando a correlação estratigráfica e as divisões sugeridas para o Complexo Jacurici. Extraído de Marques et al. (2017).

Estudos de química mineral nos segmentos Ipueira-Medrado (Marques et al. 2003) demonstraram que ao longo da UUI ocorre um gradual e lento aumento nos teores de Fo na olivina e En no piroxênio, ao passo que acima da CCP, na UUS estes teores diminuem rapidamente (Fig. 9). Esta variação indica que abaixo da CCP a câmara magmática atuou como um sistema aberto, sendo constantemente reabastecido por influxos de magma primitivo. Acima da CCP, teria ocorrido a predominância de cristalização fracionada, sem a participação de importante adição de magma primitivo. Dessa forma, a CCP representa um importante marcador petrológico, refletindo a transição de um regime magmático aberto para um regime magmático fechado.

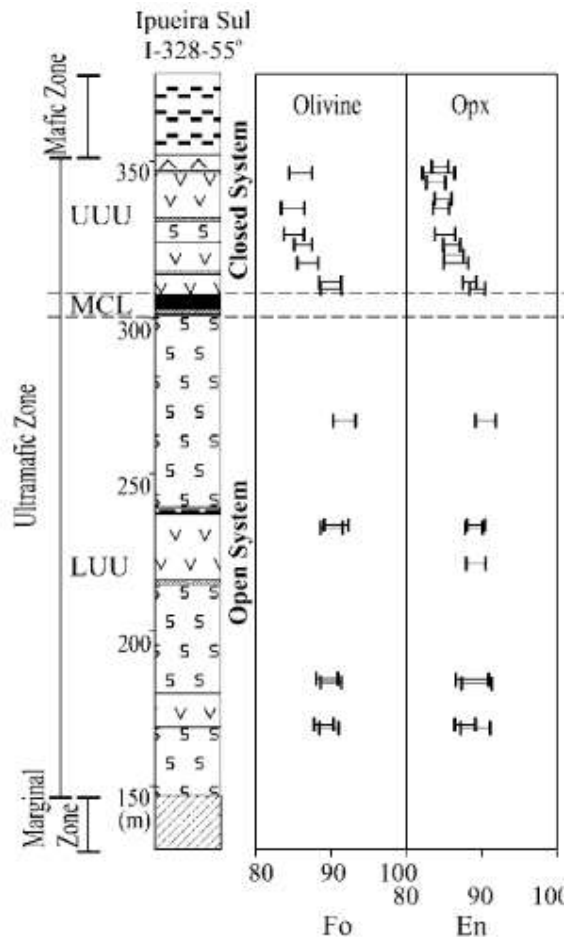


Figura 9: Variação estratigráfica de forsterita (Fo) de olivina e enstatita (En) de ortopiroxênio (Opx) através do segmento Ipueira Sul, furo I-328-55. LUU, Lower Ultramafic Unit (Unidade Ultramáfica Inferior); UUU, Upper Ultramafic Unit (Unidade Ultramáfica Superior). Extraído e modificado de Marques et al. (2003).

Marques et al. (2017) observaram a ocorrência de inclusões minerais, incluindo silicatos hidratados inclusos em cromita da CCP. Este fato, aliado à abundância de anfibólito magmático em todos os segmentos estudados, suporta o modelo de contaminação crustal do adição de fluidos proposta anteriormente (Marques et al. 2003). Neste trabalho, os autores sugerem um modelo para a formação da CCP no qual a cromita é cristalizada e acumulada ao longo das paredes do conduto,

sendo remobilizada por meio de deslizamentos e redepositada no topo da pilha cumulática, dando origem ao espesso cromitito do Complexo Jacurici (Fig. 10).

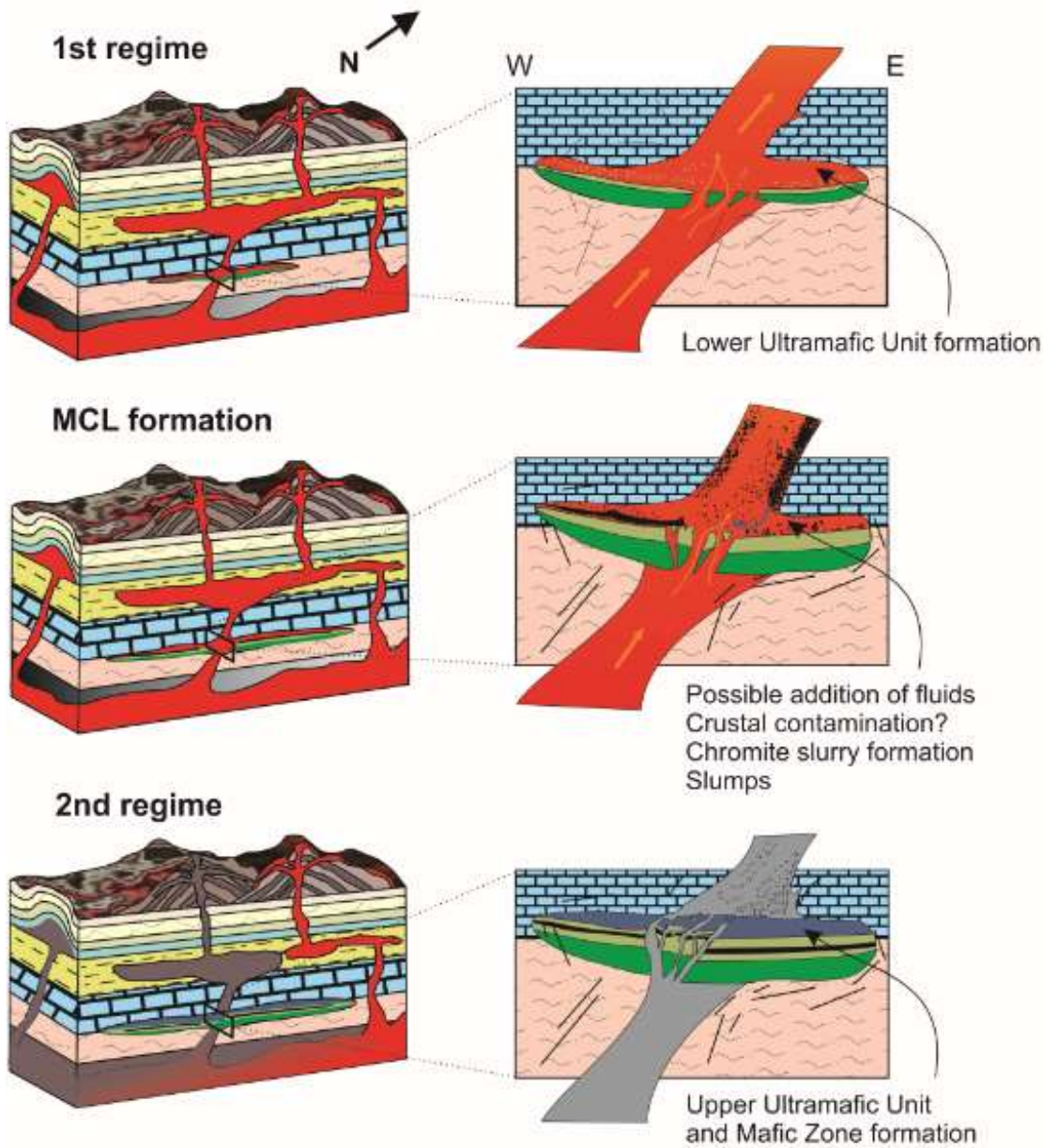


Figura 10: Diagrama esquemático que ilustra a formação do depósito de cromita do Complexo Jacurici considerando uma câmara em forma de conduto. A cromita cristalizou *in situ* ao longo das margens do conduto, formando uma lama cromitífera semi-consolidada que desmoronou e formou um cromitito espesso sobre as rochas ultramáficas acamadas previamente formadas. Posteriormente, o conduto foi obstruído e o magma residente fracionado e cristalizado, produzindo rochas mais evoluídas. Extraído de Marques et al. (2017).

## 2. MATERIAIS E MÉTODOS

### Revisão bibliográfica

Esta etapa, que se estendeu ao longo de todo o período de mestrado, fundamentou-se em pesquisa, leitura e discussão de artigos científicos e publicações técnicas, relativos à formação e posicionamento de complexos máfico-ultramáficos, modelos de formação de cromititos, relações texturais e mineralógicas entre cromita e inclusões contidas em cromita, contexto geológico e geotectônico da porção nordeste do Cráton São Francisco.

### Etapa de campo

A etapa de campo foi realizada principalmente no município de Andorinha-Ba, nas dependências da FERBASA, junto à Mina Ipueira. Esta etapa consistiu majoritariamente de descrição de furos de sondagem. Para o propósito deste estudo, três furos do Segmento Monte Alegre Sul foram detalhadamente descritos e o furo MAS-105-65 ° foi selecionado para amostragem sistemática. Amostras representativas de silicato e amostras regularmente espaçadas da Camada de Cromitito Principal foram coletadas. Além disso, foram visitadas as duas antigas lavras a céu aberto no Segmento MAS, município de Monte Santo-Ba, para fins de mapeamento e investigação da natureza dos contatos litológicos.

### Confecção de lâminas delgadas e análise petrográfica

Trinta e cinco lâminas delgadas polidas foram confeccionadas no Laboratório de Preparação de Amostras – Anexo do Centro de Estudos em Petrologia e Geoquímica (CPGq). Relações mineralógicas e texturais foram investigadas sob microscópio óptico de luz transmitida e refletida, e sob microscópio eletrônico de varredura (MEV) JEOL 6610-LV equipado com um espectrômetro de dispersão de energia (EDS) e um Detector Bruker Nano XFlash 5030, no Laboratório de Geologia Isotópica - UFRGS. Metalização com carbono foi utilizada nas lâminas investigadas com auxílio do MEV. Durante esta etapa, minerais cumulus, intercumulus e inclusões em cromita foram selecionados para investigação da química mineral.

### Química mineral

As análises pontuais sob microssonda eletrônica foram realizada em duas etapas e em dois laboratórios distintos. As microanálises em amostras da sequência silicática foram realizadas utilizando uma microssonda eletrônica JEOL JXA-8230 na Universidade de Brasília. Para olivina e piroxênios, o equipamento foi operado com potencial de aceleração de 15 kV e corrente de 20 nA usando um feixe focalizado; para anfibólio, potencial de aceleração de 15 kV, corrente de 20 nA e diâmetro de feixe de 2 µm. Padrões naturais e sintéticos foram usados para calibração. As inclusões de silicatos e sulfetos, bem como silicatos cumulus e intercumulus selecionadas na etapa anterior foram analisadas para elementos maiores e menores usando um microssonda JEOL JXA-8230 equipado com um conjunto de espectrômetros dispersivos de comprimento de onda na Queen's University. Para olivina e piroxênios, o equipamento foi operado com potencial de aceleração de 15 kV, corrente de 20 nA com feixe focalizado; para anfibólio, potencial de aceleração de 15 kV, corrente de 20 nA e diâmetro de feixe de 2 µm; para flogopita, potencial de aceleração de 15 kV, corrente de 10 nA e diâmetro de feixe de 3,5-7 µm, dependendo do tamanho

do grão; para sulfetos, tensão de aceleração de 15 kV, corrente de 10 nA e feixe focalizado. Perfis em cristais de cromita contendo inclusões e em cristais sem inclusões da CCP e imagens de raios-X de distribuição elementar em cromita também foram produzidos na Queen's University. Para tal, a microssonda foi operada a 15 kV de potencial de aceleração, 30 nA de corrente com um feixe focado. Padrões minerais naturais e sintéticos foram usados para calibração seguindo o método descrito em Pouchou e Pichoir (1991). Os teores de ferro férrico em cromita, piroxênios e anfibólios foram calculados usando parâmetros estequiométricos. Para o anfibólito, o melhor recálculo da fórmula foi obtido com as estimativas mínimas de ferro férrico, conforme descrito em Leake et al. (1997).

## REFERÊNCIAS

(Pertinentes aos Capítulos 1 e 2)

- Augé, T. 1987. Chromite deposits in the northern Oman ophiolite: Mineralogical constraints. *Mineralium Deposita*, 22: 1-10
- Borisova, A.Y., Ceuleneer, G., Kamenetsky, V.S. et al. 2012. A New View on the Petrogenesis of the Oman Ophiolite Chromitites from Microanalyses of Chromite-Hosted Inclusions. *Journal of Petrology* 53, (12):2411–40.
- Cameron, E.N. 1980. Evolution of the lower Critical Zone, central sector, Eastern Bushveld Complex, and its chromite deposits. *Economic Geology*, 75:845–871
- Cameron, E.N., Desborough, G.A. 1969. Occurrence and characteristics of chromite deposits - eastern Bushveld Complex, *Economic Geology Monograph*, vol. 4 (pg. 23-40)
- Campbell, I.H., Murck, B.W. 1993. Petrology of the G and H chromitite zones in the Mountain View area of the Stillwater Complex, Montana. *Journal of Petrology*, 34, 291–316.
- Cawthorn, R.G. 2005. Pressure fluctuations and the formation of the PGE-rich Merensky and chromitite reefs, Bushveld Complex. *Mineralium Deposita*, 40, 231–235.
- Eales, H.V. 1987. Upper Critical Zone chromitite layers at RPM Union section mine, western Bushveld complex. In: Stowe, C. W. (ed.) Evolution of Chromium Ore Fields. Van Nostrand Reinhold, pp. 144–168.
- Eales, H.V. 2000. Implications of the chromium budget of the Western Limb of the Bushveld Complex. *South African Journal of Geology*, 103:141–150
- Ferreira Filho, C.F., Araujo, S.M. 2009. Review of Brazilian Chromite Deposits Associated with Layered Intrusions: Geological and Petrological Constraints for the Origin of Stratiform Chromitites. *Applied Earth Science*, 118(3–4):86–100.
- Irvine, T.N. 1975. Crystallization Sequences in the Muskox Intrusion and Other Layered Intrusions-II. Origin of Chromitite Layers and Similar Deposits of Other Magmatic Ores. *Geochimica et Cosmochimica Acta*, 39(6–7).
- Irvine, T.N. 1977. Origin of chromitite layers in the Muskox intrusion and other layered intrusions: a new interpretation. *Geology*, 5(273–277).
- Jackson, E.D. 1961. Primary textures and mineral associations in the ultramafic zone of the Stillwater Complex, Montana. US Geological Survey, Professional Papers 358, 106 pp.
- Jackson, E.D. 1963. Stratigraphic and lateral variation of chromite composition in the Stillwater complex. *Mineralogical Society of America – Special Papers*, 1, 46–54

- Jackson, E.D. 1966. Liquid immiscibility in chromite seam formation - a discussion. *Economic Geology*, v. 61, p. 777-780.
- Jardim de Sá, E.F. 1984. Geologia da região do Vale do Jacurici. Natal, 17p. Relatório de Consultoria para CPM.
- Kamenetsky, V. 1996. Methodology for the study of melt inclusions in Cr-spinel, and implications for parental melts of MORB from FAMOUS area. *Earth and Planetary Science Letters* 142(3-4), pp. 479-486.
- Kinnaird, J.A., Kruger, F.J., Nex, P.A.M., Cawthorn, R.G. 2002. The chromitite formation - a key to understand processes of formation and platinum enrichment. *Transactions of the Institution of Mining and Metallurgy*, 111:23–35
- Kottke-Levin, J., Tredoux, M., Grab, P-J. 2009. An investigation of the geochemistry of the Middle Group of the eastern Bushveld Complex, South Africa Part 1- the chromitite layers. *Applied Earth Science (Transactions of the Institution of Mining and Metallurgy, B)*, 118:111–130
- Kropschot, S.J., Doebrich, J. 2010. Chromium - Makes stainless steel stainless: U.S. Geological Survey Fact Sheet 2010–3089, (Disponível em: <https://pubs.usgs.gov/fs/2010/3089/>.)
- Leake, B.E., Wooley, A.R., Arps, C.E.S. et al. 1997. Nomenclature of amphiboles: report of the subcommittee on amphiboles of the International Mineralogical Association, Commission on new minerals and mineral names. *American Mineralogist*, 82:1019–1037.
- Lenaz, D., Kamenetsky, V.S., Crawford, A.J., et al. 2000. Melt inclusions in detrital spinel from the SE Alps (Italy-Slovenia): a new approach to provenance studies of sedimentary basins. *Contributions to Mineralogy and Petrology*, 139: 748-758.
- Lipin, B.R. 1993. Pressure increases, the formation of chromite seams, and the development of the ultramafic series in the Stillwater Complex, Montana. *Journal of Petrology*, 34:955–976.
- Lorand, J.P., Ceuleneer, G. 1989. Silicate and base-metal sulfide inclusions in chromites from the Maqsad area (Oman ophiolite, Gulf of Oman): A model for entrapment. *Lithos*, 22: 173-190.
- Maier, W.D., Barnes, S-J. 2008. Platinum-group elements in the UG1 and UG2 chromitites, and the Bastard Reef, at Impala platinum mine, Western Bushveld Complex, South Africa: evidence for late magmatic cumulate instability and reef constitution. *South African Journal of Geology*, 111:159–176.
- Maier, W.D., Barnes, S-J., Grooves, D.I. 2013. The Bushveld Complex, South Africa: Formation of Platinum-Palladium, Chrome- and Vanadium-Rich Layers via Hydrodynamic Sorting of a Mobilized Cumulate Slurry in a Large, Relatively Slowly Cooling, Subsiding Magma Chamber. *Mineralium Deposita*, 48(3):1–56.
- Maier, W.D., Prevec, S.A., Scoates, J.S. et al. 2018. The Uitkomst Intrusion and Nkomati Ni-Cu-Cr-PGE Deposit, South Africa: Trace Element Geochemistry, Nd Isotopes and High-Precision Geochronology. *Mineralium Deposita*, 53(1):67–88.

- Mansur, E.T., Ferreira Filho, C.F. 2017. Chromitites from the Luanga Complex, Carajás, Brazil: Stratigraphic distribution and clues to processes leading to post-magmatic alteration. *Ore Geology Reviews*, 90:110–130.
- Marinho, M.M., Rocha, G.F., Deus, P.B., Viana, J.S., 1986. Geologia e potencial cromitífero do Vale do Jacurici-Bahia. *34º Congresso Brasileiro de Geologia*, Goiânia, Anais 5, 2074–2088.
- Marques, J.C., Dias, J.R.V.P., Friedrich, B.M. et al (2017) Thick Chromitite of the Jacurici Complex (NE Craton São Francisco, Brazil): Cumulate Chromite Slurry in a Conduit. *Ore Geology Reviews*, 90:131-147. Doi: 10.1016/j.oregeorev.2017.04.033
- Marques, J.C., Ferreira Filho, C.F., Carlson, R.W., Pimentel, M.M. 2003. Re-Os and Sm-Nd Isotope and Trace Element Constraints on the Origin of the Chromite Deposit of the Ipueira-Medrado Sill, Bahia, Brazil. *Journal of Petrology*, 44(4):659–78.
- Marques, J.C., Ferreira Filho, C.F. 2003. The Chromite Deposit of the Ipueira-Medrado Sill , São Francisco Craton, Bahia State, Brazil. *Economic Geology*, 98:87–108.
- McDonald, J.A. 1965. Liquid immiscibility as one factor in chromitite seam formation in the Bushyeld igneous complex. *Economic Geology*, 60:1674-1685
- Mondal, S.K., Mathez, E.A. 2007. Origin of the UG2 chromitite layer, Bushveld Complex. *Journal of Petrology*, 48:495–510
- Naldrett, A.J., Kinnaird, J.A., Wilson, A., Yudovskaya, M., McQuade, S., Chunnett, G., Stanley, C. 2009. Chromite composition and PGE content of Bushveld chromitites: Part 1—the Lower and Middle Groups. *Applied Earth Science (Transactions of the Institution of Mining and Metallurgy (B))*, 118:131–161
- Naldrett, A.J., Wilson, A., Kinnaird, J., Yudovskaya, M., and Chunnett, G., 2012, The origin of chromitites and related PGE mineralization in the Bushveld Complex: *Mineralium Deposita*, DOI10.1007/S00126-011-0366-3.
- Oliveira, E.P., Carvalho, M.J., McNaughton, N.J. et al (2004) Contrasting copper and chromium metallogenic evolution of terranes in the Paleoproterozoic Itabuna-Salvador- Curaçá orogen, São Francisco Craton, Brazil: new zircon (SHRIMP) and Sm- Nd (model) ages and their significances for orogen-parallel escape tectonics. *Precambrian Research*, 128:143-165.
- Osborn, E.F. 1978. Changes in phase relations in response to change in pressure from 1 atto to 10 kbar for the system Mg<sub>2</sub>SiO<sub>4</sub>-iron oxide-CaAlSi<sub>2</sub>O<sub>4</sub>-SiO<sub>2</sub>: Carnegie Inst. Washington Year Book 77, p. 784-790
- Peng, G., Lewis, J., Lipin, B. McGee, J., Bao, P., Wang, X. 1995. Inclusions of phlogopite and phlogopite hydrates in chromites from the Hongguleleng ophiolite in Xinjiang, northwest China. *American Mineralogist*, 80: 1307-1316.
- Pouchou, J.L., Pichoir, F. 1991. Quantitative analysis of homogeneous or stratified microvolumes applying the model “PAP”. In: Heinrich KFJ, Newbury DE (eds) *Electron Probe Quantitation*. Plenum Press, New York, pp 31–75.

- Prichard, H.M., Barnes, S.J., Godel, B. et al. 2015. The structure of and origin of nodular chromite from the Troodos ophiolite, Cyprus, revealed using high-resolution X-ray computed tomography and electron backscatter diffraction. *Lithos*, 218-219:87-98.
- Scoon, R.N., Teigler, B. 1994. Platinum-group element mineralization in the Critical Zone of the Western Bushveld Complex: I. Sulfide- poor chromitites below the UG-2. *Economic Geology*, 89:1094–1121
- Silveira, C.J.S., Frantz, J.C., Marques, J.C., Queiroz, W.J.A., Roos, S., Peixoto, V.M., 2015. Geocronologia U-Pb em zircão de rochas intrusivas e de embasamento na região do Vale do Jacurici, Cráton do São Francisco, Bahia. *Brazilian Journal of Geology*, 45:453–474.
- Shimizu, K., Komiya, T., Hirose, K., Shimizu, N. & Matuyama, S. 2001. Cr-spinel, an excellent micro-container for retaining primitive melt implications for a hydrous plume origin for komatiites. *Earth and Planetary Science Letters*, 189:177-188.
- Shimizu, K., Shimizu, N., Komiya, T., et al. 2009. CO<sub>2</sub>-rich komatiitic melt inclusions in Cr-spinsels within beach sand from Gorgona Island, Colombia. *Earth and Planetary Science Letters*, 288:33–43.
- Spandler, C., Mavrogenes, J., Arculus, R. 2005. Origin of chromitites in layered intrusions: Evidence from chromite-hosted melt inclusions from the Stillwater Complex. *Geology*, 33(11): 893-896.
- Talkington, W., Watkinson, D.H., Whittaker, P.J., Jones, P.C. 1983. Platinum-Group-Mineral Inclusions in Chromite from the Bird River Sill, Manitoba. *Mineralium Deposita*, 18(2):245–55.
- Voordouw, R., Gutzmer, J., Beukes, N.J. 2009. Intrusive origin for Upper Group (UG1, UG2) stratiform chromitite seams in the Dwars River area, Bushveld Complex, South Africa. *Mineralogy and Petrology*, 97:75–94.
- Vukmanovic, Z., Barnes, S.J., Reddy, S., Godel, B., Fiorentini, M.L. 2013. Microstructure in chromite crystals of the Merensky Reef (Bushveld Complex, South Africa). *Contributions to Mineralogy and Petrology*, 165, 1031–1050.

### 3. ARTIGO CIENTÍFICO

Este capítulo consiste no corpo principal desta Dissertação. Trata-se do artigo científico produzido pela pós-graduanda e colaboradores durante o período de Mestrado, submetido à revista Mineralium Deposita. A carta de submissão está reproduzida abaixo:



Betina Friedrich <friedrich.betina@gmail.com>

#### **MIDE-D-18-00263 - Submission Confirmation for PETROGENESIS OF THE MASSIVE CHROMITITE LAYER FROM THE JACURICI COMPLEX, BRAZIL: EVIDENCE FROM INCLUSIONS IN CHROMITE**

1 mensagem

MIDE Editorial Office <em@editorialmanager.com>

27 de dezembro de 2018 17:17

Responder a: MIDE Editorial Office <johnrichard.arrienda@springer.com>

Para: Betina Maria Friedrich <friedrich.betina@gmail.com>

Dear Mrs. Friedrich,

Your submission entitled "PETROGENESIS OF THE MASSIVE CHROMITITE LAYER FROM THE JACURICI COMPLEX, BRAZIL: EVIDENCE FROM INCLUSIONS IN CHROMITE" has been received by journal Mineralium Deposita

The submission id is: MIDE-D-18-00263

Please refer to this number in any future correspondence.

You will be able to check on the progress of your paper by logging on to Editorial Manager as an author. The URL is <https://mide.editorialmanager.com/>.

Your manuscript will be given a reference number once an Editor has been assigned.

Thank you for submitting your work to this journal.

Kind regards,

Editorial Office  
Mineralium Deposita

PETROGENESIS OF THE MASSIVE CHROMITITE LAYER FROM THE JACURICI  
COMPLEX, BRAZIL: EVIDENCE FROM INCLUSIONS IN CHROMITE

Betina Maria Friedrich<sup>1</sup>, Juliana Charão Marques<sup>1</sup>, Gema Ribeiro Olivo<sup>2</sup>, José Carlos Frantz<sup>1</sup>,  
Brian Joy<sup>2</sup>, Waldemir José Alves Queiroz<sup>3</sup>

<sup>1</sup> Instituto de Geociências – Universidade Federal do Rio Grande do Sul – Av. Bento Gonçalves 9500, Prédio 43129, Porto Alegre, RS, Brazil. CEP 91501-970 (friedrich.betina@gmail.com)

<sup>2</sup> Queen's University, Department of Geological Sciences and Geological Engineering, Kingston, Ontario K7L 3N6, Canada

<sup>3</sup> Companhia de Ferro Ligas da Bahia – FERBASA, Pojuca, Bahia, Brazil

ABSTRACT

The Jacurici Complex hosts the largest chromium deposit in Brazil in an up to 8 m thick chromitite layer within a tectonically-segmented 300 m thick intrusion. The ore has been interpreted as the result of multiple episodes of crustal contamination-driven crystallization in a magma conduit. This study addresses the stratigraphy, mineralogical and textural relationships and mineral chemistry of the Monte Alegre Sul Segment, focusing on the Main Chromitite Layer composed of massive chromitite with a semi-massive basal interval. Chromite hosts abundant and diverse primary inclusions comprising mainly silicates (enstatite, phlogopite, magnesiohornblende, diopside and olivine), carbonates (dolomite and magnesite) and sulfides (pentlandite, millerite, heazlewoodite, polydymite, pyrite and chalcopyrite). Silicate inclusions are commonly monomineralic and sub- to euhedral, and their compositions suggest that they crystallized prior to, or coeval with, the main stage of chromite crystallization. Carbonate inclusions are irregular or negative-crystal shaped, suggesting entrapment as melt droplets. Sulfides are often polymimetic, irregular or hexagonal-shaped indicating entrapment as sulfide melt and as monosulfide solid solution (mss). Collectively, these inclusions suggest an H<sub>2</sub>O- and S-saturated resident magma with immiscible droplets of carbonate melt during chromite crystallization. Inclusion-rich and inclusion-free chromites occur together, and have similar chemistries. All chromite is considered to have formed from the same magma in response to variations in the degree of Cr saturation. We propose that the basal interval is the result of in situ crystallization with additional material added by slumping of locally remobilized chromite slurries, possibly accounting for the mixing of inclusion-bearing and inclusion-free chromite grains.

KEY WORDS

Chromite deposit; origin of chromitite; hydrated inclusions in chromite; carbonate inclusions in chromite; microprobe analysis of inclusions.

INTRODUCTION

Chromite is the only ore mineral for the element chromium, used in the production of stainless steel, superalloys and in the chemical industry for pigments (Kropschot and Doebrich 2010). Stratiform chromite deposits are the main source of chromite, occurring as semi-massive to massive chromitite seams hosted in layered mafic-ultramafic intrusions. Changes in the stability field of chromite in response to composition of magma, temperature, pressure and oxygen fugacity have long been used to explain the sole chromite crystallization (eg. Irvine 1975, 1977, Murck and Campbell 1986, Lipin 1993). However, the relatively low solubility of chromium in magmas requires large amounts of silicate magma to produce a chromitite layer. The mechanism to account for massive chromitite formation remains debatable (see reviews by Naldrett et al. 2012, Maier et al. 2013) and the *in situ* formation models have been, in the last two decades, challenged by chromite remobilization models (Eales 2000, Maier and Barnes 2008; Maier et al. 2013, 2018, Marques et al. 2017, Mondal and Mathez 2007, Voordouw et al. 2009).

In the northeastern São Francisco Craton, the Jacurici Complex hosts the main Brazilian chromite deposit, explored by the Companhia de Ferro Ligas da Bahia (FERBASA), with estimated reserves of 40,000,000 tons at 39% Cr<sub>2</sub>O<sub>3</sub> (FERBASA, internal report). The ore is in a single conduit-like thin (up to 300 m) mafic-ultramafic intrusion, segmented into several bodies by folding and faulting, and is concentrated in a massive 8-m-thick chromitite layer (Marques and Ferreira Filho 2003, Marques et al. 2017). A large amount of primitive magma is considered to have flowed through the conduit, leaving behind a cumulate sequence (Marques and Ferreira Filho 2003). Marques et al. (2003) considered the addition of fluids to explain the close relation between the Os-Nd isotopic variations with modal amphibole abundance, and suggested that crustal contamination might have played an important role in the chromitite formation. This study was complemented by the work of Ferreira Filho and Araújo (2009) who suggested assimilation of marble and calc-silicate country rocks as the likely crustal contaminant.

Recently, many types of mineral inclusions in chromite from the massive chromitite layer, including hydrated silicates, were reported and considered as additional evidence that the magma was hydrated when the chromite crystallized (Marques et al. 2017). In the present study, we selected one location from the central part of the Jacurici Complex, the Monte Alegre Sul Segment, to investigate in detail the mineral compositions and textural relationships of the chromite-hosted inclusions to further the understanding of the role of volatiles in the genesis of this complex and its ore. The results reveal that the magma was enriched in volatiles during the formation of the Jacurici Complex massive chromitite layer, suggesting that these volatiles might have triggered chromite crystallization and also played a role in chromite remobilization through slumping to form the thick massive chromitite layer.

## GEOTECTONIC AND GEOLOGICAL SETTING

The São Francisco Craton (Almeida 1965, 1977) is interpreted to have been formed by collision and amalgamation of Archean terranes during the Paleoproterozoic Transamazonian Orogeny with peak metamorphism at 2.1-2.0 Ga (Barbosa 1997, Barbosa and Sabaté 2002, 2003). Barbosa and Sabaté (2003) consider the collage of four Archean crustal blocks (Gavião, Serrinha,

Jequié and Itabuna-Salvador-Curaçá) to form the Itabuna-Salvador-Curaçá orogenic belt. The basement of the Jacurici Complex comprises a set of granitic-gneiss-granulitic rocks, 3.0 to 2.7 Ga in age, metamorphosed mainly under amphibolite facies conditions at 2.1-1.9 Ga (Barbosa et al. 2012, Cunha et al. 2012). The origin of the basement of the Jacurici Complex is debatable and has been interpreted as either granulitic terranes from the Neoarchean-Paleoproterozoic Itabuna-Salvador-Curaçá Orogen (Barbosa and Sabaté 2003; Barbosa et al. 2003, 2012; Misi et al. 2012) or Mesoarchean sequences of the Serrinha Block (Teixeira et al. 2000; Oliveira et al. 2004a, 2004b; Oliveira et al. 2016). The most recent mapping performed by the Brazilian Geological Survey (CPRM) interpreted the Jacurici Complex as intrusive into the Santa Luz Complex, part of the Serrinha Block (Oliveira et al. 2016).

The Jacurici Complex, with a general N-S orientation, extends along a belt at least 70 km long (Fig. 1A) and crops out near, and parallel to, the Paleoproterozoic Itiuba Syenite ( $2084 \pm 9$  Ma SHRIMP U-Pb in zircon – Oliveira et al. 2004b). Numerous undifferentiated mafic-ultramafic intrusions (Fig. 1B) are also aligned along this trend, suggesting a complex magmatic history (Marques et al. 2017). The Jacurici Complex is divided into many segments and the main underground mine is located at the southern end of the belt, in the Ipueira Segment. Many other orebodies have already been exploited by FERBASA in open pits such as those from the Medrado Segment (near Ipueira area), and the Monte Alegre Sul and Várzea do Macaco Segments in the northern part (Fig. 1B). Oliveira et al. (2004b) dated a norite sample from the Medrado area of the Jacurici Complex at  $2085 \pm 5$  Ma (SHRIMP U-Pb in zircon), which was interpreted as the crystallization age. Silveira et al. (2015) obtained an age of  $2102 \pm 5$  Ma for a gabbronorite intrusion adjacent to the Monte Alegre Sul segment and inferred this as the age of the first pulses of the mafic-ultramafic magmatism. The Jacurici Complex rocks are crosscut by undeformed alkaline pegmatites ( $2084 \pm 6$  Ma) in sharp contact with the ultramafic rocks, and are considered to be related to the Itiuba Syenite (Marques et al. 2010). The mafic-ultramafic rocks of the Jacurici Complex intruded at the contact between quartz feldspathic gneiss and metasedimentary rocks including marble, calc-silicate rocks and metachert (Marques et al. 2017). The Jacurici Complex was deformed and affected by amphibolite to granulite facies metamorphism resulting in some segments being stratigraphically inverted (Almeida et al. 2017, Dias et al 2014, Marques and Ferreira Filho 2003, Marques et al. 2017).

The intrusive sequence is divided from the base to the top into a Marginal Zone, an Ultramafic Zone and a Mafic Zone (Marques and Ferreira Filho 2003). The Marginal Zone and Mafic Zone are represented by gabbro and norite, respectively. The Ultramafic Zone is further subdivided into a Lower Ultramafic Unit (100 to 180 m thick), the Main Chromitite Layer (MCL, 5 to 8 m thick) and an Upper Ultramafic Unit (< 50 m thick). The Lower Ultramafic Unit is composed of dunite with interlayered harzburgite showing upward evolution in mineral chemistry toward more Mg-rich compositions (Fo93 and En94). The Main Chromitite Layer predominantly comprises massive ore. The Upper Ultramafic Unit (< 50 m thick) is composed of harzburgite with minor dunite lenses, characterized by rapid evolution toward less Mg-rich compositions (Fo85 and En84). Laterally discontinuous chromitite seams up to 1 m thick occur within both the Lower and the Upper Ultramafic units. This stratigraphic division proposed by Marques and Ferreira Filho (2003) was also observed in other segments, such as the Monte Alegre Sul and Várzea do Macaco,

located respectively circa 25 and 40 km north of the Ipueira underground mine (Fig. 1B) suggesting that all studied bodies are disrupted segments of a single intrusion (Marques et al. 2017).

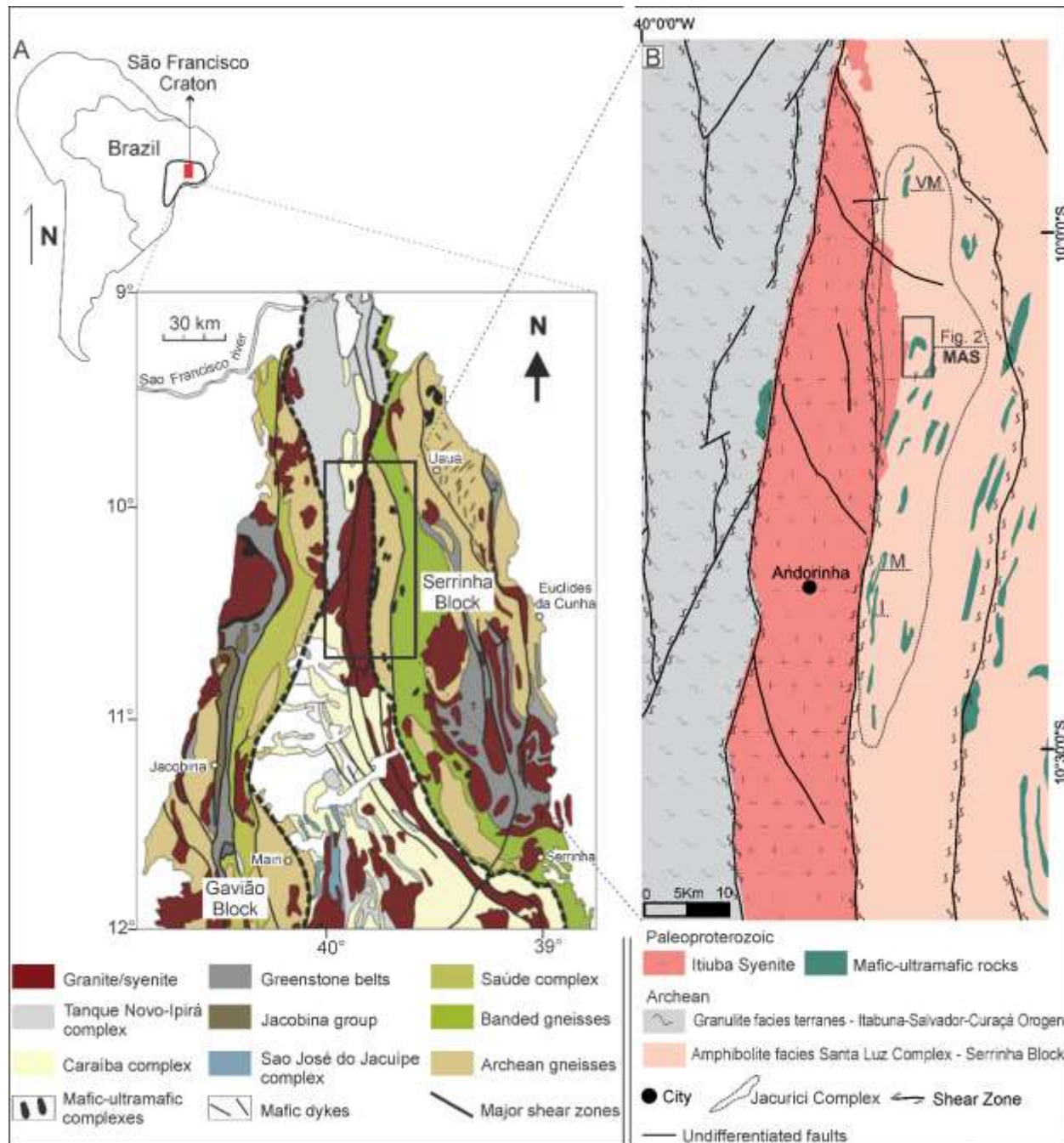


Figure 1. Geotectonic setting of the Jacurici Complex. A: North central portion of the São Francisco Craton, showing the location of the Jacurici Complex. Modified from Oliveira et al. (2010). B: Simplified geological map of the Jacurici Complex area. Mafic-ultramafic bodies within the dashed line are recognized as part of the Complex, the others are undifferentiated mafic-ultramafic bodies. The location of the Monte Alegre Sul segment and Figure 2 is highlighted, as well as of the Ipueira and Medrado segments (I-M) and Várzea do Macaco (VM) segment. Modified from Oliveira et al. (2016).

In the Monte Alegre Sul Segment, 8900t of chromite was mined from 1993 to 1995 from two different open pits with an average Cr<sub>2</sub>O<sub>3</sub> content of 35% (FERBASA, internal report). The mineralized layer varies in thickness but averages 5 m thick and occurs between 50 and 150 m below ground level (Marinho et al. 1986). The current calculated reserves occurring less than 100m deep is in the order of 600,000t but this is currently being reevaluated to include deposits up to 150 m deep (FERBASA, internal report).

## 2.1 PETROGENESIS OF THE COMPLEX AND CHROMITITE LAYERS

Considering the relative low solubility of chromium, Marques and Ferreira Filho (2003) observed that the total volume of silicate magma required for the formation of the MCL is not represented in the silicate sequence in the Jacurici Complex, leading to the suggestion that the magma chamber may have acted as a conduit through which large amounts of magma flowed. Based on mineral chemistry and isotopic data, Marques et al. (2003) proposed a model for chromitite formation considering crustal contamination in a conduit-like intrusion: the authors report more negative  $\varepsilon_{\text{Nd}}$  (mean -6.5) in the UUU where significantly larger amounts of intercumulus amphibole occur. Chromitite seams in the LUU, the MCL and the UUU record an up-stratigraphy increase in  $\gamma_{\text{Os}}$  values from -4.6 to +3. Both  $\varepsilon_{\text{Nd}}$  and  $\gamma_{\text{Os}}$  values are consistent with crustal contamination of a very high-Mg parental magma, probably originating from Archean, subcontinental, metasomatized, peridotitic lithospheric mantle. Ferreira Filho and Araujo (2009) provided a review of the chromite deposits in Brazil and suggested that assimilation of carbonate host rocks was a key factor for crystallization of chromite as a sole phase in the Jacurici Complex. Several different types of minerals were reported as inclusions in chromite from the MCL of the Jacurici Complex and are considered to provide additional evidence that the magma was hydrated during chromite crystallization (Marques et al. 2017). To explain the exceptional thickness of the chromitite, Marques et al. (2017) suggested a model in which chromite crystallized along the margins of the conduit and subsequently slumped downward into the magma chamber, producing the thick massive chromitite layer above the previously-formed dunite in the LUU.

## 3. SAMPLING AND ANALYTICAL METHODS

Several sections and mining fronts in the two open pits from the Monte Alegre Sul segment were mapped and sampled. For the purpose of this study, three drill cores were logged in detail and the core MAS-105-65° was selected for systematic sampling. Representative silicate samples and regular, closely spaced samples from the massive chromitite layer were collected. Thirty-five polished thin sections were made for transmitted and reflected light microscopy and mineral chemistry studies. Microchemical analyses of silicate rocks were carried out using a JEOL JXA-8230 electron microprobe at the Universidade de Brasília. For olivine and pyroxene, the equipment was operated at 15 kV accelerating potential and 20 nA current using a focused beam; for amphibole, 15 kV accelerating potential, 20 nA current and 2  $\mu\text{m}$  beam diameter. Natural and synthetic standards were used for calibration. Polished thin sections of chromitite were used to investigate textural relationships and mineral inclusions using a JEOL 6610-LV scanning electron microscope (SEM) equipped with an energy dispersive spectrometer (EDS) and a Bruker Nano

XFlash Detector 5030 at the Laboratório de Geologia Isotópica from the Universidade Federal do Rio Grande do Sul. The SEM was operated with 15 kV of acceleration potential and a 14 mm working distance. Wavelength dispersive analyses of selected inclusions of silicates and sulfides, as well as cumulus and intercumulus silicates, were performed using the JEOL JXA-8230 electron microprobe at Queen's University. All minerals were analyzed using a 15 kV accelerating potential. Olivine and pyroxenes were analyzed using a 20 nA beam current and fully focused beam. Amphiboles were analyzed using a 20 nA beam current and a 2  $\mu\text{m}$  spot size. For phlogopite, the beam current was 10 nA, and the beam was defocused to between 3.5 and 7  $\mu\text{m}$  depending on grain size. Chromite and sulfides were analyzed using 30 nA and 10 nA beam currents, respectively; the beam was fully focused. The generally fine-grained sulfides were analyzed at relatively low potential in an effort to prevent secondary fluorescence of enclosing or adjacent chromite. Peak and total background count times were 10-20 s for major elements and 30-60 s for minor elements. The standards used are listed in the supplementary materials in Table 16. Data reduction was performed using JEOL PC-EPMA software version 1.11.2.0. The XPP atomic number and absorption corrections of Pouchou and Pichoir (1991) were used in conjunction with mass absorption coefficients of Chantler (1995); characteristic fluorescence was treated according to the model of Reed (1965). Ferric iron content in chromite and pyroxenes was estimated by assuming a fixed number of oxygen anions and metal cations per formula unit. Ferric iron content of amphibole was assumed to be represented by the minimum stoichiometrically allowable value; in most cases, for the aluminous amphiboles, this resulted from normalization to 15 cations excluding  $\text{K}^+$  and  $\text{Na}^+$  (*i.e.*, all  $\text{Na}^+$  is placed on the A site; *cf.* Leake *et al.*, 1997, 2003). Analytical precision and detection limit were calculated according to expressions presented in Williams (1987). X-ray maps of chromite and adjacent minerals were collected using a 15 kV potential, 200 nA beam current, 0.5 or 1  $\mu\text{m}$  pixel size, and 30 ms dwell time.

## RESULTS

### 4.1 Geology of the Monte Alegre Sul (MAS) Segment

The MAS Segment is folded, metamorphosed and offset by a number of faults trending in three main directions: NW, NE and E-W (Fig. 2A). Exposure on surface is rare, mainly restricted to the two old open pits, and rocks at or close to the surface are weathered. Drilling reveals the main part of the complex down to the basal contact with the massive chromite layer. The MAS Segment is hosted by variably banded and deformed quartz-feldspathic gneiss. Further north, rocks similar to the basement gneiss were described as deformed monzogranite, and dated at  $2995 \pm 15\text{Ma}$  (U-Pb in zircon, Silveira *et al.* 2015). The stratigraphy of Monte Alegre Sul (Fig. 3) can be divided into an Ultramafic Zone and a Mafic Zone with the Ultramafic Zone further subdivided into a Lower Ultramafic Unit (LUU), the Main Chromitite Layer (MCL) and an Upper Ultramafic Unit (UUU), following the same division proposed by Marques and Ferreira Filho (2003) for the Ipueira and Medrado areas. The LUU in the MAS Segment has only its upper part recovered, being represented by serpentinized dunite. The MCL is almost 8 m thick and mainly composed of a massive (75 to 90 vol %) chromitite layer with an 80 cm thick, less massive (~50 vol %), basal part. The UUU is 35 m thick and is characterized by the predominance of orthopyroxenite with

interlayered lenses of olivine orthopyroxenite, harzburgite, websterite, olivine websterite, and a 1 m thick massive chromitite seam, with serpentinized dunite at the base. The Mafic Zone, on the top of the sequence, is represented by an up to 6 m thick, laterally discontinuous, highly sheared and weathered gabbronorite in tectonic contact with the basement. No petrographic or geochemical investigation of this interval was performed due to its poor degree of preservation. Despite the metamorphism, samples obtained from drill cores, especially those from the pyroxene-rich intervals and chromitite layers, preserved primary igneous minerals and textures which are described in the following section. The lithologies are named based only on cumulus mineral percentages.

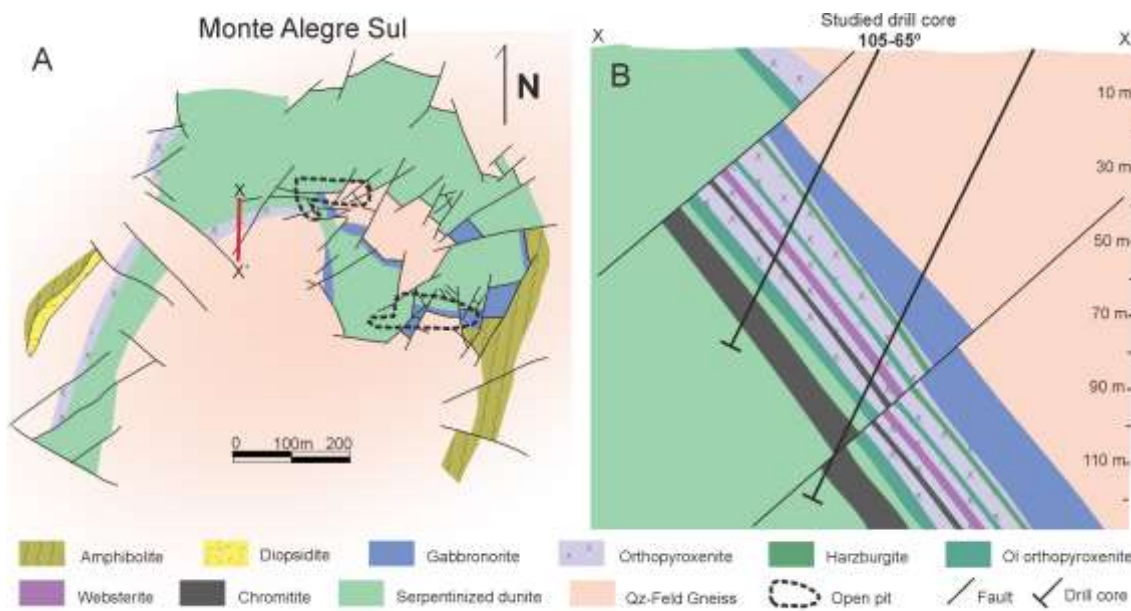


Figure 2: Geological setting of the Monte Alegre Sul segment (MAS). A: Geological map of MAS. The areas within dashed lines indicate the two old open pits (FERBASA Geology Division). B: Geological section of MAS (modified from FERBASA Geology Division, internal

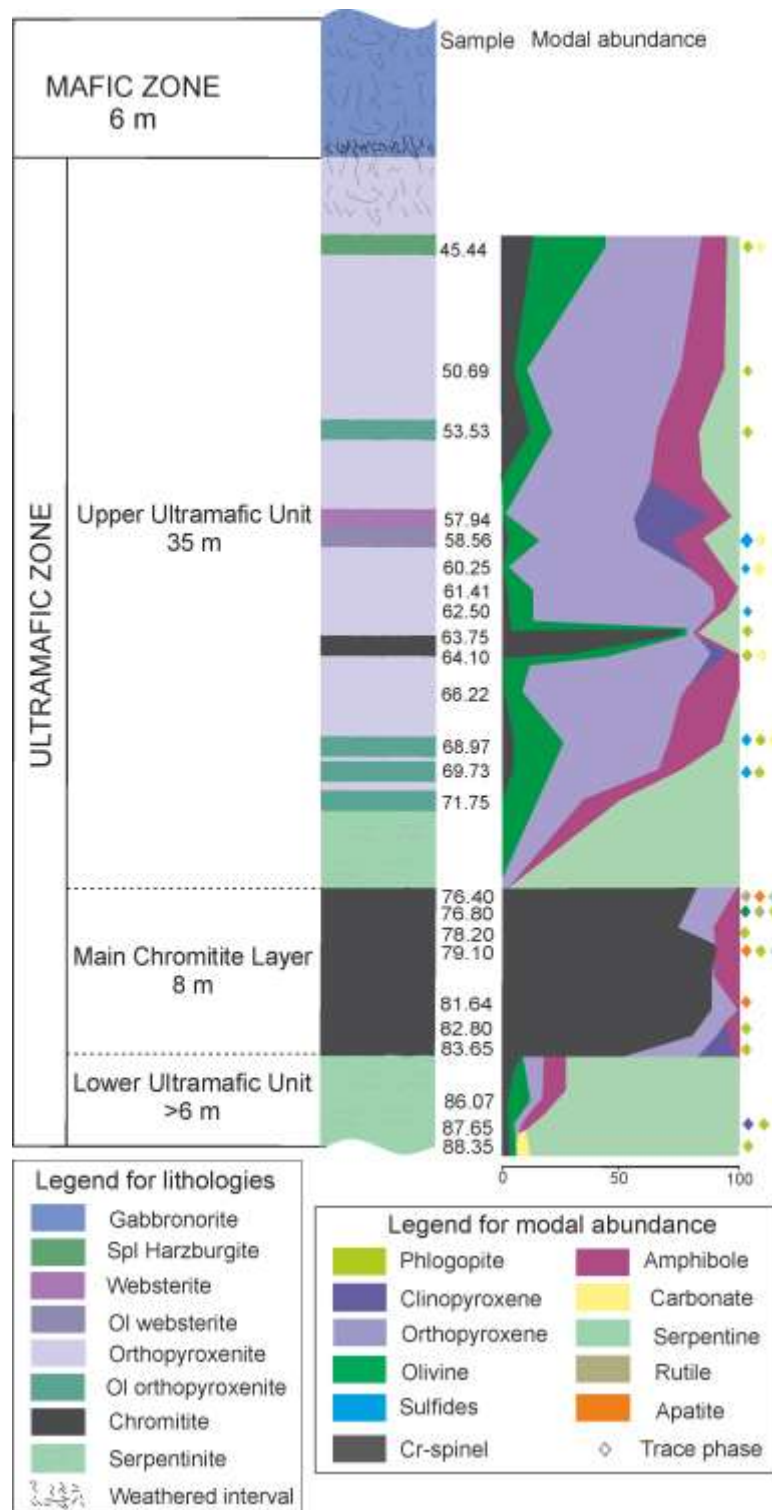


Figure 3: Schematic profile of the MAS105-65° drill core, showing the modal mineralogical abundance along stratigraphy and the cryptic variation of forsterite (Fo) and NiO contents in olivine, and enstatite (En) and Al<sub>2</sub>O<sub>3</sub> contents in orthopyroxene. Note that preserved olivine is rare and was not found in all samples.

#### 4.3 Mineralogical and textural relationships of the Lower and Upper Ultramafic Units

##### 4.3.1 Serpentinized dunite

Serpentinized dunite occurs in the LUU and in the basal part of the UUU, just above the MCL. Dunite samples are composed of 75 to 90 vol% pseudomorphic serpentine. The primary igneous textures are partially obliterated. Relicts of medium-grained cumulus-textured olivine and orthopyroxene are recognizable. Chromite occurs as fine-grained anhedral crystals and account for as much as 2 vol%. Preserved intercumulus material is comprised of amphibole (tschermakite) and minor phlogopite which increases toward the top of LUU where the orthopyroxene is also more abundant.

##### 4.3.2 Olivine orthopyroxenite

Olivine orthopyroxenite layers occur just above the dunite near the base of the UUU and near the central part of the UUU. Olivine orthopyroxenite (Fig. 4A) comprises orthopyroxene (60-85%), olivine (5-15%) and Cr-spinel (0-2%) as cumulus phases, and amphibole (5-20%) and phlogopite (1%) as intercumulus phases. Sulfides (pyrite, pyrrhotite, pentlandite and chalcopyrite) make up to 2% and occur interstitial to silicates. This rock commonly shows primary banding with laminae enriched in orthopyroxene and amphibole interlayered with laminae enriched in orthopyroxene plus Cr-spinel and olivine. In one specific interval, Cr-spinel accounts for as much as 12% of the rock (Fig. 4B). Preserved olivine occurs as up to 1 cm oikocrysts and as fine-grained (~0.5 mm) rounded crystals, but most of the crystals have been serpentized. Most of the orthopyroxene is sub-rounded, 0.3-0.6 mm in size, but may also occur as coarser oikocrystic grains. Cr-spinel grains are subhedral to anhedral ranging in size up to 1.3 mm, occurring as inclusions in orthopyroxene and olivine, and rarely hosting inclusions of orthopyroxene. In the upper part of the UUU, Cr-spinel is transformed into green Al-rich spinel, indicating metamorphic equilibration toward the top. Amphibole, identified as tschermakite, is 0.5-1 mm in size, exhibits typical intercumulus texture and is commonly oriented parallel to the banding. Phlogopite is usually fine-grained (0.2 mm), rarely forming 2 mm-sized crystals. Amphibole and phlogopite grains may show weak undulose extinction.

##### 4.3.3 Orthopyroxenite

Orthopyroxenite is the most abundant lithotype in the UUU. Orthopyroxene accounts for about 75 to 85 vol% and occurs as a cumulus phase, along with olivine (0-5 %), chromite (0-2%) and sulfides (<1%). Orthopyroxene forms mainly coarse-grained (up to 1.5 cm) oikocrystic grains, containing abundant inclusions of chromite, amphibole and olivine, or as fine-grained (0.3-0.6 mm) sub-rounded crystals. Olivine is rounded and reaches up to 3 mm in size. Chromite is usually subhedral to euhedral and 0.1-0.5 mm in size. Intercumulus material is green amphibole, associated with minor phlogopite. Amphibole (tschermakite to magnesiohornblende) representing 5 to 20 vol%, is typically 0.5-3 mm and its distribution is heterogeneous, even at a thin section scale (Fig. 4C). In zones of high strain deformation, orthopyroxene oikocrysts show undulose extinction, subgrain formation (Fig. 4D), deformed cleavage, and deformation lamellae. Olivine is highly fractured and partially transformed into iddingsite and serpentine along fractures.

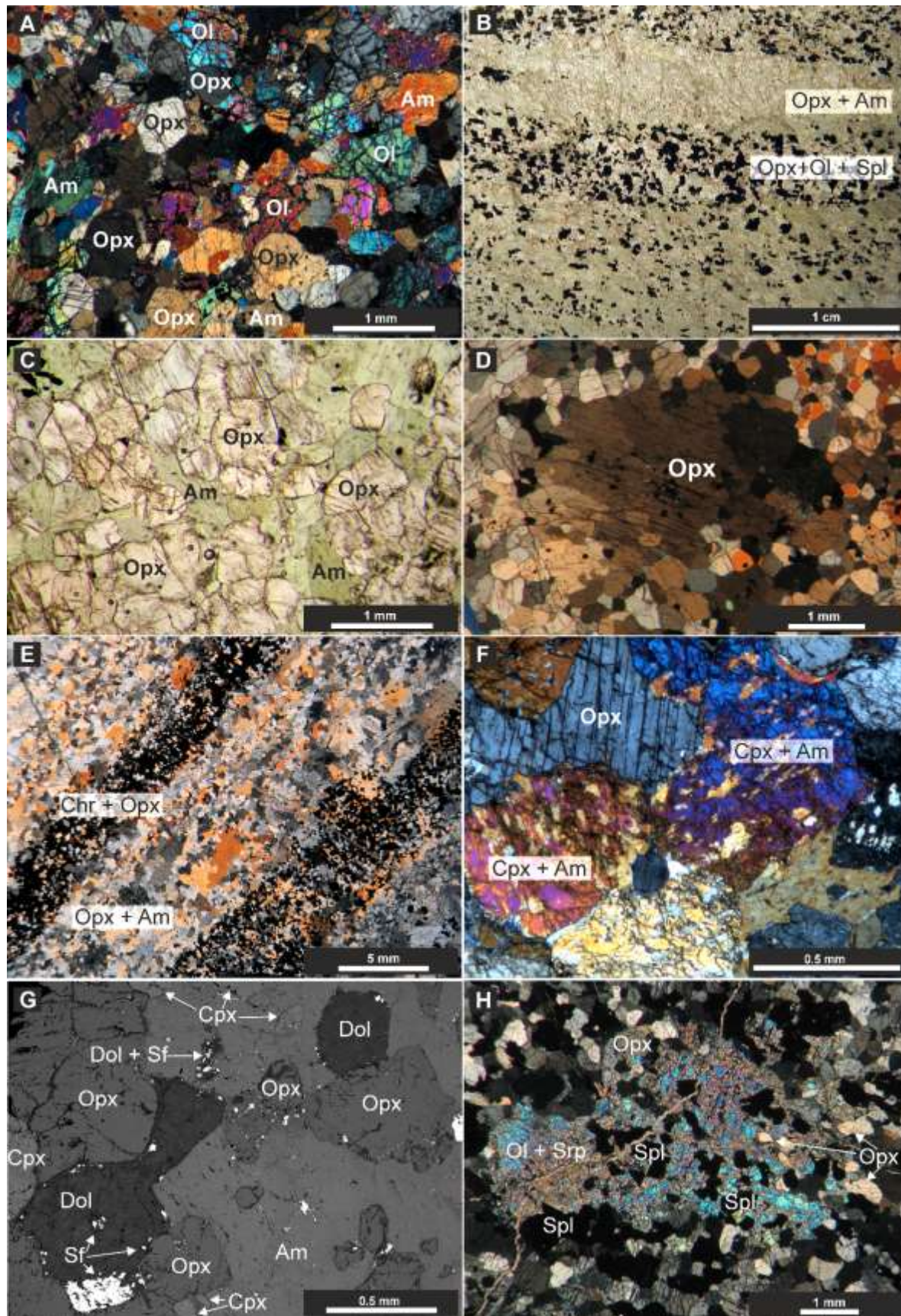


Figure 4: Transmitted light photomicrographs (A-F and H) and backscattered image (G) showing textural variation in rocks from the UUU. A: Olivine orthopyroxenite interval showing granular texture. B: Banding of spinel-rich olivine orthopyroxenite, marked by laminae composed mainly of orthopyroxene and amphibole with laminae enriched in olivine and green spinel. C: Orthopyroxenite showing heterogeneous distribution of intercumulus amphibole (magnesiohornblende). D: Poikilitic orthopyroxenite affected by metamorphism and deformation showing an orthopyroxene oikocryst grain with undulose extinction and subgrain formation. E: Layering in the basal portion of a chromitite seam in the UUU. F: Typical texture of websterite, with highly fractured clinopyroxene partially replaced by amphibole. G: Pockets containing dolomite and sulfides in the websterite interval. H: Olivine oikocrysts from the poikilitic harzburgite interval, showing abundant spinel and orthopyroxene inclusions.

#### 4.3.4 Chromitite seam

The 1-m-thick chromitite seam that occurs in the UUU comprises massive chromitite with a basal (about 10 cm thick) banded chromitite. The massive chromitite is made up of 75% of chromite, along with orthopyroxene (5%) and olivine, amphibole and phlogopite as minor phases. Interstitial minerals are affected by serpentinization. The basal banded interval (Fig 4E) is composed of interlayered 2-4 mm thick chromitiferous laminae (40-75% chromite and orthopyroxene) and 2-12 mm thick silicate laminae, which are composed mainly of orthopyroxene and amphibole, with minor chromite, clinopyroxene (diopsidite) and phlogopite. Chromite grains in this chromitite seam show mineral inclusions and textures similar to those in the MCL, which will be detailed in section 4.5.

#### 4.3.5 Olivine websterite and websterite

These rocks occur in the central part of the UUU, with olivine websterite in the lower part transitioning to websterite towards the top. These rocks are composed of orthopyroxene (35-45%), clinopyroxene (diopsidite) (10-36%), olivine (0-10%) and Cr-spinel (0-2%) as cumulus minerals with amphibole (tschermakite-magnesiohornblende) as an intercumulus mineral (15-25%). Both ortho- and clinopyroxene are fine-grained (0.5 mm), sub-rounded or adcumulate-textured. Intercumulus amphibole is also fine-grained (0.5 mm) and tends to be spatially associated with sulfides (1-3%). Undulose extinction in orthopyroxene and microfractures in clinopyroxene are observed in zones of high strain. Clinopyroxene is locally replaced by amphibole (magnesiohornblende-tremolite), which is interpreted to be metamorphic in origin (Fig. 4F).

A very common feature in these rocks is small (up to 1 mm) rounded or irregular-shaped carbonate-rich pockets (Fig. 4G). Most of these pockets are affected by subsequent replacement by low temperature minerals, but when preserved, they are totally or partially filled with dolomite crystals up to 0.1 mm in size and commonly contain sulfide crystals (pyrite, pyrrhotite, pentlandite and chalcopyrite), which can form sulfide aggregates (Fig. 4G). Although these carbonate-rich pockets are especially common in the websterite - olivine websterite interval, they can be found in all silicate rocks from the UUU.

#### 4.3.6 Spinel Harzburgite

One interval of spinel harzburgite occurs close to the upper part of the UUU (Fig. 3). It contains about 35% orthopyroxene, 30% olivine and 15% Cr-spinel as cumulus minerals, with amphibole (15%) and minor phlogopite as intercumulus phases. Olivine in this interval is oikocrystic (up to 7 mm in size) and contains numerous inclusions of spinel and orthopyroxene

(Fig. 4H). In contrast, orthopyroxene is fine-grained (0.5 mm), rounded or adcumulate, depending on the abundance of intercumulus material, and rarely host inclusions. Cr-spinels are 1 to 2 mm in size, commonly occur connected along an axis and may contain inclusions of orthopyroxene. Amphibole ranges from 0.5 to 1 mm and shows undulose extinction. Cr-spinels are altered into green spinels with exsolutions of magnetite.

#### Mineralogical and textural relationships of the Main Chromitite Layer

The MCL shows internal layering with distinct textures and variable proportions of chromite and intercumulus minerals as illustrated in Figure 5A. It comprises mainly massive layers containing 70-90 vol% of chromite (Fig. 5B), however the basal layer (80 cm-thick) contains approximately 50-60 vol% chromite, and is hereafter referred to as the “semi-massive interval” (Fig. 5C). Basal and top intervals are mainly adcumulate, showing virtually no intercumulus material, while the central intervals contain up to 10 vol% intercumulus amphibole (magnesiohornblende - Fig. 5A and G). The basal contact is gradual, starting as centimeter-thick disseminated chromitite laminae in dunite with an upward increase in chromite content, and the upper contact is abrupt and irregular, resembling a truncated surface.

Chromite granulometry varies from 0.02 mm to 0.8 mm, with a modal grain size in 0.2-0.4 mm. Most of the grains are subhedral (Fig. 5D), but the finer grains are usually anhedral. Euhedral crystals are rare, found mainly in the uppermost part (sample 76.40 – Fig. 5E). Chromite hosts abundant mineral inclusions, which will be detailed in the next section. Annealed chromite grains contain interstitial minerals that mark the limits of previous smaller grains.

Orthopyroxene is the second most abundant cumulus phase. At the basal semi-massive interval, it occurs as up to 5 mm oikocrysts enclosing dozens of chromite grains (Fig. 5F). Oikocrysts of orthopyroxene decrease in size and abundance upwards, where fine-grained crystals are more abundant as the cumulus silicate phase (Fig. 5D). In the central portion of the MCL, orthopyroxene becomes almost absent and chromite occurs enclosed in magmatic amphibole (Fig. 5G). Above this interval, orthopyroxene occurs as both oikocrysts and granular crystals grading upwards to granular textured crystals. Sub-grains are locally observed along the borders of the oikocrysts.

Clinopyroxene (diopside) is abundant in the basal semi-massive interval and forms oikocrysts up to 5 mm in size (Fig. 5F), and is partially replaced by metamorphic amphibole along grain margins and fractures (Fig. 5H). Olivine is rare and only found in the upper part of the MCL. Rutile is also a minor phase in this upper interval (Fig. 5E), and occurs in trace amounts close to the base. Zircon grains (5-30 µm) are zoned, tend to be rounded or oval-shaped, and commonly occur in the contact between orthopyroxene and chromite (Fig. 5I) or in the contact between chromite and intercumulus phlogopite and amphibole and rarely semi-included in chromite rims or in annealed grains.

Phlogopite occurs in almost all samples as inclusions in chromite or orthopyroxene and as intercumulus minerals (Fig. 5J). Hydroxyapatite commonly rimmed by chlorapatite (Fig. 5K) is

found as an interstitial phase along the MCL, but these minerals also occur as interdigitated or isolated crystals.

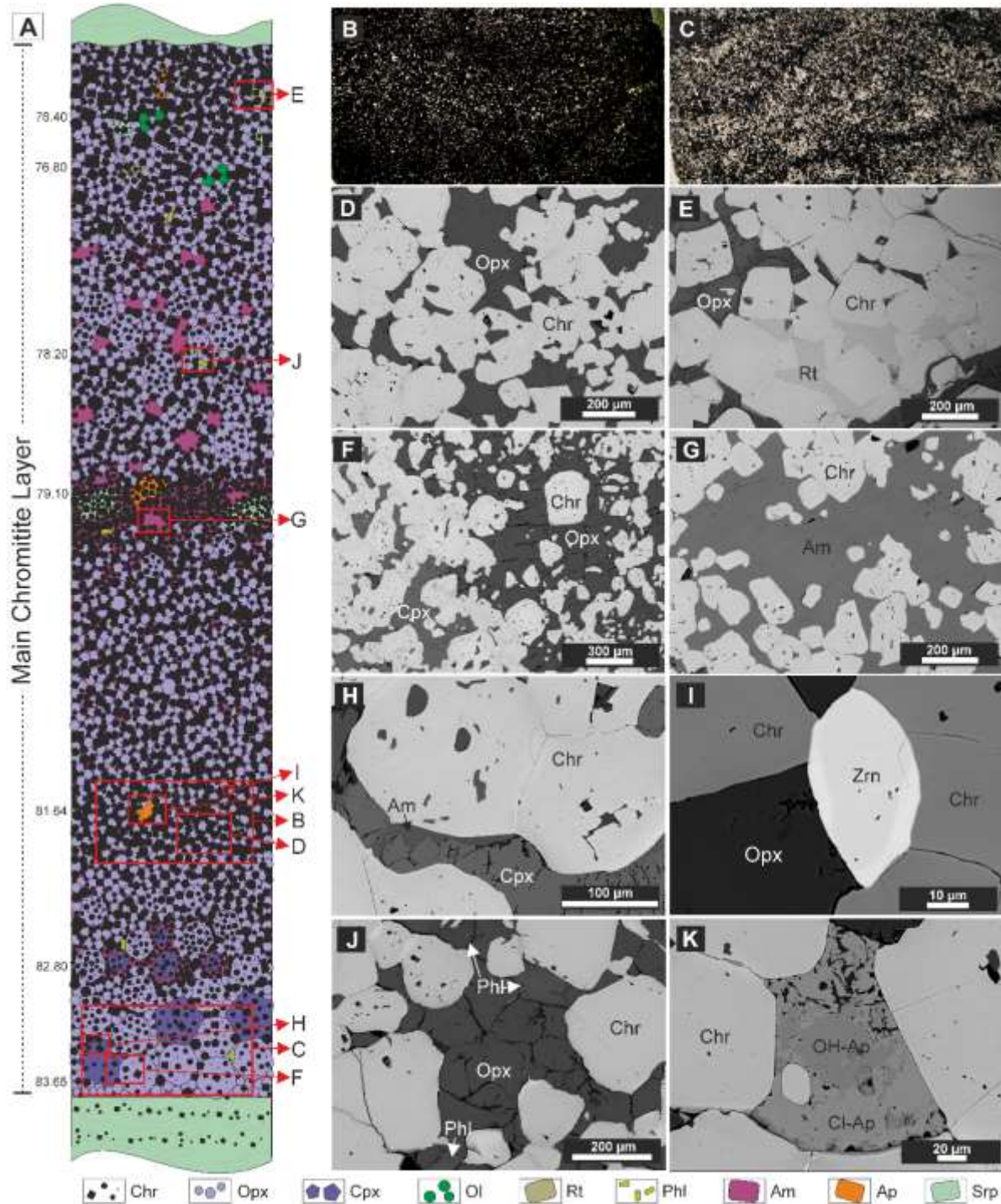


Figure 5: A: Schematic profile of the Main Chromitite Layer. The proportion of chromite to other minerals is modified to better characterize variation in mineralogy and textures of silicates. B: Typical massive chromitite. C: Basal semi-massive chromitite. D: Typical assemblage of chromite with granular orthopyroxene. E: Euhedral chromite grains and intercumulus rutile of the

uppermost interval. F: Oikocrysts of ortho- and clinopyroxene in the basal sample. G: Intercumulus amphibole (magnesiohornblende). H. Clinopyroxene oikocryst being transformed into amphibole (magnesiohornblende-tremolite) along the border of the grain. I Intercumulus zircon in the contact of orthopyroxene with chromite. J: Intercumulus phlogopite. K: Intercumulus hydroxyapatite rimmed by chlorapatite.

Magnesiohornblende (up to 10 vol% Fig. 5A and G) occurs mainly as intercumulus amphibole in the central intervals, and as a minor phase in the basal semi-massive interval (sample 83.65) replacing diopside. Tremolite is more common in areas where the replacement is more pervasive.

Pentlandite, millerite and minor heazlewoodite occur in trace amounts interstitial to chromite. Interstitial sulfides are mostly associated with serpentinized grains, and less commonly as inclusions in preserved ortho- and clinopyroxene and intercumulus amphibole.

Tiny grains of barite and galena (<5 µm) may occur in association with serpentine and minor chlorite where interstitial silicates are affected by alteration. Calcite and dolomite veinlets (1-2 mm thick) crosscut the chromitite with no preferential direction.

#### 4.5 Mineral inclusions in chromite

Mineral inclusions in chromite are abundant along the entire Main Chromitite Layer (Figures 6, 7 and 8). In the massive intervals about 70% of the chromite crystals host at least one inclusion. In the semi-massive interval, at the base of the MCL, 90% or more of the chromite grains contain mineral inclusions. The occurrence of inclusion-bearing grains side-by-side with inclusion-free grains is very common (Fig. 6A). In inclusion-rich chromite grains, inclusions may represent up to 15-20% of the host mineral surface. Inclusions are commonly isolated within the host chromite grain, and can reach up to 70 µm but with the majority ranging from 5-20 µm. Most of the inclusions are randomly distributed, but they can be either oriented parallel to the crystallographic axes of the host chromite (Fig. 6B) or spirally oriented (Fig. 6C). Inclusions also form internal coronas, following the chromite growth zones (Fig. 6D), or they are concentrated in the core of the host crystal, with an outer inclusion-free rim (Fig. 6E). Their compositions and textures are described below.

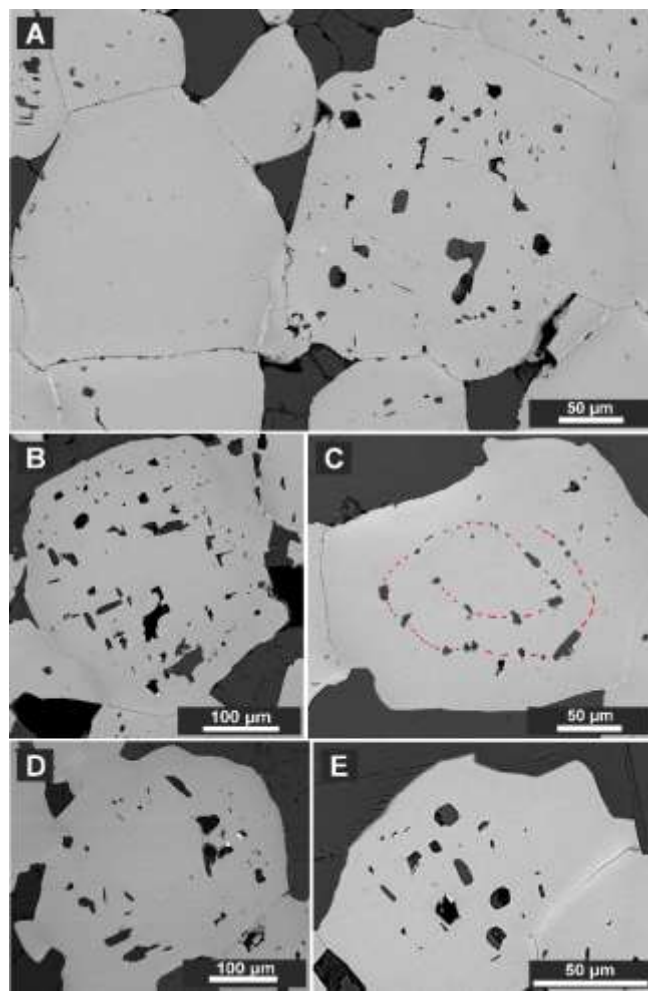


Figure 6: Textures of chromite-bearing inclusions. A: Inclusion-free chromite grain coexisting with inclusion-bearing chromite. B: Inclusions oriented parallel to crystallographic axes of the host chromite. C: Inclusions spirally oriented. D: Inclusions forming an internal corona, along chromite growth zone. E: Inclusions concentrated in the center of the host chromite.

#### 4.5.1 Silicate inclusions

Silicates are the most abundant type of mineral enclosed in chromite. Most of the silicate inclusions consist of a single phase, and comprise orthopyroxene, amphibole, phlogopite, clinopyroxene, and olivine in decreasing order of abundance. Orthopyroxene, amphibole and phlogopite inclusions occur in all samples, whereas clinopyroxene inclusions were only found at the base of the layer (sample 83.65) and olivine inclusions were only identified at the top of the sequence (sample 76.80), where these phases also occur as cumulus minerals. Semi-included zircon grains also occur. Olivine and orthopyroxene inclusions are mainly rounded or somewhat irregular (Fig. 7A); orthopyroxene also occurs as euhedral short prisms (Fig. 7B). Only one microprobe analysis of an olivine inclusion (Fo 96.4) was possible due to its scarcity and generally small size (<10 μm). In contrast, inclusions of orthopyroxene (En 92.6-95.1) are the most common silicate inclusions and tend to be larger (<30 μm) and consequently more suitable for analysis. Amphibole inclusions (magnesiohornblende) occur as mainly irregular or subhedral prismatic

grains (Fig. 7C and D) and tend to be larger and more abundant in the basal interval (samples 81.64 and 83.65) where there is virtually no amphibole as an intercumulus mineral. Phlogopite inclusions are common in all samples, and exhibit euhedral to subhedral prismatic habit (Fig. 7E and F). They are often too small ( $<10\text{ }\mu\text{m}$ ) for reliable microanalysis in the massive intervals, whereas in the basal semi-massive interval (sample 83.65), phlogopite inclusions are larger ( $<40\text{ }\mu\text{m}$ ) and more abundant. Clinopyroxene (diopside: Wo48.6En48.5Fs2.9) inclusions occur solely in the semi-massive interval, as oval, rounded or irregular isolated crystals (Fig. 7C) or in association with amphibole.

Orthopyroxene and amphibole inclusions are found in annealing contacts among chromite grains (Fig. 8A, B). Chlorite  $\pm$  serpentine ( $<1\text{ }\mu\text{m}$ ) occur along parallel trails. These are considered post-magmatic inclusions.

#### 4.5.2 Carbonate inclusions

Carbonates are the second most abundant type of mineral inclusion, comprising magnesite, dolomite and calcite, in order of abundance. Calcite is rare, only found in the central intervals. Carbonate inclusions occur in highly irregular (Fig. 7D) or negative-crystal shapes (Fig. 7G and H), and dolomite and magnesite commonly occur as composite inclusions, sometimes with concentric zoning (Fig. 7G and H). Carbonates are commonly associated with sulfides (Fig. 7I), and, to a lesser degree, with oxides and silicates (enstatite, phlogopite and magnesiohornblende). Carbonate inclusions may produce thin reaction halos in the host chromite, which are poorer in iron and chromium and richer in aluminum, compared to non-altered chromite.

#### 4.5.3 Sulfide inclusions

Sulfide inclusions ( $<70\text{ }\mu\text{m}$ ) comprise mainly pentlandite, millerite and heazlewoodite; polydymite, pyrite and chalcopyrite are less common phases and occur as very small grains. Most of these inclusions have hexagonal/pseudohexagonal outlines (Fig. 7F, I, K and L) or irregular shapes (Fig. 7J), and are commonly associated with carbonate or hydrous silicate inclusions along the entire MCL (Fig. 7F, I, J). Sulfide inclusions may occur mantling fine-grained chromite grains (Fig. 7L) in chromite cumulus. Although sulfide inclusions are usually composed of at least two sulfide minerals, pentlandite and more rarely heazlewoodite occur as single phase inclusions. The bulk of the polymimetic sulfide inclusions comprise pentlandite (Fig. F, I and J), followed by millerite (Fig. K and L), and, less frequently, heazlewoodite. In inclusions dominated by Ni-sulfides, the contact between pentlandite and millerite or pentlandite and heazlewoodite is usually irregular. Where pentlandite is the major phase, millerite and heazlewoodite usually occur in flame-like textures (Fig. 7 I and J). Millerite and heazlewoodite show diffuse contacts and commonly occur interdigitated (Fig. 7J). Contacts between polydymite and millerite or polydymite and pentlandite are irregular to sharp (Fig. 7K). Pyrite and chalcopyrite only occur as minor exsolved phases within composite inclusions. Pyrite is found as spots within Ni-sulfides (Fig. 7K and L), and may also occur as oriented sub- to euhedral crystals (Fig. 7K). Chalcopyrite is located at one margin of the inclusion walls, and typically shows sharp contacts with other phases (Fig. 7L).

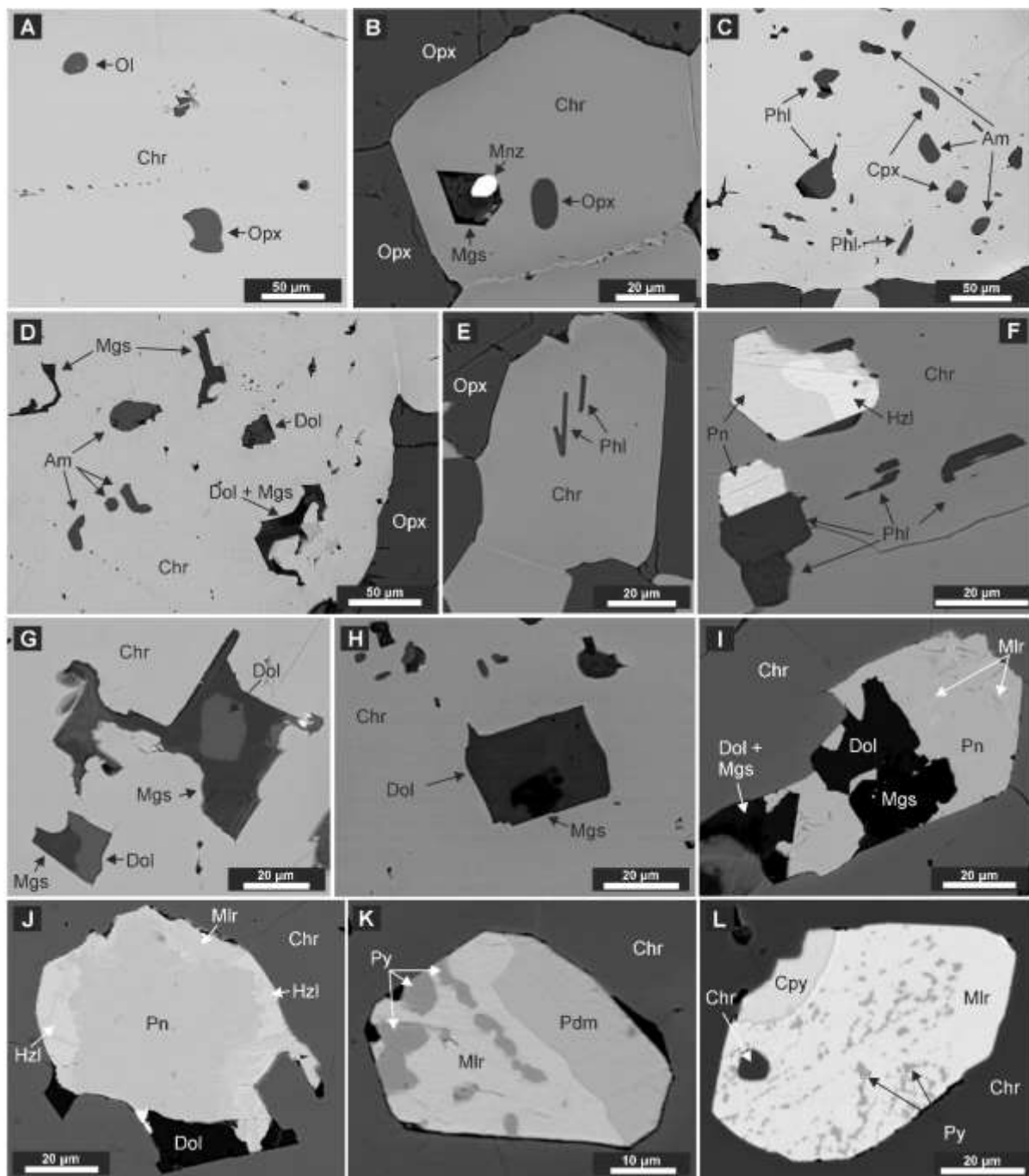


Figure 7: Types of mineral inclusions trapped in chromite. A: Rounded olivine and irregular orthopyroxene. B: Monazite and magnesite composite inclusion and orthopyroxene prism. C: Irregular and prismatic phlogopite and amphibole, and irregular clinopyroxene inclusions. D: Irregular crystals and hexagonal basal section of amphibole and highly irregular carbonate inclusions. E: Prismatic phlogopite grains. F: Euhehedral phlogopite inclusions in association with pentlandite and heazlewoodite. G, H: Negative crystal-shaped composite carbonate inclusions (magnesite+ dolomite). I, J: Sulfide and carbonate inclusions; sulfide is pentlandite with (I) minor exsolution of millerite and (J) minor millerite plus heazlewoodite. K: Sulfide inclusion with millerite and exsolution of polydymite and pyrite. L: Millerite sulfide inclusion with exsolution of pyrite, chalcopyrite after iss, and inclusion of chromite. Am: amphibole; Cpx: clinopyroxene; Cpy: chalcopyrite; Dol: dolomite; Hzl: heazlewoodite; Mgs: magnesite; Mir: millerite; Mnz: monazite; Ol: olivine; Opx: orthopyroxene; Pdm: polydymite; Phl: phlogopite; Pn: pentlandite; Py: pyrite.

Some rare secondary pyrrhotite occurs in inclusions showing multiple cracks, and is spatially related to serpentinized interstitial minerals. These are interpreted to be formed by later, post-magmatic processes.

#### 4.5.4 Other mineral inclusions

Other minor mineral phases included in chromite comprise rutile, barite, apatite, monazite and scheelite. Rutile inclusions are found in the upper interval where it is also a minor intercumulus mineral. Rare barite inclusions ( $5\text{ }\mu\text{m}$  or less) occur isolated in chromite or in association with Ni-sulfides, amphibole or carbonates. Barite is also included in unaltered cumulus orthopyroxene, confirming that it is a primary inclusion. Two apatite grains ( $25\text{ }\mu\text{m}$  and  $6\text{ }\mu\text{m}$  across), one scheelite and one monazite inclusion in association with magnesite (Fig. 7B) were also identified within chromite.

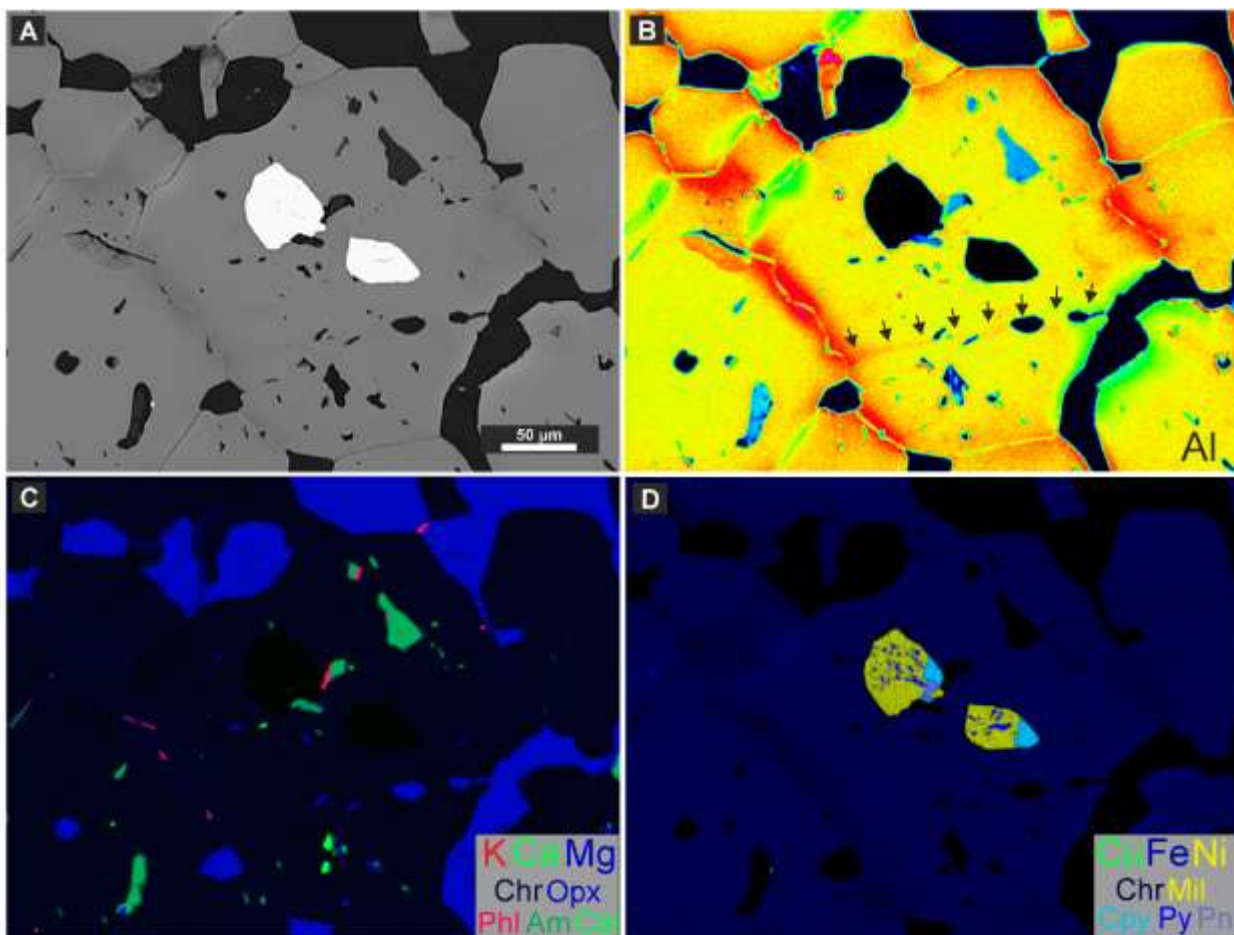


Figure 8: Element maps of chromite grains containing silicate, sulfide and carbonate inclusions. A: Electron backscattered image of analyzed field. B: Element map for Al; arrows indicate secondary inclusions trapped by annealing of grains. C: Composite element map enhancing silicate and carbonate inclusions. D: Composite element map highlighting sulfide inclusions. Abbreviations are the same as Figure 7. Cal: calcite.

## 4.6 Mineral chemistry

### 4.6.1 Cryptic variation of silicate rocks

Systematic analyses of pyroxene, olivine and amphibole from the rocks of the UUU and LUU were performed and representative results are shown in Tables 1 to 3 with the full dataset available in the Supplementary Materials. Figure 9 shows the cryptic variations for olivine and orthopyroxene.

The forsterite content in olivine varies from 86.6 to 90.2 and the enstatite content of orthopyroxene varies from 84.4 to 89. The highest Fo values occur just below the MCL and above the chromitite seam in the UUU, following the same trend shown by orthopyroxene, whose highest En values occur immediately below the MCL and below and above the chromitite seam in the UUU. NiO content in olivine varies from 0.06 to 0.56 wt. % following a positive correlation with Fo content. The Al<sub>2</sub>O<sub>3</sub> content in orthopyroxene (0.7-3.6 wt. %) shows an inverse correlation with En content.

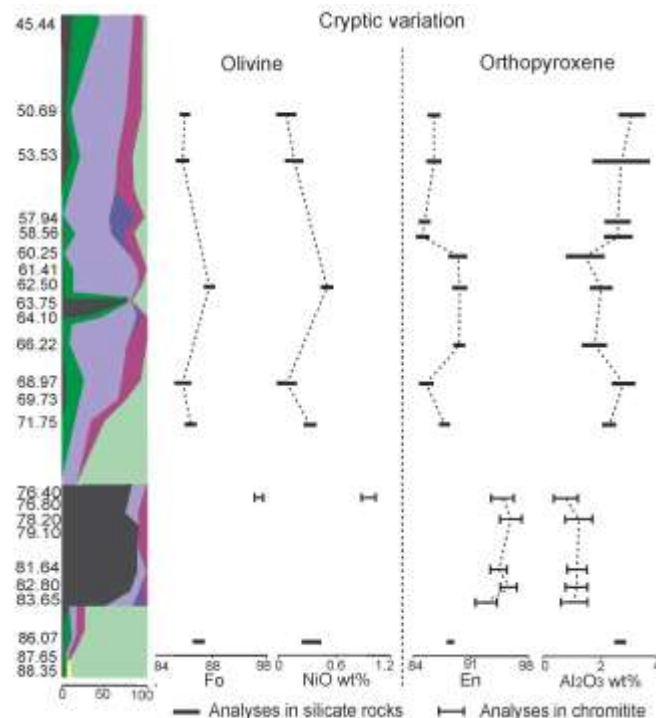


Figure 9: Cryptic variation of olivine and orthopyroxene along the drill core MAS-105-65°, showing consistent variation of Fo tenor and NiO in olivine and Al<sub>2</sub>O<sub>3</sub> and En content in orthopyroxene. Each bar represent 4 to 9 analyses in olivine and 6 to 24 analyses in orthopyroxene (except in sample 86.07, where only 2 orthopyroxene analyses were obtained).

### 4.6.2 Mineral chemistry of the Main Chromitite Layer

Microprobe profiles across inclusion-bearing and inclusion-free chromite grains were collected for comparison. Microanalyses of chromite-hosted inclusions and of cumulus and

intercumulus silicates of the MCL were performed in order to compare their chemistry throughout the stratigraphy. Sulfide inclusions and interstitial minerals were also analyzed. Care was taken while analyzing mineral inclusions to avoid fractures and interference from the host chromite. Representative analyses are available in Tables 4 to 8 and the full dataset is provided in the Supplementary Materials.

Both inclusion-free and inclusion-bearing chromite types show similar chemistry when comparing grains from the same stratigraphic interval. They show homogeneous compositions throughout the grains with minor disturbances only at some borders (Fig. 10), interpreted as subsolidus or low temperature local reequilibration.

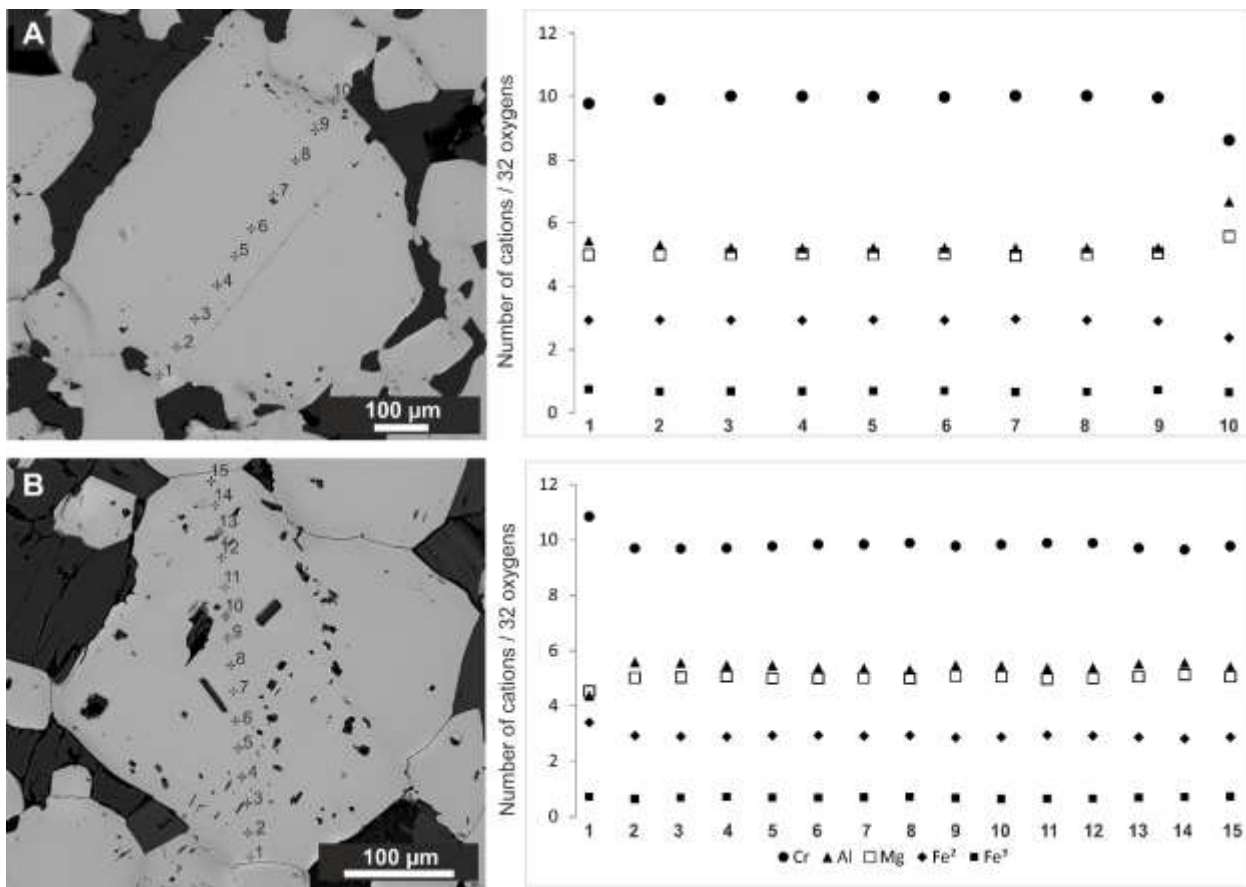


Figure 10: Line traverses comparing mineral chemistry of inclusion-free (A) and inclusion-bearing (B) chromite grains.

Orthopyroxene occurring as inclusions, cumulus granular grains and oikocrysts are all enstatite, and all clinopyroxene inclusions and oikocrysts are diopside (Fig 11A). However, orthopyroxene has a distinct composition in the basal semi-massive interval compared to the massive interval. As shown in Figure 11B, the basal interval (sample 83.65) shows lower En contents for both oikocrysts and orthopyroxene inclusions compared to all other intervals from the MCL. Within the massive intervals, oikocrysts are chemically similar to granular orthopyroxene (Fig 11B). Enstatite inclusions show enrichment in Cr and depletion in Al compared to cumulus enstatite, leading to a higher Cr/ (Cr+Al+Fe<sup>3+</sup>) ratio in the inclusions (Fig. 11B). Diopside

inclusions also show a higher Cr/(Cr+Al+Fe<sup>3+</sup>) ratio (Fig. 11C) and lower Ca and Ti contents (Fig. 11D) compared to the diopside oikocrysts.

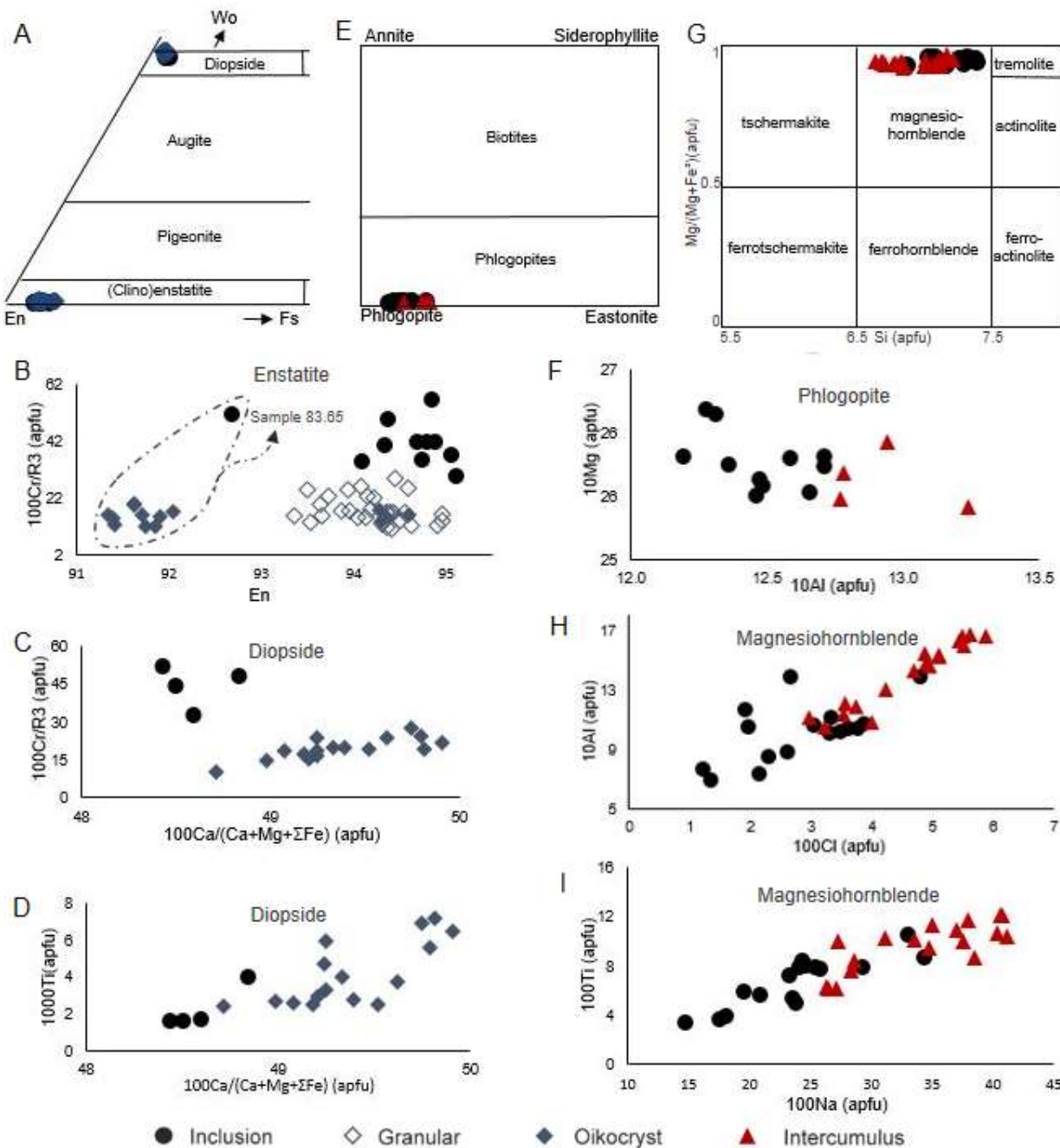


Figure 11: Mineral chemistry of chromite-hosted silicate inclusions, cumulus and intercumulus minerals in the MCL. A: Pyroxene classification diagram (Morimoto 1989). B: En content X  $100\text{Cr}/R3$  diagram for orthopyroxene, showing that inclusions are richer in Cr compared to granular and oikocryst orthopyroxene ( $R3 = \text{Cr}+\text{Al}+\text{Fe}^{3+}$ ); orthopyroxene from the basal interval shows lower En content than the massive interval. C and D:  $100\text{Ca}/(\text{Ca}+\text{Mg}+\Sigma\text{Fe}^{3+})$  X  $100\text{Cr}/R3$  and  $100\text{Ca}/(\text{Ca}+\text{Mg}+\Sigma\text{Fe}^{3+})$  X  $1000\text{Ti}$  diagrams for clinopyroxene, showing that clinopyroxene oikocrysts are enriched in Ca and Ti and have lower Cr compared to the inclusions. E: Phlogopite classification diagram (Bailey 1984), showing intercumulus phlogopite tend to be richer in the eastonite member. F:  $10\text{Al}$  X  $10\text{Mg}$  diagram for phlogopite, showing intercumulus grains are richer in Al and have a tendency to be

slightly poorer in Mg. Amphibole classification diagram (Leake et al. 1997), showing that all magmatic amphiboles classify as magnesiohornblende. H and I:  $100^*\text{Cl} \times 10^*\text{Al}$  and  $100^*\text{Na} \times 100^*\text{Ti}$  diagrams for magmatic amphibole, showing that intercumulus amphibole tend to be richer in Cl, Al, Na and Ti compared to the inclusions.

Intercumulus phlogopite is enriched in the eastonite member ( $\text{Al}$  in octahedral site/ $\text{Mg}$ ) (Fig 11E), reflecting an enrichment in  $\text{Al}$  and a slight depletion in  $\text{Mg}$  when compared to phlogopite inclusions (Fig. 11F). Amphibole inclusions and magmatic intercumulus amphiboles are classified as magnesiohornblende (Fig. 11G). Intercumulus amphibole contains, in general, more  $\text{Cl}$ ,  $\text{Al}$ ,  $\text{Na}$  and  $\text{Ti}$  compared to amphibole inclusions in chromite (Fig. 11H and I). Metamorphic amphibole is classified as a transition from magnesiohornblende to tremolite (Fig. 12A). It contains more  $\text{Ca}$ , less  $\text{Cr}$  and slightly less  $\text{K}$  when compared to magmatic amphiboles (Fig. 12B).

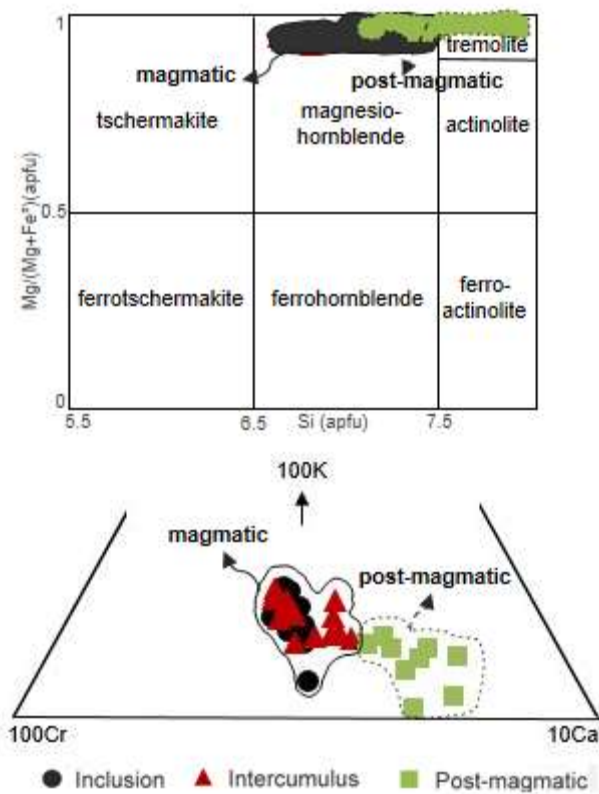


Figure 12: Chemical comparison of primary and post-magmatic amphiboles. A: Amphibole classification diagram (Leake et al. 1997) showing magmatic amphibole classified as magnesiohornblende, and metamorphic amphibole transitioning from magnesiohornblende to tremolite. B: In a K-Cr-Ca ternary diagram, showing the fields of magmatic and metamorphic amphibole.

Note that only enstatite and diopside inclusions are enriched in Cr compared to the respective interstitial minerals. It is interpreted not to be an analytical effect caused by fluorescence of Cr from host chromite, considering other types of inclusions do not show Cr enrichment.

The MCL shows slight internal chemical variation with stratigraphy. The chemical variation of cumulus chromite and orthopyroxene, as well as inclusions of pentlandite is shown in Figure 13. En content in cumulus orthopyroxene varies from 91.1 to 95, and Fo content in olivine

from 96.2 to 96. The MCL shows a general upward increase in enstatite content with a slight decrease in the uppermost sample (Fig. 13). The  $\text{Al}_2\text{O}_3$  content in orthopyroxene (0.46-1.63) shows an inverse correlation with enstatite content.

The basal interval has more distinct compositions compared to the rest of the layer with lower  $\text{MgO}$ ,  $\text{Cr}_2\text{O}_3$  and  $\text{Al}_2\text{O}_3$  and higher total Fe in chromite, and lower En content in orthopyroxene.  $\text{TiO}_2$  contents in both chromite and enstatite are very low and do not show any particular trend. Chromite-hosted pentlandite inclusions show the lowest Ni ratio ( $100\text{Ni}/(\text{Ni}+\text{Fe})$ ) and highest Co content in the basal interval.

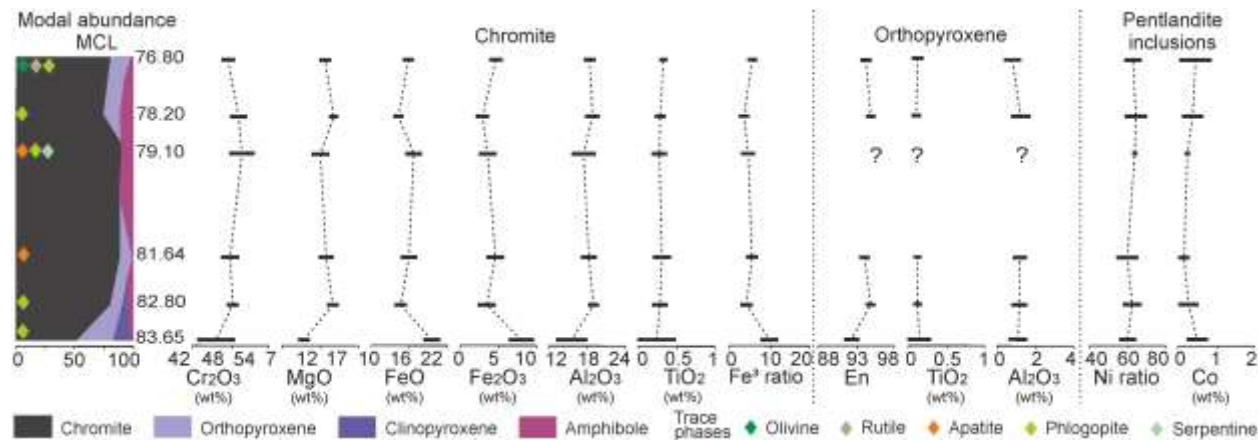


Figure 13: Cryptic variation of chromite, cumulus orthopyroxene and pentlandite inclusions in chromite from the MCL. Each bar represents 10 to 18 analyses in chromite, 5 to 20 analyses in orthopyroxene, and 5 to 11 analyses in pentlandite (except in sample 79.10, where only 1 analysis was obtained). Data from chromite in cryptic variation are from Marques et al. (2017).

## DISCUSSION

### 5.1 The crystallization timeline of the MCL at the Monte Alegre Sul Segment

The abundant and varied types of minerals found enclosed in chromite raises the question of whether they were trapped as melt that crystallized after cooling, or as previously crystallized minerals. Before any attempt is made to organize a crystallization order for the MCL, it is important to understand this issue.

Regarding silicates, the single-phase character of most inclusions and the common sub- to euhedral habits of the silicate inclusions in chromite point to entrapment as previously crystallized minerals rather than melt as the likely mechanism. Melt inclusions usually crystallize into more than one mineral phase upon cooling, leading to compound silicate inclusions with preferentially rounded or negative-crystal shapes (e.g. McDonald 1965, Irvine 1975, Spandler et al. 2005).

Cumulus and intercumulus silicates are slightly enriched in lighter and more incompatible elements compared to chromite-hosted silicate inclusions (Fig. 11). This is consistent with the inclusion silicates having crystallized earliest, from a more primitive magma, and for the cumulus and intercumulus phases to have crystallized during subsequent stages from a magma undergoing

fractional crystallization and magmatic differentiation. Cr enrichment in ortho- and clinopyroxene inclusions compared to the respective cumulus minerals (Fig. 11B and C) indicates that they crystallized before any substantial Cr extraction from the magma, i.e., before extensive chromite crystallization. The chemical composition variation is consistent with a scenario in which most silicate inclusions represent minerals that crystallized prior to or coeval with chromite, and the cumulus and intercumulus phases crystallized after the main stage of chromite formation.

In contrast to the commonly prismatic shapes of silicate inclusions, carbonate inclusions have highly irregular, rounded or negative-crystal shapes suggesting entrapment as droplets of a carbonate-rich melt phase, which subsequently crystallized as magnesite, dolomite and calcite. As for the sulfides, the hexagonal/pseudohexagonal shape of the sulfide inclusions suggest that at least part of them were entrapped as a crystallized mss; however the irregular sulfide inclusions may have been entrapped as sulfide droplets revealing a possible contemporaneity of sulfide immiscibility and crystallization of mss and chromite. Subsequent cooling of the system led to recrystallization of mss into the observed sulfide assemblage (pentlandite, pyrite, heazlewoodite, millerite, polydymite) and exsolution of an intermediate solid solution (iss), which further recrystallized into chalcopyrite.

As for the other inclusions in chromite such as rutile, barite, apatite, monazite and scheelite it is still unclear if all crystallized from the magma or if they might have been incorporated as xenocrysts. The occurrence of rutile and apatite as late magmatic intercumulus minerals is suggestive of crystallization of these phases from the magma.

After addressing the nature of the mineral inclusions, it is possible to propose a magmatic crystallization order for the Main Chromitite Layer from the Monte Alegre Sul Segment (Fig. 14). The silicate minerals found in chromite (enstatite, magnesiohornblende, phlogopite, diopsidite and olivine) were already crystallized or still crystallizing during chromite formation, and mss, sulfide melt and carbonate melt coexisted with chromite during its crystallization. Olivine, enstatite and diopsidite continued crystallizing during chromite formation as cumulus phases while phlogopite and magnesiohornblende occur either as inclusions or as intercumulus minerals suggesting two different crystallization stages. Mineral chemistry suggests a continuous evolution in composition toward a more differentiated composition of silicates when inclusions, cumulus and intercumulus minerals are compared (Fig. 11). During the late magmatic stage, zircon crystallized from intercumulus liquid, which is suggested by its occurrence as both an interstitial phase (Fig. 5I) and included in intercumulus amphibole. Apatite and rutile also show intercumulus textures, being considered as post-cumulus phases. During cooling, mss, sulfide melt and carbonate melt enclosed by chromite equilibrated into the various sulfide and carbonate minerals. The same may have occurred in sulfides interstitial to chromite, but in this case, a hydrothermal origin for heazlewoodite and millerite cannot be discarded, especially in sulfides associated with serpentinitized silicates.

After crystallization, subsolidus chemical reequilibration may have occurred causing an increase in MgO in both the olivine and enstatite cumulus phases. However, despite the shift, the chemical variations along the silicate rocks show a trend suggestive of a more primitive magma

composition during chromite crystallization, in agreement with previously reported data from the Ipueira-Medrado segments (Marques and Ferreira Filho 2003).

Local recrystallization of oikocrystic orthopyroxene in response to high temperatures during regional metamorphism gives rise to a third generation of enstatite, and, under lower temperatures, magnesiohornblende-tremolite forms by replacement of diopside (Fig. 5H). Rare pyrrhotite, galena, barite and chlorite are associated with low temperature serpentinization. The latest phase observed is carbonate in veinlets crosscutting the chromitite.

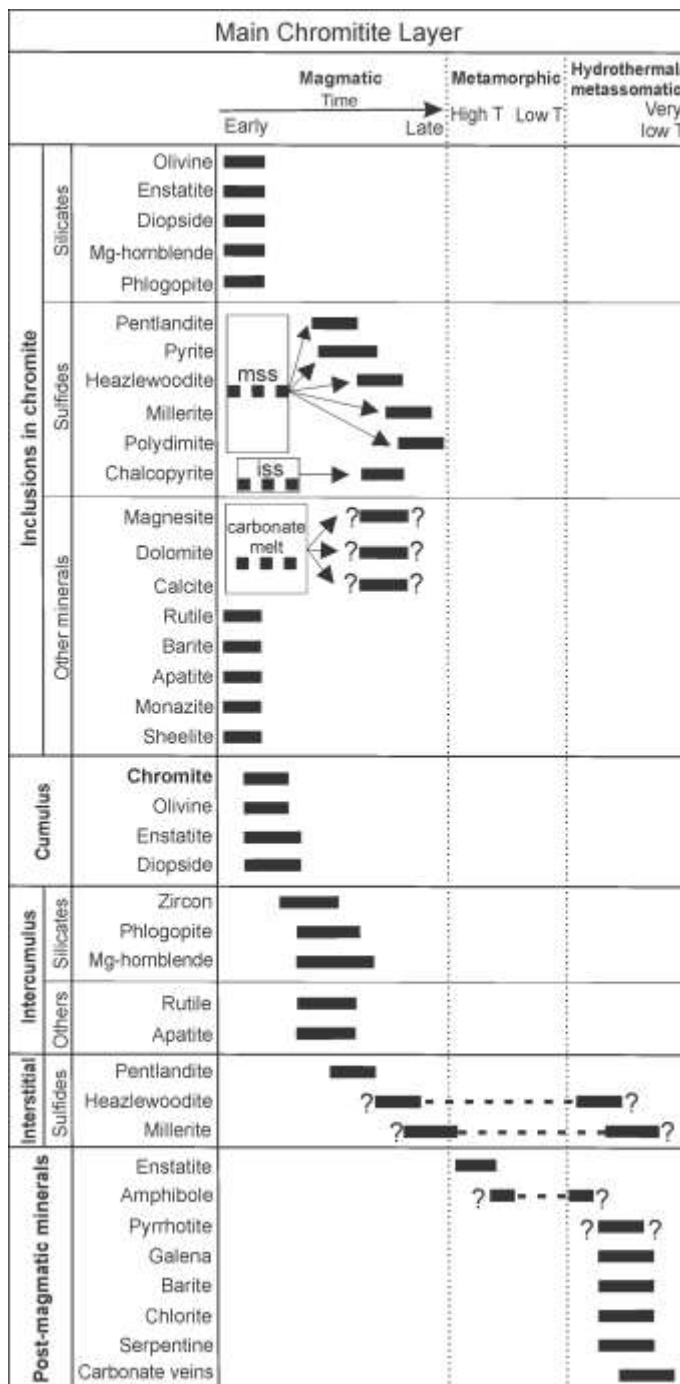


Figure 14: Paragenetic sequence of MCL.

## 5.2 What chromite-hosted inclusions tell about the parental magma of MCL

The primary inclusions in chromite represent early crystallized silicate minerals, carbonate melt, sulfide melt and mss. The existence of comagmatic hydrous silicates, sulfides and carbonates

included in chromite attest to saturation in water and S, and indicate the presence of immiscible droplets of carbonate melt in the magma during chromite crystallization.

Previous studies in the Jacurici Complex (Marques et al. 2003; Marques and Ferreira Filho 2003) have proposed that the mafic-ultramafic segments are located along a conduit structure where large amounts of primitive magma have flowed in order to explain the anomalously large amount of chromite preserved in a relatively thin intrusion. The MCL marks a major petrologic shift in the chamber, under which the chamber was continuously replenished by influxes of primitive magma; after the MCL formation, the magmatic system was dominated by fractional crystallization without continuous injections of fresh magma (Marques et al. 2003). The cryptic variation in the UUU for the MAS Segment is consistent with magma fractionation up-stratigraphy (Fig. 9), with a local disturbance caused by influxes of primitive magma, recorded at the chromitite seam level in the UUU. Os and Nd isotopic studies (Marques et al. 2003) suggested that crustal contamination with the addition of water occurred at the MCL interval, which triggered chromite crystallization. Assimilation of carbonate rocks, as indicated by the presence of marble xenoliths in Ipueira and Medrado areas, was considered relevant in the mineralization process (Ferreira Filho and Araujo 2009), and this suggestion is supported by the presence of abundant carbonate inclusions observed in the present study.

The fact that the UUU in the MAS Segment contains a higher abundance of intercumulus amphibole (as much as 20 vol%) in comparison to the LUU (Fig. 3) is in agreement with the observations of Marques and Ferreira Filho (2003) for the Ipueira-Medrado areas, suggesting that the entire complex records evidence of important water saturation at and above the MCL. Isotopic studies (Marques et al. 2003) revealed that amphibole-rich samples show more negative  $\epsilon_{\text{Nd}}$  than amphibole-free samples, implying that amphibole-rich samples formed from a more crustal-contaminated magma. Abundant inclusions of magmatic amphibole and phlogopite in chromite from the MCL points to magma hydration before chromite crystallization, raising questions about the role of these contamination processes in the formation of the thick chromitite layer.

Further evidence for assimilation lies in the occurrence of inclusions and oikocrysts of diopside at the base of the MCL (Fig. 5A). Experiments show that the addition of calcite and dolomite to mafic magmas favors crystallization of clinopyroxene and other Ca-rich phases (Iacono-Marziano et al. 2007). Oikocrysts are considered cumulus minerals formed by supercooling (Campbell 1968) or supersaturation of the magma with regards to this phase (Barnes et al. 2016) rather than crystallization from intercumulus liquid. Ca-rich clinopyroxene is also found in the basal interval of the chromitite seam in the UUU (Fig. 3) suggesting a close relationship between the trigger for chromite crystallization and the possible addition of Ca and CO<sub>2</sub>. The highest abundance of droplets of dolomite in websterite and olivine websterite in the UUU (Fig. 4G) further indicates the addition of carbonate to the magma, and its close relationship with diopside crystallization. Crystallization of abundant Ca-rich clinopyroxene as a response to carbonate assimilation is also described in other mafic-ultramafic intrusions (e.g. Wenzel et al. 2002; Barnes et al. 2005; Maier et al. 2018).

Furthermore, sulfide inclusions in chromite indicate sulfide saturation prior to or during chromite crystallization. It is noteworthy that all chromitite samples contain Ni-enriched sulfide

inclusions in chromite. Besides, the chemical variation of pentlandite inclusions along stratigraphy is consistent with the variation of comparable parameters in chromite (Fig. 13) indicating that sulfide inclusions experienced the same magmatic fractionation as shown by chromite. It is therefore likely that the enrichment in Ni represents a magmatic feature rather than hydrothermal overprint. One of the ways to form anomalously Ni-rich primary sulfides is by very high R factor (silicate/sulfide mass ratio) (Barnes et al. 2013), which seems to be applicable to the Jacurici Complex, considering that most of the segments contain only traces of sulfides. An alternative mechanism could be by exchange of Ni and Fe between mss and the host chromite during chromite crystallization, as also theorized by Page (1971) to explain Ni enrichment in chromite-hosted sulfide inclusions in the Stillwater Complex.

The common association of carbonates and sulfides as inclusions in chromite (Fig. 7I and J) is a remarkable feature. Similarly, high-temperature carbonates associated with sulfide inclusions have also been reported in orthopyroxene crystals below the J-M reef in the Stillwater Complex (Aird and Boudreau 2013). The preference of sulfide melt to carbonate liquid may indicate sulfide transport in carbonate-sulfide drops, similar to what is proposed for sulfide-volatile compound drops in Ni sulfide ores from komatiites in the Yilgarn Craton (Dowling et al. 2004) and from Noril'sk (Le Vaillant et al. 2017), and observed in experimental investigations (Iacono-Marziano et al. 2017, Mungall et al. 2015).

The mineralogy observed in chromite-hosted inclusions supports previous suggestions of crustal contamination with the addition of water (Marques et al. 2003) and assimilation of carbonate rocks (Ferreira Filho and Araujo 2009) during chromitite formation. Additionally, sulfide inclusions demonstrate that S saturation and crystallization of mss is contemporary with chromite crystallization. Sulfide saturation may have been triggered by incorporation of S from supracrustal rocks during host rock assimilation. It is therefore suggested that the origin of the hydrated silicates, carbonate and sulfide minerals included in chromite might be related to the contamination processes as previously suggested in other parts of the complex (Marques et al. 2003, Ferreira Filho and Araujo 2009).

### 5.3 Why does inclusion-poor chromite coexist with inclusion-rich chromite?

The identical chemistry of inclusion-bearing and inclusion-free chromite grains suggests that they crystallized from the same parental magma, but this feature poses problems for the understanding of how such different textures could be formed at the same level if *in situ* crystallization is assumed. A reasonable way to explain the occurrence of inclusion-bearing chromite is through skeletal or dendritic growth of the crystals. Skeletal or dendritic chromite grains hosting both mineral and melt inclusions are recognized in komatiites (Barnes 1985; Dowling et al. 2004; Godel et al. 2013), ophiolite complexes (Greenbaum 1977; Leblanc 1980, Prichard et al. 2015) and in layered intrusions (Bushveld Complex, Vukmanovic et al. 2013). Dendritic growth of chromite is explained by a fast growth rate provoked by supercooling (Godel et al. 2013, Vukmanovic et al. 2013) or supersaturation in chromite (Prichard et al. 2015).

It has long been known that the solubility of  $\text{Cr}^{3+}$  in the melt decreases with increasing oxygen fugacity (Ulmer 1969, Hill and Roeder 1974, Barnes 1986, Murck and Campbell 1986), which led Ulmer (1969) to propose a model for the crystallization of large amounts of chromite and formation of chromitite layers being triggered by an abrupt increase in  $f\text{O}_2$ . This idea, however, has not received large acceptance since “no reasonable geologic mechanism has been proposed which can produce a sudden increase in  $f\text{O}_2$ , at constant or near constant temperature” (Murck and Campbell 1986). More recently, Wenzel et al. (2002) demonstrated by means of modeling that the very high #Mg of olivine and very low #Cr of spinel forming close to calc-silicate xenoliths is consistent with crystallization under very high oxygen fugacities. They attributed the dramatic change in the redox state of the magma to the introduction of  $\text{CO}_2$  released from dolomite xenoliths. Addition of water to a tholeiitic basalt has been experimentally shown as a feasible way to drastically increase the magma’s  $f\text{O}_2$ : only ~3 wt% water added to an originally dry basalt increases  $f\text{O}_2$  from QFM+1 to QFM+4.2 at 100 MPa (Feig et al. 2006). We therefore argue that large amounts of hot primitive magma flowing through a narrow conduit or chonolith-like intrusion could heat and devolatilize carbonate wall-rocks, introducing  $\text{CO}_2$  into the magma. The assimilation process would probably also introduce water, since the carbonates contained water-bearing minerals as impurities, indicated by the presence of muscovite and biotite in the marbles (Gama 2014). Both water and  $\text{CO}_2$  additions to magma increase  $f\text{O}_2$  pushing the system into the chromite supersaturation field, and consequently favoring chromite crystallization. Therefore, the addition of  $\text{CO}_2$  and water to an originally nearly volatile-free magma would be an alternative way to promote fast growth rates in chromite, explaining the presence of inclusion-rich chromite. We thus interpret that inclusion-rich chromite initially formed as skeletal crystals, allowing entrapment of co-crystallizing minerals and melt droplets, with further textural maturation taking place during slow cooling leading to the formation of inclusion-rich chromite. Figure 15 summarizes the proposed model.

Chromite crystallizing at a lower growth rate from a saturated magma forms inclusion-free crystals (Fig.15A). When the introduction of volatiles sufficiently increased  $f\text{O}_2$  the magma became supersaturated in chromium, causing skeletal growth of chromite due to fast growth. Skeletal chromite growth allows co-crystallizing minerals to be arranged parallel to crystallographic axes in the host chromite (e.g. Fig.15B). Rapid crystallization of spinning chromite in a dynamic/chaotic system may explain the spiral-like oriented inclusions (Fig.15C). Inclusions forming an internal corona in chromite grains could be explained by overgrowths of skeletal chromite on a core of inclusion-free chromite (Fig.15D). This situation could be achieved by increasing saturation of the magma with regards to chromium, caused by the addition of volatiles. Contrarily, chromite morphology in which inclusions are concentrated in the center of the host chromite, with an outer clean (free of inclusions) chromite aureole (Fig.15E) could be explained by a skeletal grain crystallizing under supersaturated conditions, followed by a decrease in the degree of supersaturation. In this mechanism, the decrease in the degree of supersaturation would cause skeletal chromite to stop crystalizing and tiny chromite grains would start crystallizing along the edges of the previously formed skeletal chromite. This model was originally proposed by Prichard et al. (2015) to explain nodular chromites with dendritic cores in the Troodos ophiolite.

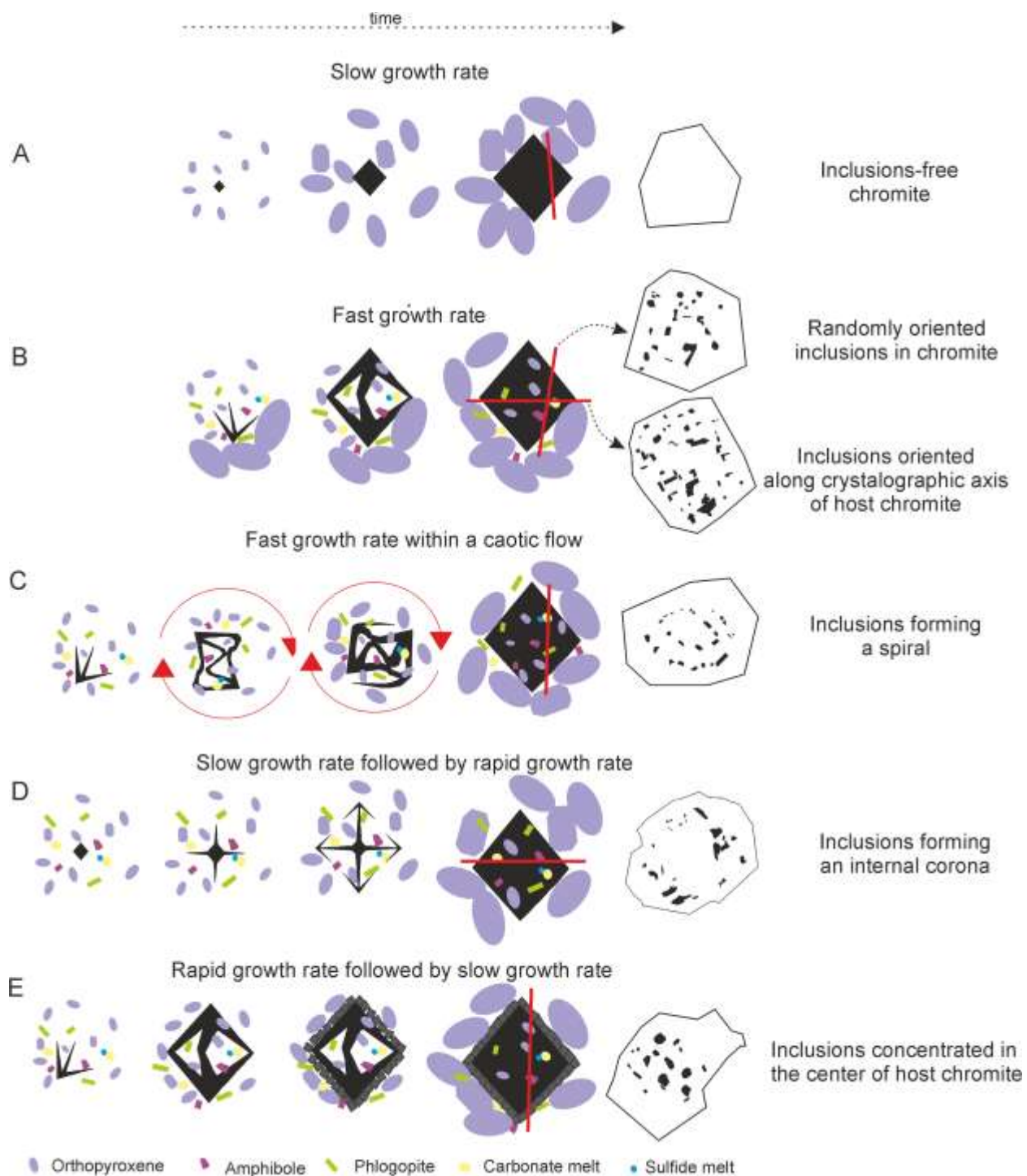


Figure 15: Model for the formation of the different patterns of inclusions in chromite. A: inclusion-free chromite. B: randomly oriented inclusions and inclusions oriented along crystallographic axes of host chromite. C: inclusions forming a spiral. D: Inclusions forming an internal corona. E: Inclusions concentrated in the center of host chromite.

#### 5.4 A model for chromitite formation at the Jacurici Complex

It has been postulated that in the Jacurici Complex the magma was emplaced at the contact between orthogneisses and a supracrustal sequence along a conduit in which hot primitive magma ascended from the mantle and spread laterally into the crust, preferentially along weakness planes between quartz-feldspathic gneisses and olivine marbles, producing elongated sill-like or chonolith-like magma chambers (Marques and Ferreira Filho 2003, Ferreira Filho and Araújo 2009, Marques et al. 2003, 2017). In the Monte Alegre Sul Segment, continuous replenishment of hot magma caused superheating of the wall rocks, provoking devolatilization of marbles. Wall-rock heating and magmatic erosion resulted in the incorporation of xenoliths (Ferreira Filho and Araújo 2009). Carbonate was potentially assimilated, along with possibly also minor gneisses. Further heating of wall-rocks and xenoliths caused dissolution and melting of carbonates. Melting of dolomitic xenoliths by mafic magma was predicted for the Ioko-Doviren intrusion in Russia (Wenzel et al. 2002) and demonstrated at the Hortavær igneous complex in Norway (Barnes et al. 2005). In both cases, the predicted and identified carbonate melt was calcitic. In the Jacurici Complex, the derived carbonate melt is mainly Mg-rich, possibly due to the reaction of an originally calcitic melt with the Mg-rich silicate melt.

The changes in chromite and enstatite composition (Fig. 13) from the basal semi-massive interval to the main chromite seam, and the occurrence of diopside in the basal interval (Fig. 5A), strongly support a model in which  $fO_2$  and  $aCa$  were high at the beginning of the crystallization of large amounts of chromite. These features could be explained by devolatilization and digestion of carbonate wall rocks, and the consequent introduction of  $CO_2$  and  $H_2O$  as volatile phases, as well as Ca and possibly phosphates into the magma. Inclusions of dolomite and magnesite in chromite and dolomite pockets found in the UUU provide further support for this hypothesis. During this process, contamination with S from the wall rock may also have occurred, causing sulfide saturation and inducing partitioning of Ni, Fe and Cu into the liquid S.

Values of  $-7.5$  to  $-8 \log fO_2$  were obtained for the basal interval (sample 83.65 -  $Fe^{3+}$  ratio varies from 8.3 to 11.5; Fig 13) and  $-8.5$  to  $-11 \log fO_2$  for samples in the massive sequence ( $Fe^{3+}$  ratio varies from 2.8 to 6.2; Fig 13), according to the method of Murck and Campbell (1986) and considering a temperature of  $1250^\circ C$  for chromite formation. The basal sample contains higher  $FeO$  and  $Fe_2O_3$ , and lower  $MgO$ ,  $Cr_2O_3$  and  $Al_2O_3$  compared to the overlying sequence, which is also in accordance with crystallization of the basal interval under higher oxygen fugacities (Murck and Campbell 1986). Assuming that inclusion-rich chromite crystallized under fast growth rate conditions driven by higher  $fO_2$ , the higher proportion of chromite with mineral inclusions in the basal interval (about 90% or more against circa 70% at the overlying massive intervals) also supports crystallization of the basal interval under higher oxygen fugacity.

A model for the formation of the MCL is summarized in Figure 16. During the crystallization of chromite, minerals are assumed to accumulate preferentially along the walls of the conduit and the roof of the chonolith-like magma chamber, where the heat loss is more pronounced. An initial in situ crystallization period is supported by the gradual basal contact of the MCL with the underlying dunite with upward increase of chromite, and the higher proportion of inclusion-bearing chromite grains in the basal interval (Fig. 16A). Throughout the period of

chromite crystallization, the degree of supersaturation gradually decreases allowing crystallization of inclusion-free chromite crystals and overgrowths on the previously-formed skeletal chromite (Fig. 16B). Injection of a new batch of magma destabilizes the mixture of crystals accumulated along the conduit walls and chonolith-like magma chamber roof, causing slumping of chromite-enriched semi-consolidated crystal slurries downward towards the floor, accumulating on top of the semi-massive basal chromitite (Fig. 16C). This process is facilitated by the abundance of CO<sub>2</sub> and H<sub>2</sub>O bubbles in the magma which lowers the magma's viscosity (Ghosh and Karki 2017), especially in high shear rate systems (Lesher and Spera 2015), making it more mobile. A slumping event may also partly re-expose wall-rocks to the incoming hot primitive magma, aiding in further crustal contamination and resulting in the addition of more volatiles, oxidation, and supersaturation in chromite. As a result, rapid crystallization of skeletal chromite crystals is boosted again, restarting the cycle. Recharging of the magma chamber and slumpings may have occurred several times during the formation of the MCL, with varying degrees of interaction with host rocks, leading to the variation observed in mineral compositions in the MCL (Fig. 13). Mixing of crystals during slumping may have been responsible for arranging inclusion-bearing and inclusion-free chromite grains side by side.

Experiments by Forien et al. (2015) demonstrated that slumps of crystal slurries can be an effective mechanism to produce layering, and they showed that multiple slumping events is a feasible way to thicken early-formed layers if they are not yet completely crystallized. Sorting triggered by slumps resulting in layering and thickening of chromitite layers has been also proposed for the Bushveld Complex (Cameron and Desborough 1969; Maier and Barnes 2008; Maier et al. 2013) and Uitkomst intrusion (Maier et al. 2018). Mechanical sorting caused by slumping could explain both the thickness and the massive nature of the Main Chromitite Layer of the Jacurici Complex.

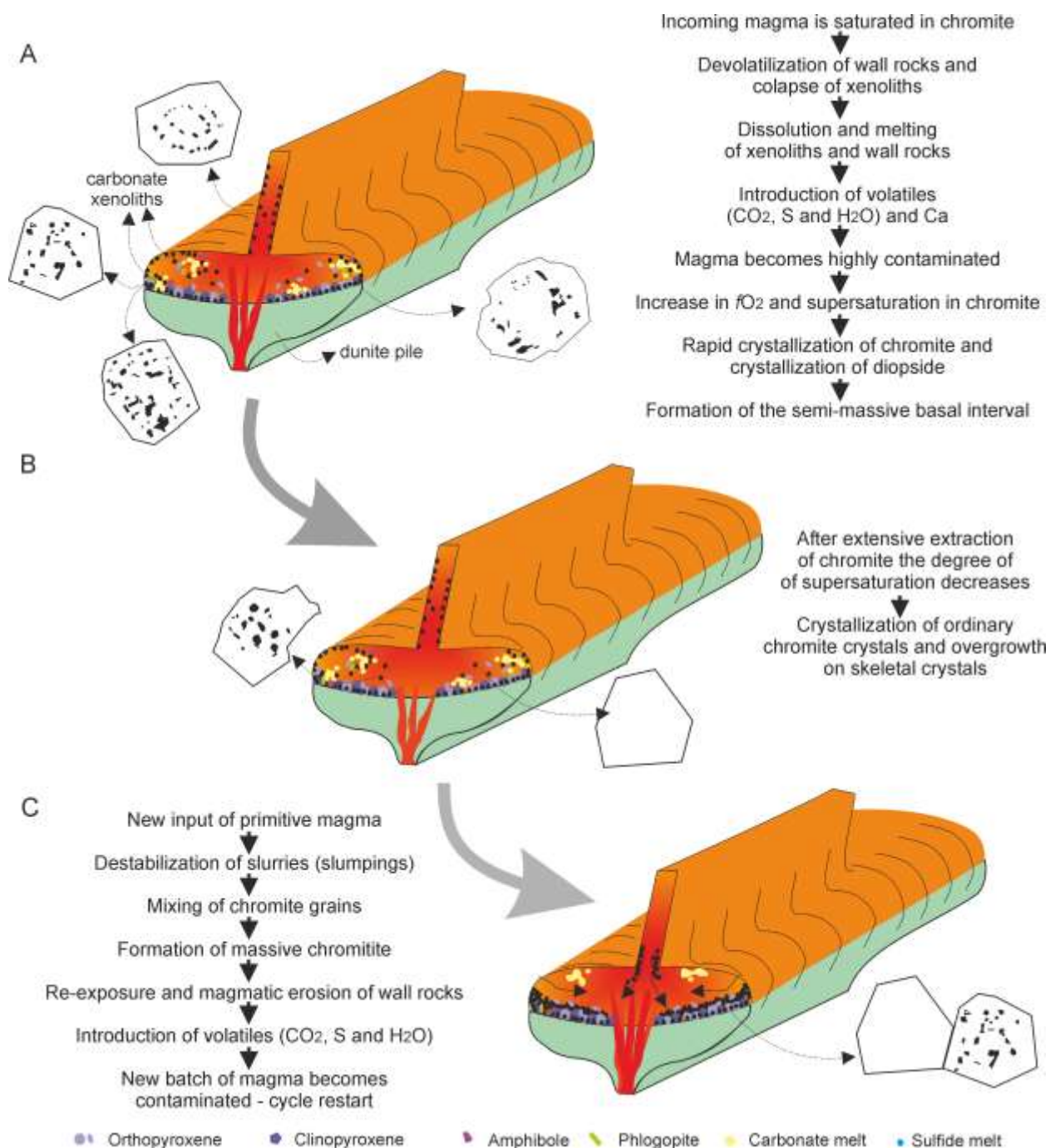


Figure 16: Model for chromitite formation in the Jacurici Complex. A: Devolatilization and digestion of carbonates in the wall rocks introduced volatiles into the magma, causing an increase in  $f\text{O}_2$  and supersaturation in chromite. This led to rapid crystallization of chromite and incorporation of inclusions. B: After extensive extraction of chromite, the degree of supersaturation decreased, favoring formation of inclusion-free overgrowths and formation of new crystals of chromite. C: New input of primitive magma causes destabilization and slumping of chromite-rich crystal slurries. Reworking of the slurries formed layering with mixed populations of inclusion-free and inclusion-bearing chromite grains. The walls of the conduit were re-exposed, enabling contamination of the primitive magma and initiation of a new cycle.

## 6. CONCLUSIONS

The major conclusions of this study are:

1. Chromite from the Main Chromitite Layer in the Jacurici Complex hosts abundant mineral inclusions, comprising mainly silicates (enstatite, phlogopite, magnesiohornblende, diopside and olivine), carbonates (mainly dolomite and magnesite), sulfides (pentlandite, millerite, heazlewoodite, polydymite, pyrite and chalcopyrite) and rutile.
2. Most of the silicate inclusions are monomineralic and represent previously crystallized phases trapped by growing chromite.
3. The chemical composition variation is consistent with a scenario in which most silicate inclusions represent minerals that crystallized prior to, or coeval with, chromite, and the cumulus and intercumulus phases crystallized after the main stage of chromite formation.
4. Textures indicate carbonate inclusions were entrapped as carbonate melt, whereas sulfide inclusions were captured as both sulfide melt and mss, suggesting contemporaneity between chromite and sulfide crystallization.
5. Inclusion-bearing chromite occurs spatially associated with inclusion-free chromite.
6. Inclusion-bearing and inclusion-free chromite grains from the same stratigraphic level have similar chemical compositions, suggesting that both crystallized from similar parental magma.
7. The presence or absence of primary inclusions is interpreted to be due to different growth rates in chromite. Fast-growing skeletal chromite grains were able to trap abundant primary inclusions, whereas chromite growing at slower rates could not easily.
8. Fast chromite growth is attributed to supersaturation in chromium, possibly induced by the presence of volatiles ( $H_2O$  and  $CO_2$ ) that increased oxygen fugacity in the magma.
9. The origin of the volatiles is interpreted as the result of crustal contamination as previously suggested by isotopic studies (Marques et al. 2003). During magma ascent and emplacement, hot primitive magma could heat and devolatilize carbonate wall-rocks, introducing  $CO_2$  and probably water into the system.
10. It is proposed that the semi-massive basal interval has an in situ origin. On the other hand, the very massive nature of the overlying intervals, the striking thickness of the MCL, and the mixing of inclusion-bearing with inclusion-free chromite grains provide lines of evidence for its formation by local remobilization and sorting during slumping events. Slumping might have been facilitated by the presence of volatiles in the system.
11. Successive recurring episodes of slumping were possibly responsible for periodically re-exposing wall-rocks to new incoming primitive magma, allowing for long periods of contamination and facilitating the crystallization of huge amounts of chromite.
12. The proposed genetic model has implications for exploration, and we suggest that Intrusions of mafic-ultramafic magmas in contact with carbonate rocks is a favorable setting to explore for deposits of chromite.

## ACKNOWLEDGEMENTS

Companhia de Ferro Ligas da Bahia (FERBASA) and its staff are gratefully acknowledged for field support, geological information and allowing sampling of the drill cores. Betina M. Friedrich holds a scholarship from CNPq (Conselho Nacional de Desenvolvimento Científico e Tecnológico), project 131133/2016-0 and this study is part of her M.Sc. thesis developed at the Instituto de Geociências, Universidade Federal do Rio Grande do Sul.

Table 1: Representative electron microprobe analyses of olivine of the UUU and LUU

Unit	UUU	UUU	UUU	UUU	UUU	UUU	LUU
Sample	50.69	53.53	62.50	68.97	71.75	71.75	86.07
<b>Oxides (wt.%)</b>							
SiO <sub>2</sub>	38.97	38.44	38.91	38.58	38.09	38.20	38.75
MgO	48.09	47.26	50.43	48.06	49.48	48.98	49.42
FeO	12.55	12.84	9.42	12.90	11.66	12.06	10.70
MnO	0.23	0.35	0.19	0.30	0.31	0.21	0.22
NiO	0.05	0.25	0.53	0.10	0.35	0.35	0.36
Cr <sub>2</sub> O <sub>3</sub>	0.00	0.00	0.01	0.00	0.03	0.02	0.08
Total	99.95	99.40	99.66	100.01	100.00	99.89	99.85
<b>Number of 62+ cations per 4 oxygens</b>							
Si4+	0.97	0.97	0.96	0.96	0.95	0.95	0.96
Mg2+	1.79	1.77	1.86	1.79	1.84	1.82	1.82
Fe2+	0.26	0.27	0.19	0.27	0.24	0.25	0.22
Mn2+	0.00	0.01	0.00	0.01	0.01	0.00	0.00
Ni	0.00	0.00	0.01	0.00	0.01	0.01	0.01
Cr3+	0.00	0.00	0.00	0.00	0.00	0.00	0.00
Total	3.03	3.03	3.03	3.03	3.04	3.04	3.02
Fo	87.22	86.77	90.51	86.91	88.32	87.86	89.17

Table 2: Representative electron microprobe analyses of pyroxene of the UUU and LUU

Orthopyroxene											Clinopyroxene		
Unit	UUU	UUU	UUU	UUU	UUU	UUU	UUU	UUU	LUU		UUU	UUU	UUU
Sample	50.69	53.53	57.94	58.56	60.25	62.50	66.22	68.97	71.75	86.07	57.94	58.56	66.22
Oxides (wt.%)													
SiO <sub>2</sub>	53.69	53.46	53.70	53.77	55.69	53.91	55.49	54.17	54.39	54.38	51.86	51.39	52.42
Al <sub>2</sub> O <sub>3</sub>	3.25	3.57	2.65	2.85	1.09	2.16	1.53	2.82	2.17	2.75	2.34	2.13	1.79
TiO <sub>2</sub>	0.00	0.06	0.00	0.11	0.13	0.00	0.00	0.00	0.00	0.00	0.02	0.31	0.06
Cr <sub>2</sub> O <sub>3</sub>	0.10	0.11	0.04	0.11	0.12	0.26	0.11	0.14	0.14	0.16	0.26	0.16	0.23
Fe <sub>2</sub> O <sub>3</sub>	3.77	4.36	3.79	0.00	3.45	6.44	4.90	2.02	3.97	4.17	3.35	3.64	3.01
FeO	5.48	5.35	6.56	10.10	4.22	1.37	2.66	7.94	4.68	4.06	0.00	0.23	0.25
MnO	0.16	0.19	0.23	0.35	0.14	0.16	0.07	0.23	0.13	0.18	0.18	0.03	0.04
MgO	32.75	32.54	32.31	32.14	34.73	34.99	35.27	32.10	33.66	33.81	16.89	17.09	17.54
CaO	0.38	0.36	0.24	0.42	0.27	0.19	0.43	0.47	0.31	0.51	24.93	24.58	24.21
Na <sub>2</sub> O	0.00	0.01	0.00	0.01	0.00	0.04	0.03	0.01	0.01	0.00	0.10	0.08	0.16
Total	99.57	100.20	99.69	99.90	99.92	99.67	100.64	100.00	99.55	100.32	100.14	99.88	99.79
Number of cations per 6 oxygens													
Si <sub>4+</sub>	1.88	1.86	1.89	1.88	1.93	1.87	1.90	1.89	1.90	1.88	1.89	1.88	1.91
Al <sub>3+</sub>	0.13	0.15	0.11	0.12	0.04	0.09	0.06	0.12	0.09	0.11	0.10	0.09	0.08
Ti <sub>4+</sub>	0.00	0.00	0.00	0.00	0.00	0.00	0.00	0.00	0.00	0.00	0.00	0.01	0.00
Cr <sub>3+</sub>	0.00	0.00	0.00	0.00	0.00	0.01	0.00	0.00	0.00	0.00	0.01	0.00	0.01
Fe <sub>3+</sub>	0.10	0.11	0.10	0.00	0.09	0.17	0.13	0.05	0.10	0.11	0.10	0.10	0.08
Fe <sub>2+</sub>	0.16	0.16	0.19	0.30	0.12	0.04	0.08	0.23	0.14	0.12	0.00	0.01	0.01
Mn <sub>2+</sub>	0.00	0.01	0.01	0.01	0.00	0.00	0.00	0.01	0.00	0.01	0.01	0.00	0.00
Mg <sub>2+</sub>	1.71	1.69	1.69	1.67	1.79	1.81	1.80	1.67	1.75	1.74	0.92	0.93	0.95
Ca <sub>2+</sub>	0.01	0.01	0.01	0.02	0.01	0.01	0.02	0.02	0.01	0.02	0.97	0.96	0.95
Total	4.00	4.00	4.00	4.00	4.00	4.00	4.00	4.00	4.00	4.00			
En	86.61	85.97	84.95	84.57	89.23	89.49	89.80	85.14	87.74	88.28			

Table 3: Representative electron microprobe analyses of amphibole of the UUU and LUU. Mag: magmatic; p-mag: post-magmatic; Ts: Tshermakite; Tr: tremolite; Mg-Hbl: magnesiohornblende

Unit	UUU	UUU	UUU	UUU	UUU	UUU	UUU	UUU	UUU	UUU	UUU	LUU	LUU
Sample	50.69	53.53	57.94	57.94	58.55	58.55	60.25	62.50	66.22	68.97	71.75	86.07	88.35
	mag	mag	mag	p-mag	mag	p-mag	mag	mag	mag	mag	mag	mag	mag
Classification	Ts	Ts	Ts	Tr	Ts	Tr	Mg-Hbl	Mg-Hbl	Ts	Ts	Ts	Ts	Ts
Oxides (wt.%)													
SiO <sub>2</sub>	43.08	43.46	45.62	55.28	44.21	55.46	45.99	46.47	45.16	43.77	44.18	43.87	43.94
Al <sub>2</sub> O <sub>3</sub>	12.93	13.65	10.22	2.36	12.33	2.17	10.81	10.58	11.35	12.11	11.47	12.12	12.05
TiO <sub>2</sub>	1.10	0.58	0.38	0.02	0.40	0.00	0.34	0.66	0.55	0.66	0.41	1.02	1.08
Cr <sub>2</sub> O <sub>3</sub>	0.29	0.17	0.45	0.11	0.49	0.13	1.24	0.71	1.21	0.70	0.90	0.87	1.00
Fe <sub>2</sub> O <sub>3</sub>	4.11	4.29	6.70	2.41	5.93	2.98	2.94	2.48	4.09	4.27	5.54	4.70	4.82
FeO	3.09	2.92	0.35	0.00	1.48	0.00	1.68	2.15	0.98	2.70	0.83	1.05	0.80
MnO	0.00	0.06	0.00	0.04	0.09	0.09	0.10	0.00	0.06	0.12	0.05	0.04	0.00
MgO	17.45	17.25	18.82	23.51	17.44	23.46	18.95	19.19	18.98	17.51	18.51	18.60	18.75
CaO	12.17	12.62	12.88	13.36	12.94	13.55	12.52	12.70	12.68	12.56	12.66	12.62	12.59
Na <sub>2</sub> O	1.83	1.98	1.21	0.28	1.31	0.30	1.53	1.59	1.60	1.77	1.62	1.77	1.56
K <sub>2</sub> O	0.89	0.77	0.73	0.07	0.89	0.05	0.77	0.80	0.88	0.91	0.97	0.88	1.07
F	0.18	0.04	0.13	0.03	0.06	0.12	0.12	0.28	0.30	0.08	0.34	0.10	0.12
Cl	0.40	0.47	0.34	0.05	0.43	0.03	0.27	0.29	0.38	0.39	0.42	0.36	0.37
H <sub>2</sub> O (assumed)	2.20	2.20	2.20	2.20	2.20	2.20	2.20	2.20	2.20	2.20	2.20	2.20	2.20
Total	99.14	99.95	99.55	99.63	99.72	100.39	99.06	99.52	99.72	99.28	99.34	99.74	99.84
Number of cations and anions per 23 anhydrous oxygens													
Si <sup>4+</sup>	6.21	6.20	6.49	7.58	6.31	7.57	6.55	6.58	6.41	6.30	6.32	6.25	6.25
Al <sup>3+</sup>	2.20	2.30	1.71	0.38	2.07	0.35	1.81	1.77	1.90	2.05	1.94	2.03	2.02
Ti <sup>4+</sup>	0.12	0.06	0.04	0.00	0.04	0.00	0.04	0.07	0.06	0.07	0.04	0.11	0.12
Cr <sup>3+</sup>	0.03	0.02	0.05	0.01	0.05	0.01	0.14	0.08	0.14	0.08	0.10	0.10	0.11
Fe <sup>3+</sup>	0.45	0.46	0.72	0.35	0.64	0.41	0.31	0.26	0.44	0.46	0.60	0.50	0.52
Fe <sup>2+</sup>	0.37	0.35	0.04	0.00	0.18	0.00	0.20	0.25	0.12	0.32	0.10	0.13	0.09
Mg <sup>2+</sup>	3.75	3.67	3.99	4.81	3.71	4.77	4.02	4.05	4.01	3.76	3.95	3.95	3.98
Mn <sup>2+</sup>	0.00	0.01	0.00	0.00	0.01	0.01	0.01	0.00	0.01	0.01	0.01	0.01	0.00
Ca <sup>2+</sup>	1.88	1.93	1.96	1.96	1.98	1.98	1.91	1.93	1.93	1.94	1.94	1.93	1.92
Na <sup>+</sup>	0.51	0.55	0.33	0.07	0.36	0.08	0.42	0.44	0.44	0.49	0.45	0.49	0.43
K <sup>+</sup>	0.16	0.14	0.13	0.01	0.16	0.01	0.14	0.15	0.16	0.17	0.18	0.16	0.19
Total	15.67	15.69	15.46	15.19	15.52	15.20	15.56	15.58	15.60	15.66	15.63	15.65	15.62
Mg/(Mg+Fe <sup>2+</sup> )	0.91	0.91	0.99	1.00	0.95	1.00	0.95	0.94	0.97	0.92	0.98	0.97	0.98

Table 4: Representative electron microprobe analyses of inclusion-free and inclusion-bearing chromite of the MCL

Sample	78.20	78.20	78.20	78.20	78.20	78.20
	Inclusion-free chromite			Inclusion-bearing chromite		
<b>Oxides (wt.%)</b>						
SiO <sub>2</sub>	0.00	0.00	0.00	0.03	0.00	0.00
TiO <sub>2</sub>	0.27	0.24	0.25	0.21	0.22	0.18
Al <sub>2</sub> O <sub>3</sub>	18.03	17.63	17.77	18.59	18.03	18.36
Cr <sub>2</sub> O <sub>3</sub>	50.22	50.35	50.88	49.15	50.05	50.24
V <sub>2</sub> O <sub>3</sub>	0.12	0.11	0.14	0.08	0.12	0.10
Fe <sub>2</sub> O <sub>3</sub>	3.55	3.61	3.51	3.79	3.73	3.46
FeO	14.05	13.96	14.05	13.76	14.01	14.01
MnO	0.32	0.33	0.37	0.34	0.37	0.34
MgO	13.44	13.37	13.50	13.57	13.41	13.48
ZnO	0.09	0.07	0.03	0.06	0.06	0.08
NiO	0.20	0.16	0.17	0.15	0.16	0.17
CaO	0.00	0.00	0.00	0.02	0.00	0.00
Total	100.29	99.84	100.67	99.77	100.16	100.44
<b>Number of cations per 32 oxygens</b>						
Si <sup>4+</sup>	0.00	0.00	0.00	0.01	0.00	0.00
Ti <sup>4+</sup>	0.05	0.05	0.05	0.04	0.04	0.03
Al <sup>3+</sup>	5.30	5.21	5.21	5.47	5.31	5.38
Cr <sup>3+</sup>	9.90	9.99	10.01	9.70	9.88	9.88
V <sup>3+</sup>	0.02	0.02	0.03	0.02	0.02	0.02
Fe <sup>3+</sup>	0.67	0.68	0.66	0.71	0.70	0.65
Fe <sup>2+</sup>	2.93	2.93	2.92	2.87	2.93	2.91
Mn <sup>2+</sup>	0.07	0.07	0.08	0.07	0.08	0.07
Mg <sup>2+</sup>	5.00	5.00	5.01	5.05	4.99	5.00
Zn <sup>2+</sup>	0.02	0.01	0.01	0.01	0.01	0.01
Ni <sup>2+</sup>	0.04	0.03	0.03	0.03	0.03	0.03
Ca <sup>2+</sup>	0.00	0.00	0.00	0.01	0.00	0.00
Total	24.00	24.00	24.00	24.00	24.00	24.00

Table 5: Representative electron microprobe analyses of pyroxene inclusions, cumulus and poikilitic of the MCL. Cr/R3: 100Cr/(Al+Cr+Fe<sup>3+</sup>)

Orthopyroxene											Clinopyroxene			
Sample	76.80	76.80	78.20	81.64	81.64	82.80	82.80	82.80	83.65	83.65		82.80	83.65	83.65
	Cum	Inc	Cum	Inc	Cum	Poik	Cum	Inc	Inc	Poik		Poik	Inc	Poik
Oxides (wt.%)														
SiO <sub>2</sub>	57.83	57.91	57.28	57.77	57.32	57.30	57.97	58.14	58.19	56.77	53.87	53.90	54.03	
Al <sub>2</sub> O <sub>3</sub>	0.74	0.42	1.63	0.77	1.44	0.88	1.10	0.65	0.48	1.24	1.27	0.62	0.77	
TiO <sub>2</sub>	0.06	0.07	0.09	0.08	0.09	0.07	0.09	0.12	0.03	0.04	0.25	0.06	0.09	
Cr <sub>2</sub> O <sub>3</sub>	0.29	0.90	0.48	0.75	0.45	0.47	0.40	0.99	1.02	0.43	0.73	1.20	0.29	
Fe <sub>2</sub> O <sub>3</sub>	0.58	0.71	0.83	0.29	0.29	1.25	0.48	0.46	0.29	1.49	1.06	0.24	0.54	
FeO	3.43	2.89	3.02	3.63	4.09	2.52	3.27	3.01	4.66	4.10	0.00	1.63	1.39	
MnO	0.12	0.12	0.16	0.18	0.17	0.12	0.15	0.13	0.16	0.15	0.05	0.07	0.07	
MgO	36.69	37.17	36.49	36.44	35.84	36.92	36.80	37.13	36.20	35.46	17.36	17.91	17.79	
CaO	0.17	0.12	0.34	0.25	0.31	0.16	0.30	0.16	0.21	0.30	24.79	24.87	24.87	
Na <sub>2</sub> O	0.00	0.00	0.00	0.00	0.00	0.00	0.00	0.01	0.00	0.01	0.16	0.09	0.10	
TOTAL	99.92	100.32	100.33	100.16	99.99	99.70	100.55	100.81	101.24	99.98	99.55	100.59	99.95	
Number of cations per 6 oxygens														
Si <sub>4+</sub>	1.97	1.97	1.95	1.97	1.96	1.96	1.96	1.97	1.97	1.95	1.96	1.95	1.96	
Al <sub>3+</sub>	0.03	0.02	0.07	0.03	0.06	0.04	0.04	0.03	0.02	0.05	0.05	0.03	0.03	
Ti <sub>4+</sub>	0.00	0.00	0.00	0.00	0.00	0.00	0.00	0.00	0.00	0.00	0.01	0.00	0.00	
Cr <sub>3+</sub>	0.01	0.02	0.01	0.02	0.01	0.01	0.01	0.03	0.03	0.01	0.02	0.03	0.01	
Fe <sub>3+</sub>	0.01	0.02	0.02	0.01	0.01	0.03	0.01	0.01	0.01	0.04	0.00	0.04	0.04	
Fe <sub>2+</sub>	0.10	0.08	0.09	0.10	0.12	0.07	0.09	0.09	0.13	0.12	0.03	0.01	0.02	
Mn <sub>2+</sub>	0.00	0.00	0.00	0.01	0.00	0.00	0.00	0.00	0.00	0.00	0.00	0.00	0.00	
Mg <sub>2+</sub>	1.87	1.88	1.85	1.85	1.83	1.88	1.86	1.87	1.83	1.82	0.94	0.97	0.96	
Ca <sub>2+</sub>	0.01	0.00	0.01	0.01	0.01	0.01	0.01	0.01	0.01	0.01	0.97	0.96	0.97	
Na <sub>+</sub>	0.00	0.00	0.00	0.00	0.00	0.00	0.00	0.00	0.00	0.00	0.01	0.01	0.01	
Total	4.00	4.00	4.00	4.00	4.00	4.00	4.00	4.00	4.00	4.00	4.00	4.00	4.00	
En	94.12	94.80	94.31	94.10	93.37	94.60	94.45	94.89	92.68	91.86	49.74	48.59	48.71	
Cr/R3	15.05	41.05	12.93	34.58	15.72	15.69	15.82	41.19	50.93	11.63	19.07	30.00	8.49	

Table 6: Representative electron microprobe analyses of phlogopite inclusions and intercumulus of the MCL

Sample	76.80	78.20	79.10	79.10	82.80	83.65
	Inclusion	Intercumulus	Intercumulus	Inclusion	Inclusion	Inclusion
<b>Oxides (wt.%)</b>						
SiO <sub>2</sub>	40.16	40.53	39.54	40.18	40.29	40.52
Al <sub>2</sub> O <sub>3</sub>	14.86	15.49	15.62	14.90	14.76	14.87
TiO <sub>2</sub>	1.96	1.84	2.33	2.24	2.27	1.74
Cr <sub>2</sub> O <sub>3</sub>	1.82	1.33	1.52	1.63	1.83	1.57
FeOT	1.41	1.45	1.50	1.58	1.58	1.84
MnO	0.01	0.00	0.03	0.00	0.02	0.00
MgO	24.95	24.63	24.75	24.55	24.71	25.08
CaO	0.02	0.02	0.00	0.04	0.01	0.00
BaO	0.09	0.31	0.21	0.35	0.12	0.42
Na <sub>2</sub> O	0.57	0.65	0.29	0.57	0.09	0.40
K <sub>2</sub> O	9.13	9.01	9.39	8.85	9.98	9.09
F	0.35	0.54	0.11	0.37	0.10	0.00
Cl	0.15	0.26	0.13	0.14	0.25	0.09
H <sub>2</sub> O (assumed)	4.00	4.00	4.00	4.00	4.00	4.00
Total	99.48	100.05	99.42	99.40	100.01	99.62
<b>Number of cations per 11 anhydrous oxygens</b>						
Si <sup>4+</sup>	2.82	2.84	2.78	2.83	2.82	2.84
Al <sup>3+</sup>	1.23	1.28	1.29	1.24	1.22	1.23
Al <sup>3+</sup> in Z	1.18	1.16	1.22	1.17	1.18	1.16
Al <sup>3+</sup> in Y	0.05	0.11	0.07	0.06	0.04	0.06
Ti <sup>4+</sup>	0.10	0.10	0.12	0.12	0.12	0.09
Cr <sup>3+</sup>	0.10	0.07	0.08	0.09	0.10	0.09
FeT	0.08	0.08	0.09	0.09	0.09	0.11
Mn <sup>2+</sup>	0.00	0.00	0.00	0.00	0.00	0.00
Mg <sup>2+</sup>	2.61	2.57	2.59	2.58	2.58	2.62
Ca <sup>2+</sup>	0.00	0.00	0.00	0.00	0.00	0.00
Ba <sup>2+</sup>	0.00	0.01	0.01	0.01	0.00	0.01
Na <sup>+</sup>	0.08	0.09	0.04	0.08	0.01	0.05
K <sup>+</sup>	0.82	0.80	0.84	0.80	0.89	0.81
F <sup>-</sup>	0.08	0.12	0.02	0.08	0.02	0.00
Cl <sup>-</sup>	0.02	0.03	0.02	0.02	0.03	0.01
Total cations	7.86	7.84	7.85	7.83	7.85	7.85
Al(VI)/Mg	0.02	0.04	0.03	0.02	0.02	0.02
FeT/Mg	0.03	0.03	0.03	0.04	0.04	0.04

Table 7: Representative electron microprobe analyses of inclusions, intercumulus and post-magmatic of the MCL

Sample	78.20	79.10	79.10	81.64	82.80	82.80	83.65	83.65
Oxides (wt.%)	Inter	Inter	Inc	Inc	p-mag	Inter	Inc	p-mag
SiO <sub>2</sub>	47.81	51.29	48.86	50.13	54.04	50.22	52.91	51.62
Al <sub>2</sub> O <sub>3</sub>	9.35	6.62	8.47	6.77	4.02	7.24	4.76	6.08
TiO <sub>2</sub>	1.04	0.60	1.01	0.74	0.49	0.95	0.35	0.58
Cr <sub>2</sub> O <sub>3</sub>	2.05	1.33	1.99	2.07	0.68	1.36	1.79	0.91
Fe <sub>2</sub> O <sub>3</sub>	0.20	0.16	0.91	1.41	0.49	0.02	1.44	1.66
FeO	1.71	1.89	1.44	0.76	0.87	1.78	0.92	0.87
MnO	0.03	0.04	0.06	0.01	0.03	0.04	0.05	0.03
MgO	20.04	21.08	20.68	21.17	22.50	20.82	22.03	21.47
CaO	12.71	13.02	12.77	12.99	13.22	12.86	13.07	13.10
Na <sub>2</sub> O	1.36	1.01	1.23	0.96	0.53	1.01	0.66	0.80
K <sub>2</sub> O	0.63	0.36	0.73	0.58	0.20	0.45	0.36	0.30
F	0.38	0.00	0.03	0.00	0.13	0.03	0.04	0.17
Cl	0.20	0.17	0.20	0.14	0.09	0.16	0.05	0.15
H <sub>2</sub> O (assumed)	2.20	2.20	2.20	2.20	2.20	2.20	2.20	2.20
TOTAL	99.72	99.76	100.59	99.93	99.49	99.15	100.64	99.96
Number of cations and anions per 23 anhydrous oxygens								
Si <sup>4+</sup>	6.74	7.14	6.81	7.00	7.47	7.05	7.29	7.17
Al <sup>3+</sup>	1.55	1.09	1.39	1.11	0.66	1.20	0.77	1.00
Ti <sup>4+</sup>	0.11	0.06	0.11	0.08	0.05	0.10	0.04	0.06
Cr <sup>3+</sup>	0.23	0.15	0.22	0.23	0.07	0.15	0.19	0.10
Fe <sup>3+</sup>	0.02	0.02	0.10	0.15	0.05	0.00	0.15	0.17
Fe <sup>2+</sup>	0.20	0.22	0.17	0.09	0.10	0.21	0.11	0.10
Mg <sup>2+</sup>	4.21	4.38	4.30	4.40	4.64	4.35	4.52	4.44
Mn <sup>2+</sup>	0.00	0.00	0.01	0.00	0.00	0.01	0.01	0.00
Ca <sup>2+</sup>	1.92	1.94	1.91	1.94	1.96	1.93	1.93	1.95
Na <sup>+</sup>	0.19	0.14	0.17	0.13	0.07	0.14	0.09	0.11
K <sup>+</sup>	0.06	0.03	0.07	0.05	0.02	0.04	0.03	0.03
F <sup>-</sup>	0.17	0.00	0.01	0.00	0.06	0.01	0.02	0.08
Cl <sup>-</sup>	0.05	0.04	0.05	0.03	0.02	0.04	0.01	0.04
Total cations	15.24	15.17	15.23	15.18	15.09	15.18	15.12	15.13
Mg/(Mg+Fe <sup>2+</sup> )	0.95	0.95	0.96	0.98	0.98	0.95	0.98	0.98

Table 8: Electron microprobe analyses of sulfide inclusions of the MCL. Ni ratio = 100Ni/(Ni+Fe)

## REFERENCES

- Almeida FFM (1965) Precambrian geology of North Eastern Brazil and Western Africa and the theory of Continental Drift. In: Symposium on the granites of West Africa, Ivory Coast, Nigeria and Cameron, 1965. Proceedings, Paris, UNESCO, p. 151-162 .
- Almeida FFM (1977) The São Francisco Craton. Rev Bras Geoc 7(4): 349-364 (in Portuguese).
- Almeida HL, Cabral EB, Bezerra FX (2017) Deformational evolution of the Vale do Jacurici rocks: implications for the structuration of the mafic-ultramafic chromite bodies. Geo USP Sér Cient 17(2):71-88. doi 0.11606/issn.2316-9095.v17-398.
- Aird HM, Boudreau AE (2013) High-temperature carbonate minerals in the Stillwater Complex, Montana, USA. Contrib Mineral Petrol 166:1143–1160.
- Bai ZJ, Zhong H, Zhu WG et al (2018) The genesis of the newly discovered giant Wuben magmatic Fe–Ti oxide deposit in the Emeishan Large Igneous Province: a product of the late-stage redistribution and sorting of crystal slurries. Miner Deposita (2018). doi: 10.1007/s00126-018-0801-9.
- Bailey SW (1984) Reviews in mineralogy-Micas, 13, 584 pp.
- Barbosa JSF (1997) Summary of the knowledge about the geotectonic evolution of the Archean and Paleoproterozoic rocks of the basement of the São Francisco Craton in Bahia. Rev Bras Geoc 27(3):241-256. (In Portuguese).
- Barbosa JSF, Sabaté P (2002) Geological Features and the Paleoproterozoic Collision of Four Archean Crustal Segments of the São Francisco Craton, Bahia, Brazil. A Synthesis. An Acad Bras Ciênc 74(2):343–59.
- Barbosa JSF, Sabaté P (2003) Paleoproterozoic collage of Archean plates of the São Francisco Craton in Bahia. Rev Bras Geoc 33(1):7–14. (In Portuguese).
- Barbosa JSF, Sabaté P, Marinho MM (2003) O Cráton São Francisco na Bahia: uma síntese. Rev Bras Geoc 33(1):3-6. (In Portuguese).
- Barbosa JSF, Mascarenhas SJF, Correa Gomes LC et al. (2012) Geology of Bahia: research and update. Companhia Baiana de Pesquisa Mineral, Salvador. (In Portuguese).
- Barnes CG, Prestvik T, Sundvoll B, Surratt D (2005) Pervasive assimilation of carbonate and silicate rocks in the Hortavær igneous complex, north-central Norway. Lithos 80, 179–199.
- Barnes SJ (1985) The petrography and geochemistry of Komatiite flows from the Abitibi greenstone-belt and a model for their formation. Lithos 18(4):241–270. doi: 10.1016/0024-4937(85)90030-1
- Barnes SJ (1986) The distribution of chromium among orthopyroxene, spinel and silicate liquid at atmospheric pressure. Geochim Cosmochim Acta. 50:1889-1909.
- Barnes SJ, Godel B, Gürer D et al. (2013) Sulfide-Olivine Fe-Ni Exchange and the Origin of Anomalously Ni Rich Magmatic Sulfides. Econ Geol 108:1971–1982.

- Barnes SJ, Mole DR, Le Vaillant M et al. (2016) Poikilitic Textures, Heteradcumulates and Zoned Orthopyroxenes in the Ntaka Ultramafic Complex, Tanzania: Implications for Crystallization Mechanisms of Oikocrysts. *J Petrol* 57(6):1171–1198. doi: 10.1093/petrology/egw036
- Campbell IH (1968) The origin of heteradcumulate and adcumulate textures in the Jimberlana Norite. *Geol Mag* 105:378–383.
- Cameron EN, Desborough GA (1969) Occurrence and characteristics of chromite deposits—eastern Bushveld Complex, Economic Geology Monograph , 1969, vol. 4 (pg. 23-40)
- Chantler CT (1995): Theoretical form factor, attenuation and scattering tabulation for  $Z = 1\text{--}92$  from  $E = 1\text{--}10 \text{ eV}$  to  $E = 0.4\text{--}1.0 \text{ MeV}$ . *J Phys Chem Ref Data* 24:71–643.
- Cunha JC, Barbosa JSF, Mascarenhas JF (2012) Greenstone Belts and similar sequences. In: Barbosa JSF, Mascarenhas SJF, Correa Gomes LC et al (eds.) *Geology of Bahia: research and update*. Companhia Baiana de Pesquisa Mineral, Salvador, pp 203–326. (In Portuguese).
- Dias JRVP, Marques JC, Queiroz WJA (2014) The chromium and copper-nickel mineralized Várzea do Macaco body, Jacurici Mafic-ultramafic Complex, São Francisco Craton, Bahia, Brazil. *Braz J Geol* 44(2): 289–308.
- Dowling SE, Barnes SJ, Hill RET, Hicks JD (2004) Komatiites and Nickel Sulfide Ores of the Black Swan Area, Yilgarn Craton, Western Australia. 2: Geology and Genesis of the Orebodies. *Miner Deposita* 39(7):707–28.
- Eales HV (2000) Implications of the chromium budget of the Western Limb of the Bushveld Complex. *S Afr J Geol* 103:141–150
- Feig ST, Koepke J, Snow JE (2006) Effect of Water on Tholeiitic Basalt Phase Equilibria: An Experimental Study under Oxidizing Conditions. *Contrib Mineral Petrol* 152(5):611–38.
- Ferreira Filho CF, Araujo SM (2009) Review of Brazilian Chromite Deposits Associated with Layered Intrusions: Geological and Petrological Constraints for the Origin of Stratiform Chromitites. *Applied Earth Science* 118(3–4):86–100.
- Forien M, Tremblay J, Barnes S-J, et al (2015) The Role of Viscous Particle Segregation in Forming Chromite Layers from Slumped Crystal Slurries: Insights from Analogue Experiments. *J Petrol* 56(12):2425–44.
- Gama MA (2014) Petrographic characterization and lithogeochemistry of metacarbonate and calcisilicate rocks from Vale do Rio Jacurici. Dissertation, Federal University of Bahia. (In portuguese).
- Ghosh DB, Karki B (2017) Transport Properties of Carbonated Silicate Melt at High Pressure. *Sci Adv* 3(12):1–8.
- Greenbaum D (1977) The chromitiferous rocks of the Troodos ophiolite complex, Cyprus. *Econ Geol* 72:1175–1194

- Godel B, Barnes SJ, Gürer D et al (2013) Chromite in Komatiites: 3D Morphologies with Implications for Crystallization Mechanisms. *Contrib Mineral Petrol* 165(1):173–89.
- Hill RET, Roeder PL (1974) The crystallization of spinel from a basaltic liquid as a function of oxygen fugacity. *J Geol* 82:709–729.
- Iacono-Marziano G, Gaillard F, Pichavant M (2007) Limestone assimilation by basaltic magmas: an experimental re-assessment and application to Italian volcanoes. *Contrib. Mineral. Petrol.* 155, 719–738
- Iacono-Marziano G, Ferraina F, Gaillard F et al. (2017) Assimilation of sulfate and carbonaceous rocks: Experimental study, thermodynamic modeling and application to the Noril'sk-Talnakh region (Russia). *Ore Geol Rev* 90:399–413
- Irvine TN (1975) Crystallization Sequences in the Muskox Intrusion and Other Layered Intrusions-II. Origin of Chromitite Layers and Similar Deposits of Other Magmatic Ores. *Geochim Cosmochim Acta* 39(6–7).
- Kropschot SJ, Doebrich J (2010) Chromium—Makes stainless steel stainless: U.S. Geological Survey Fact Sheet 2010–3089, 2 p. (Also available at <https://pubs.usgs.gov/fs/2010/3089/>.)
- Le Vaillant M, Barnes SJ, Mungall JE, Mungall EL (2017) Role of degassing of the Noril'sk nickel deposits in the Permian–Triassic mass extinction event. *Proc Natl Acad Sci* 114(10):2485–2490
- Leake BE, Wooley AR, Arps CES et al (1997) Nomenclature of amphiboles: report of the subcommittee on amphiboles of the International Mineralogical Association, Commission on new minerals and mineral names. *Amer Miner* 82:1019–1037.
- Leake BE, Woolley AR, Burch WD, et al. (2003) Nomenclature of amphiboles: additions and revisions to the International Mineralogical Association's amphibole nomenclature. *Canadian Mineralogist* 41:1355–1370.
- Leblanc M (1980) Chromite growth, dissolution and deformation from a morphological view point: SEM investigations. *Miner Deposita* 15(2):201–210. doi:10.1007/bf00206514
- Lesher CE, Spera FJ (2015) Thermodynamic and Transport Properties of Silicate Melts and Magma. In Sigurdsson H, Houghton B, McNutt S, et al (eds) *The Encyclopedia of Volcanoes*, 2nd edn. Academic Press, London.
- Maier WD, Barnes S-J (2008) Platinum-group elements in the UG1 and UG2 chromitites, and the Bastard Reef, at Impala platinum mine, Western Bushveld Complex, South Africa: evidence for late magmatic cumulate instability and reef constitution. *S Afr J Geol* 111: 159–176.
- Maier WD, Barnes S-J, Groves DI (2013) The Bushveld Complex, South Africa: Formation of Platinum-Palladium, Chrome- and Vanadium-Rich Layers via Hydrodynamic Sorting of a Mobilized Cumulate Slurry in a Large, Relatively Slowly Cooling, Subsiding Magma Chamber. *Miner Deposita* 48(3):1–56.

- Maier WD, Prevec SA, Scoates JS et al (2018) The Uitkomst Intrusion and Nkomati Ni-Cu-Cr-PGE Deposit, South Africa: Trace Element Geochemistry, Nd Isotopes and High-Precision Geochronology. *Miner Deposita* 53(1):67–88.
- Marinho MM, Rocha GF, Deus PB, Viana JS (1986) Geology and chromitiferous potential from Vale do Jacurici. In 34th Congr Bras Geol, Proceedings, Goiânia, pp. 2074–88. (In Portuguese).
- Marques JC, Dias JRVP, Friedrich BM et al (2017) Thick Chromitite of the Jacurici Complex (NE Craton São Francisco, Brazil): Cumulate Chromite Slurry in a Conduit. *Ore Geol Rev* 90:131–147. Doi: 10.1016/j.oregeorev.2017.04.033
- Marques JC, Ferreira Filho CF, Carlson RW, Pimentel MM (2003) Re-Os and Sm-Nd Isotope and Trace Element Constraints on the Origin of the Chromite Deposit of the Ipueira-Medrado Sill, Bahia, Brazil. *J Petrol* 44(4):659–78.
- Marques JC, Ferreira Filho CF (2003). The Chromite Deposit of the Ipueira-Medrado Sill, São Francisco Craton, Bahia State, Brazil. *Econ Geol* 98:87–108.
- Marques JC, Frantz JC, Pimentel MM, et al (2010) U-Pb zircon geochronology of alkaline pegmatites: new constraints on the age of the Jacurici Complex, São Francisco Craton, Brazil. In: South American Symposium on Isotope Geology, Proceedings. Brasília.
- McDonald JA (1965) Liquid immiscibility as one factor in chromitite seam formation in the Bushveld igneous complex: *Econ Geol* 60:1674–1685.
- Misi A, Teixeira JBG, Silva Sá JH, et al (2012) Main Metallogenetic Domains. Gold of the Greenstone Belt of the Rio Itapicuru. In: Misi A, Teixeira JBG, Silva Sá JH. Digital metallogenetic map of the State of Bahia and main mineral provinces. Scale 1:1.000.000. Explnatory Text. Salvador, Companhia Baiana de Pesquisa Mineral, pp. 109–126. (In Portuguese).
- Mondal SK, Mathez EA (2007) Origin of the UG2 chromitite layer, Bushveld Complex. *J Petrol* 48:495–510
- Morimoto N (1989) Nomenclature of Pyroxenes. *Canad Mineral* 27:143–156.
- Mungall JE, Brenan JM, Godel B et al (2015) Transport of Metals and Sulphur in Magmas by Flotation of Sulphide Melt on Vapour Bubbles. *Nat Geosci* 8(3):216–19.
- Murck BW, Campbell IH (1986) The effects of temperature, oxygen fugacity and melt composition on the behaviour of chromium in basic and ultrabasic melts. *Geochim Cosmochim Acta* 50:1871–1887.
- Naldrett AJ, Wilson A, Kinnaird J et al (2012) The origin of chromitites and related PGE mineralization in the Bushveld Complex: new mineralogical and petrological constraints. *Miner Deposita* 47(3):209–32.
- Oliveira EP, Carvalho MJ, McNaughton NJ (2004a). Evolution of the north segment of the Itabuna-Salvador-Curaçá Orogen: Chronology of arc accretion, continental collision and terrains scape. *Geo USP Sér Cient* 4:41–53. (In Portuguese).
- Oliveira EP, Carvalho MJ, McNaughton NJ et al (2004b) Contrasting copper and chromium metallogenetic evolution of terranes in the Paleoproterozoic Itabuna-Salvador-

Curaçá orogen, São Francisco Craton, Brazil: new zircon (SHRIMP) and Sm- Nd (model) ages and their significances for orogen-parallel escape tectonics. *Precambr Res* 128:143-165.

Oliveira RCLM, Neves JP, Pereira LHM et al (2016) Geologic chart - sheet SC.24-Y-B-II Andorinha - scale 1:100.000. CPRM, Salvador.

Oliveira EP, McNaughton N, Armstrong R (2010) Mesoarchaean to palaeoproterozoic growth of the northern segment of the Itabuna-Salvador-Curaçá orogen, São Francisco craton, Brazil. In: Kusky T, Mingguo Z, Xiao Z (Eds.) *The Evolving Continents Understanding Processes of Continental Growth*. Geological Society Special Publication, pp. 263-286.

Page NJ (1971) Sulfide Minerals in the G and H Chromitite Zones of the Stillwater Complex, Montana. U.S. Geol. Survey Prof Paper 694: 20 p.

Pouchou JL, Pichoir F (1991) Quantitative analysis of homogeneous or stratified microvolumes applying the model “PAP”. In: Heinrich KFJ, Newbury DE (eds) *Electron Probe Quantitation*. Plenum Press, New York, pp 31–75.

Prichard HM, Barnes SJ, Godel B et al (2015) The structure of and origin of nodular chromite from the Troodos ophiolite, Cyprus, revealed using high-resolution X-ray computed tomography and electron backscatter diffraction. *Lithos* 218-219:87-98.

Reed SJB (1965) Characteristic fluorescence corrections in electron-probe microanalysis. *Br J Appl Phys* 16:913-926.

Silveira CJS, Frantz JC, Marques JC, et al (2015) U-Pb geochronology in zircon of intrusive and basement rocks in the region of the Jacurici Valley, São Francisco Craton, Bahia. *J Braz Geol* 45:453–474. (In Portuguese).

Spandler C, Mavrogenes J, Arculus R (2005) Origin of chromitites in layered intrusions: evidence from chromite-hosted melt inclusions from the Stillwater Complex. *Geology* 33(11):893–96.

Teixeira W, Sabaté P, Barbosa J et al (2000) Archean and Paleoproterozoic tectonic evolution of the São Francisco Craton, Brazil. In: Cordani UG, Milani EJ, Thomaz Filho A, Campos DA (eds) *Tectonic evolution of South America*, International Geological Congress, Rio de Janeiro, pp. 101-137.

Ulmer GC (1969) Experimental investigations of chromite spinels. In Wilson HDB (ed) *Magmatic ore deposits, a symposium*. Econ Geol Mon 4, pp. 114- 131.

Voordouw R, Gutzmer J, Beukes NJ (2009) Intrusive origin for Upper Group (UG1, UG2) stratiform chromitite seams in the Dwars River area, Bushveld Complex, South Africa. *Mineral Petrol* 97, 75–94. Vukmanovic Z, Barnes SJ, Reddy SM, et al (2013) Morphology and microstructure of chromite crystals in chromitites from the Merensky Reef (Bushveld Complex, South Africa). *Contrib Mineral Petrol* 165(6):1031-1050. DOI: 10.1007/s00410-012-0846-1

Wenzel T, Lukas PB, Brügmann GE et al (2002) Partial Melting and Assimilation of Dolomitic Xenoliths by Mafic Magma: The Ioko-Dovyren Intrusion (North Baikal Region, Russia). *J Petrol* 43(11):2049–2074.

Williams KL (1987) Introduction to X-ray spectrometry. Allen and Unwin, London, 370 p.

#### 4. ANEXOS

##### 4.1 Resumos e resumos expandidos de autoria da pós-graduanda publicados em anais de eventos durante o período de Mestrado

###### 4.1.1 13th International Platinum Symposium (IPS)

#### VOLATILE-RICH MINERALS ENCLOSED IN CHROMITE OF THE MASSIVE LAYER FROM THE JACURICI COMPLEX: EVIDENCE OF CRUSTAL CONTAMINATION

Betina Maria Friedrich<sup>1</sup>, Juliana Charão Marques<sup>2</sup>, Gema Olivo<sup>3</sup>, Brian Joy<sup>4</sup>, José Carlos Frantz<sup>5</sup>

<sup>1</sup>*Post-graduate student, Universidade Federal do Rio Grande do Sul, Brazil, [friedrich.betina@gmail.com](mailto:friedrich.betina@gmail.com);*

<sup>2</sup>*Associate professor, Universidade Federal do Rio Grande do Sul, Brazil; <sup>3</sup>Full professor, Queens University, Canada; <sup>4</sup>Queens University, Canada; <sup>5</sup>Full professor, Universidade Federal do Rio Grande do Sul, Brazil*

#### ABSTRACT

Mineral inclusions in chromite from the thick chromitite layer of the Jacurici Complex (Brazil) show evidences of H<sub>2</sub>O and CO<sub>2</sub> enriched magma during ore formation supporting crustal contamination as a trigger for chromite crystallization with subsequent slumping of unconsolidated slurry.

Several models have been invoked to explain the formation of massive chromitite layers<sup>1,2</sup>, however it remains debatable. In the NE São Francisco Craton, the Jacurici Complex hosts the largest chromite deposit in Brazil. The complex is interpreted as a single conolith-type intrusion, oriented N-S along more than 70-km, tectonically disrupted forming many different segments. It is emplaced between quartz-feldspathic orthogneiss at the base and calc-silicate rocks and marbles at the top. The basal part of the intrusion is mostly composed by dunites with increase abundance of pyroxene towards the top. It is followed by a 5 to 8 m thick massive chromitite layer (MCL). Above the MCL, normal fractionation trends occur forming norite and gabbronorites<sup>3-5</sup>. The parental magma is interpreted as very primitive (Fo up to 94). Petrological studies suggest a magma derived from partial melt of a sub-continental lithospheric mantle that was submitted to contamination at the interval of ore formation<sup>4</sup>. Carbonate rocks from the top of the complex were suggested to have been assimilated and triggered chromite crystallization<sup>5,6</sup>.

The aim of this study is to characterize the chromite-hosted inclusions in the MCL interval. Chromite is a refractory mineral that can preserve primary magmatic phases allowing for a better

understanding of the petrogenetic processes responsible for the deposit formation.

We selected the samples chromitite layer of the Monte Alegre Sul (MAS) segment, located in the central part of the complex, about 25 km north of the current underground operation (Ipueira Mine). The MAS segment is folded and offset by a number of faults. The MCL is 8 m thick and is mainly represented by a massive chromitite containing 70-90 vol% of chromite, with an 80 cm thick semi-massive basal interval, with approximately 50 vol% chromite. The basal contact with serpentinite is gradual and the upper contact is abrupt and irregular, resembling erosive contact. Detailed petrographic studies of the chromite-hosted inclusions were performed using transmitted and reflected light microscopy, and scanning electron microscope (SEM) at Universidade Federal do Rio Grande do Sul. Quantitative microanalyses were carried out using a JEOL JXA-8230 Electron Microprobe at Queens University.

Individual chromite grains are mainly anhedral to subhedral with rare well-formed crystals. Chromite granulometry varies from 25 µm to 800 µm (0.8 mm), with modal grain size around 0.3-0.4 mm. Chromite grains in the MCL contain abundant inclusions. Orthopyroxene is the second most abundant cumulus phase and occurs as fine-grained crystals and as large

poikilitic crystals enclosing dozens of chromite grains. Diopside and olivine are minor cumulus phases. Chromitite samples are ad- to mesocumulates, showing up to 10% intercumulus minerals, composed mainly by magnesiohornblende and minor phlogopite and rutile.

Circa 70-90% of the chromite crystals host inclusions. Inclusion-bearing grains occur side-by-side with inclusion-free grains. The distribution of the inclusions within chromite grains is random. Inclusions can reach up to 50 µm, the majority ranging around 5-20 µm, and comprise silicates, carbonates, sulphides and oxides, in decreasing order of abundance. Silicate inclusions are usually monophase and comprise enstatite, magnesiohornblende, phlogopite, diopside and olivine. Amphibole and phlogopite commonly show sub- to euhedral prismatic habits. Among carbonate inclusions, magnesite dominates over dolomite, and they usually have rounded or irregular shapes, or negative-crystal shapes. Dolomite and magnesite commonly occur as composite inclusions associated to sulphides. Sulphide inclusions are predominately pentlandite and millerite, with minor reequilibrium to heazlewoodite, pyrite and chalcopyrite and rare pyrrhotite. Rutile inclusions are described in the top of the MCL sequence.

Cumulus and intercumulus minerals have slight enrichment in lighter and more incompatible elements in comparison to inclusions suggesting that all derived from the same magma. The isolated character and sub- to euhedral habits of most of the silicate inclusions suggest they were already crystallized when trapped by chromite indicating early hydration of the magma. On the other hand, the shape of the carbonate inclusions suggests entrapment of a liquid phase. Common association of carbonate and sulphide in inclusions imply that sulphide liquid could have been transported in compound drops of sulphide liquid-carbonated volatile, as suggested by experiments

## REFERENCES

1. NALDRETT, A. J., WILSON, A., KINAIRD, J., YUDOVSAYA, M. & CHUNETT, G. (2012): The origin of chromitites and related PGE mineralization in the Bushveld Complex: New mineralogical and petrological constraints. *Miner. Depos.* 47, 209–232.
2. MAIER, W. D. BARNE S. J., GROOVES, D. I. (2013): The Bushveld Complex, South Africa: Formation of platinum-palladium, chrome- and vanadium-rich layers via hydrodynamic sorting of a mobilized cumulate slurry in a large, relatively slowly cooling, subsiding magma chamber. *Miner. Depos.* 48, 1–56.
3. MARQUES, J.C., FERREIRA FILHO, C. F. (2003): The Chromite Deposit of the Ipueira-Medrado Sill , São Francisco Craton , Bahia State , Brazil. *Econ. Geol.* 98, 87–108.
4. MARQUES, J.C., FERREIRA FILHO, C. F, CARLSON, R.W., PIMENTEL, M. M. (2003): Re-Os and Sm-Nd Isotope and Trace Element Constraints on the Origin of the Chromite Deposit of the Ipueira-Medrado Sill, Bahia, Brazil. *J. Petrol.* 44, 659–678.
5. MARQUES, J. C., DIAS, J.R.V., FRIEDRICH, B.M., FRANTZ, J.C., QUEIROZ, V.J.A., BOTELHO, N.F. (2017): Thick chromitite of the Jacurici Complex (NE Craton São Francisco, Brazil): Cumulate chromite slurry in a conduit. *Ore Geol. Rev.*

performed by<sup>7</sup>, and were then entrapped together in the chromite crystals.

Os and Nd isotopic data and the presence of amphibole near and after the MCL suggest crustal contamination and addition of fluids to explain chromite formation<sup>4</sup>. Similar processes and assimilation of carbonate rocks are proposed by other authors<sup>4,6</sup>. The large amount of hydrated minerals enclosed in chromite and as intercumulus phases confirm the magma was substantially hydrated during the time of chromitite formation.

Our findings also confirm the presence of CO<sub>2</sub> and S-saturation previous or during chromite crystallization. The addition of CO<sub>2</sub>, S and water to the magma due possibly to assimilation of marbles and calc-silicate host rocks could explain the formation of all observed inclusions. Contamination with water and CO<sub>2</sub> affect oxygen fugacity<sup>8,9</sup> and favour crystallization of chromite.

Marques et al.<sup>5</sup> suggested a semi-consolidate slurry had sagged from the conduit to explain the thickness of the MCL. Inclusion-bearing and inclusion-free chromite grains is related to crystallization as a response to fast and lower chromite grow rate, respectively, as already proposed for chromites in the Ylgarn Craton<sup>10</sup>. Remobilization of accumulated chromite crystals by dense slurries could explain the two types of chromite occurring at the same interval. The presence of CO<sub>2</sub> bubbles in the magma of the Jacurici Complex could facilitate slumping of incompletely solidified cumulates, as also suggested for the Uitkomst intrusion<sup>11</sup>.

## Acknowledgements

The authors acknowledge the FERBASA Group for providing support for the fieldwork and allowing access and sapling of the drill core.

6. FERREIRA FILHO, C. F. & ARAUJO, S. M. (2009): Review of Brazilian chromite deposits associated with layered intrusions: geological and petrological constraints for the origin of stratiform chromitites. *Appl. Earth Sci.* 118, 86–100.
7. MUNGALL, J. E., BRENNAN, J. M., GODEL, B., BARNES, S. J. & GAILLARD, F. (2015): Transport of metals and sulphur in magmas by flotation of sulphide melt on vapour bubbles. *Nat. Geosci.* 8, 216–219.
8. FEIG, S. T., KOEPKE, J. & SNOW, J. E. (2006): Effect of water on tholeiitic basalt phase equilibria: An experimental study under oxidizing conditions. *Contrib. to Mineral. Petrol.* 152, 611–638.
9. WENZEL, T., BAUMGARTNER, L. P., KONNIKOV, E. G., BRU, G. E. & KISLOV, E. V. (2002): Partial Melting and Assimilation of Dolomitic Xenoliths by Mafic Magma: the Ioko-Dovyren Intrusion (North Baikal Region, Russia). *J. Petrol.* 43, 2049–2074.
10. GODEL, B., BARNES, S. J., GÜRER, D., AUSTIN, P. & FIORENTINI, M. L. (2013): Chromite in komatiites: 3D morphologies with implications for crystallization mechanisms. *Contrib. to Mineral. Petrol.* 165, 173–189.
11. MAIER, W. D., PREVEC, S. A., SCOATES, J. S., WALL, C. J., BARNES, S.-J., GOMWE, T. (2018): The Uitkomst intrusion and Nkomati Ni-Cu-Cr-PGE deposit, South Africa: trace element geochemistry, Nd isotopes and high-precision geochronology. *Miner. Depos.* 53, 67–88.

#### 4.1.2 VIII Simpósio Brasileiro de Exploração Mineral (SIMEXMIN) / I Encontro Nacional dos Estudantes de Geologia Econômica (ENAGE)

#### **Inclusões minerais em cromita da Camada de Cromitito Principal como novas evidências de contaminação crustal para o Complexo Jacurici, BA**

Friedrich. B.M.<sup>1</sup>; Marques, J.C.<sup>1</sup>; Olivo, G.<sup>2</sup>, Joy, B.<sup>2</sup>, Frantz, J.C.<sup>1</sup>  
<sup>1</sup>: Universidade Federal do Rio Grande do Sul; <sup>2</sup>: Queen's University

O Complexo Jacurici contém o maior depósito de cromo do Brasil e apresenta mineralização de Ni-Cu. É composto por várias intrusões máfico-ultramáficas delgadas (<300 m) que hospedam uma camada de 5-8 m de espessura de cromitito maciço. As intrusões são interpretadas como partes tectonicamente segmentadas de um conduto alimentador de um volumoso magmatismo. Os mecanismos de formação deste cromitito, assim como de outros em vários locais do mundo permanecem pouco compreendidos. Neste estudo caracterizamos minerais inclusos em cromita da Camada de Cromitito Principal (CCP) do corpo Monte Alegre Sul, localizado cerca de 25 km a norte da Mina de Ipueira. O trabalho teve por objetivo entender os processos petrogenéticos responsáveis pela formação do depósito. Os estudos petrográficos foram realizados na UFRGS e as análises de microssonda na Queen's University (Canadá). A CCP possui 8 m de espessura, em sua maior parte composta por cromitito contendo 70-90% de cromita como fase cumulus principal. Enstatita é a segunda fase cumulus mais abundante, ocorrendo ainda diopsídio e olivina de forma restrita. As amostras contém até 10% de magnesiohornblenda e, subordinadamente, flogopita e rutilo como minerais intercumulus. Cristais de cromita incluem grande quantidade e variedade de minerais. Inclusões silicáticas são geralmente monofásicas e compostas por enstatita, magnesiohornblenda, flogopita, diopsídio e olivina. É comum anfibólio e flogopita apresentarem hábitos prismáticos. Inclusões carbonáticas (magnesita e dolomita) possuem formas arredondadas, irregulares, ou formas de cristais negativos. Inclusões de sulfetos são compostas por pentlandita e millerita, com

reequilíbrios a heazlewoodita, pirita e calcopirita, e mais raro pirrotita. Inclusões de rutilo ocorrem no topo da sequência. A química das inclusões, minerais cumulus e intercumulus sugere que todos cristalizaram a partir do mesmo magma. O caráter isolado e hábitos sub- a euédricos das inclusões hidratadas apontam para aprisionamento de fases previamente cristalizadas, indicando hidratação precoce do magma. Já as formas das iclusões carbonáticas sugerem aprisionamento de fase líquida, indicando presença de gotas de líquido carbonático imiscível no magma silicatado. Saturação precoce em S é sugerida pelas abundantes inclusões de sulfetos. As observações confirmam que o magma estava saturado em H<sub>2</sub>O, CO<sub>2</sub> e S previamente ou durante a cristalização da cromita. A presença de voláteis é entendida como facilitadora de fluxos de massa dentro de câmaras magmáticas, interpretados como responsáveis por promover acamamento e espessamento de camadas de minério nos mais recentes modelos de formação de cromititos maciços. Contaminação por rochas carbonáticas foi também identificada na intrusão considerada conduto alimentador da maior província mineral do mundo, o Complexo de Bushveld. As observações reforçam a ideia de que assimilação de rochas carbonáticas e adição de água tiveram papel importante na formação do cromitito no Complexo Jacurici e retomam a discussão sobre a importância de contaminação crustal na origem de grandes depósitos de óxidos e sulfetos magmáticos em intrusões mafico-ultramáficas.

#### 4.1.3 14th SGA Biennial Meeting

## The mafic-ultramafic Jacurici Complex (NE Brazil): a chromite-hosted mineral inclusions study

**Betina M. Friedrich, Juliana C. Marques, João Rodrigo V. P. Dias, José Carlos Frantz**  
*Universidade Federal do Rio Grande do Sul*

**Nilson F. Botelho**  
*Universidade de Brasília*

**Abstract.** The Monte Alegre Sul is a segment of the mafic-ultramafic intrusion Jacurici Complex and hosts an up to 8-m-thick chromitite layer. Chromite-hosted inclusions are abundant along the entire chromitite layer. Inclusions are usually 10-20 µm in size, normally randomly distributed and composed of a single mineral phase that comprises olivine, ortho- and clinopyroxene, amphibole, phlogopite, magnetite and pentlandite. Chromite-hosted hydrated silicate inclusions indicate that the magma in which chromite crystallized contained early formed hydrous minerals or became hydrated. The chromitite massive layer interval occurs at a stratigraphic level where significant petrological changes occur. We suggest in this study that crustal contamination releasing fluids into the magma during magma ascent through conduits could have played an important role in the extensive chromite crystallization and formation of the thick chromitite layer.

### 1 Introduction

Solid inclusions within chromite grains have been described in disseminated and massive chromitites both in ophiolitic and stratiform tectonic environments. The association of solid inclusions in chromite has been recognised as being related to the factors controlling the formation of chromitites since the 1960s (McDonald 1965). Since then, several attempts have been made to understand the mechanisms of entrapment and the relationship of the chromite-hosted solid inclusions and the origin of massive chromitites (e.g. Irvine 1975; Peng et al. 1995; Li et al. 2005; Spandler et al. 2005). Although the Jacurici Complex hosts one of the thickest

chromitite layer in the world and represents the Brazilian largest chromium deposit, no attempt has been made so far to investigate its origin in the light of chromite-hosted solid inclusions. This study aimed to better constraint magma conditions at the time of chromite crystallization and shed some light on chromitite formation.

## 2 Geological setting

The Jacurici Complex, located in the São Francisco Craton, Northeastern Brazil, is composed by several mafic-ultramafic bodies, many of them mineralized with chromite. The bodies are believed to be disrupted segments of a single intrusion (Marques et al. 2017, *in press*). The Complex intrudes gneisses of the Mesoarchean Santa Luz Complex (Silveira et al. 2015) and presents a general N-S orientation cropping out parallel to the Paleoproterozoic Itiuba Syenite (Fig. 1) and extending along a belt of at least 70 km long. The bodies are thin (up to 300 m) and host massive chromitite layers of variable thickness, ranging up to 8 m thick in some segments. The Monte Alegre Sul (MAS) segment occurs in the central part of the Complex and was mined in the 1970's in open pit by the FERBASA Group. The mineralized layer has an average thickness of 5 m and is found between 50 and 150 m deep (Marinho et al. 1986).

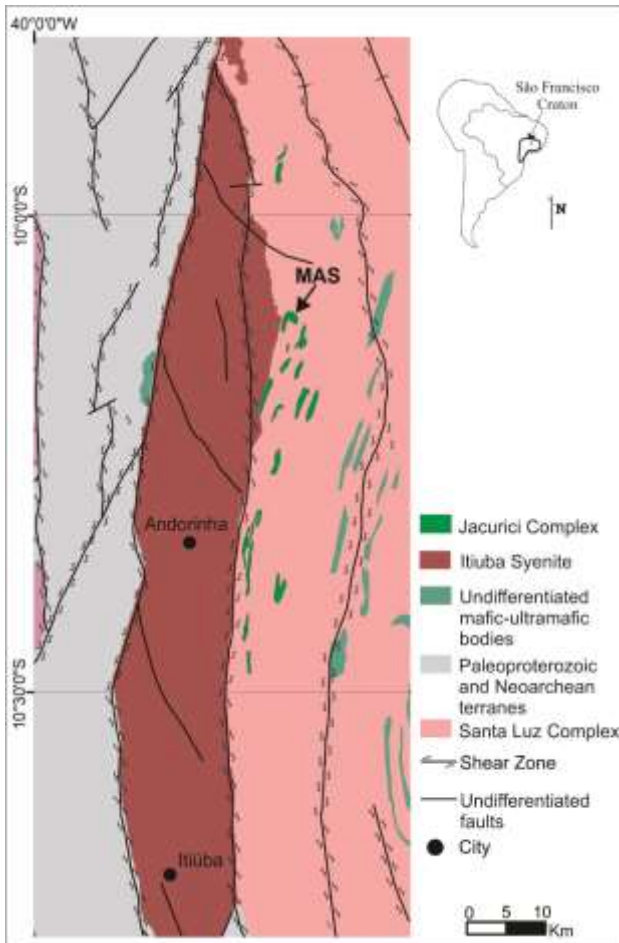


**Figure 1.** Simplified geological map of the Jacurici Complex area. Monte Alegre Sul segment is indicated by an arrow. Geology from Kosin et al. (2004)

## 3 Sampling and analytical procedures

The drill core MAS-105-65° of the Monte Alegre Sul segment was selected and carefully described. Representative silicate samples and regularly close spaced massive chromitite samples were collected. Polished thin sections of chromitite were analysed using a scanning electron microscope (SEM), JEOL 6610-LV, equipped with an energy dispersive spectrometer (EDS), Bruker Nano XFlash Detector 5030, at the Laboratório de Geologia Isotópica from the Universidade Federal do Rio Grande do Sul. The aim was to identify chromite-hosted mineral inclusions. The SEM was operated with 15 kV acceleration potential and 14 mm working distance. The standard ZAF calibration method was applied. Complementary analyses for major and minor elements of selected inclusions were performed using an electron microprobe, JEOL JXA-8230 at Universidade de Brasília. The equipment was operated with 15 kV acceleration potential and a 20 nA beam current, using natural mineral standards and standard ZAF matrix corrections. Care was taken to avoid fractures and interference with the host chromite.

## 4 Results

### 4.1 Stratigraphy of the Monte Alegre Sul

The MAS-105-65° borehole intercepts 55 m of a mafic-ultramafic intrusion hosting an almost 8 m thick massive chromitite layer. The stratigraphy of the Monte Alegre Sul (Fig. 2) fits in the division proposed by Marques & Ferreira-Filho (2003) for the Ipueira and Medrado areas, located about 30 km to the south, and can be divided into a Mafic Zone and an Ultramafic Zone. The Mafic Zone is only represented by an interval of about 6 m thick and is constituted by an altered gabbro in tectonic contact with basement rocks. The Ultramafic Zone can be subdivided into an Upper Ultramafic Unit, a Main Chromitite Layer (MCL) and a Lower Ultramafic Unit. The Upper Ultramafic Unit is 35 m thick and is represented by the predominance of pyroxenite with lenses of lherzolite. The MCL will be detailed in the next section. The Lower Ultramafic Unit has only its upper part recovered and is represented by serpentinite.

### 4.2 Main Chromitite Layer

The contacts between the MCL and the host rocks are faulted though it is possible to observe a banding at the basal contact, marked by interlayered centimetre-tick silicate lamina and millimetre-tick chromitite lamina (Fig. 3a), followed by an upward increasing in chromite content. Most of the MCL is represented by massive chromitite containing 90 vol% or more of chromite (Fig. 3b), showing interstitial pyroxene, amphibole and serpentine. Chromite grains are mainly subhedral, well preserved and very fine-grained, ranging 0.25 mm and, in a few cases, up to 1 mm.

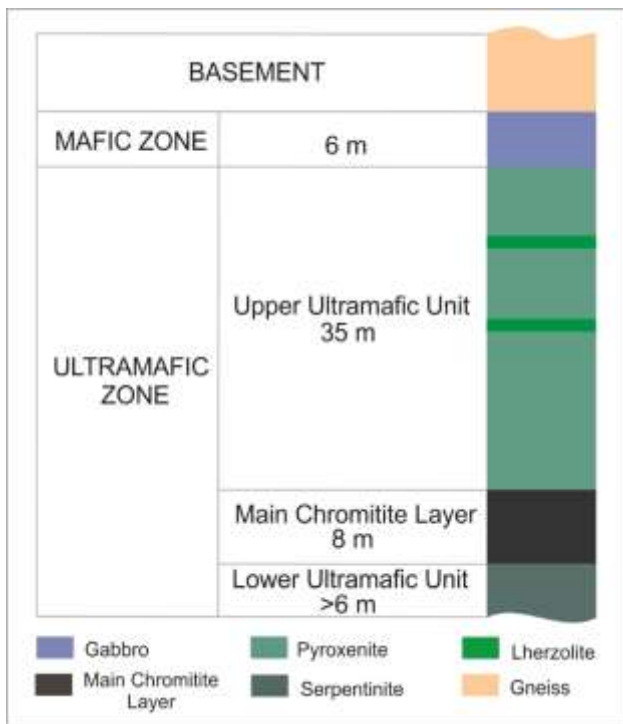


**Figure 2.** Stratigraphy of the MAS-105-65° drill core. The Lower Ultramafic Unit is not completed once the drilling stopped after achieving the MCL.

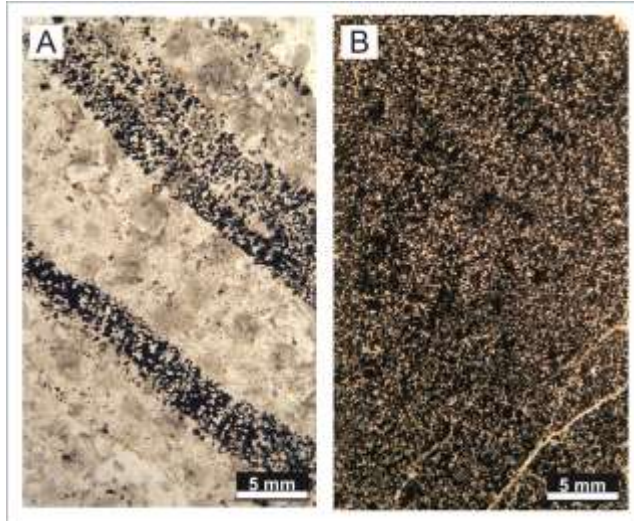


**Figure 3.** General aspect of a banded chromitite closed to the basal contact and **b** fine-grained massive ore.

#### 4.3 Chromite-hosted solid inclusions

Along the entire MCL interval inclusions within chromite grains are abundant, though they are less frequent near the layer's core. Most of the chromite grains host at least one inclusion, but the number of inclusions is variable. In a single thin section inclusion-free chromite grains can occur side by side with inclusion-bearing grains (Fig. 4a). In inclusion-rich chromite, the inclusions can account for as much as 15% of the host grain surface (Fig. 4b). Most of the inclusions are randomly distributed, though in some cases they can form an internal corona, following the chromite crystallography (Fig. 4c). Inclusions can

reach the size of 50 µm, the majority ranging around 10-20 µm. Spherical and anhedral inclusions are common (Fig. 4a and b), however several show subhedral prismatic habit (Fig. 4c) or show outlines that appear to follow chromite symmetry (Fig. 4d); tiny hexagonal euhedral inclusions are rare. Most of the inclusions consist of a single silicate phase, among which phlogopite (Fig. 4e), olivine, clinopyroxene, orthopyroxene and amphibole (Fig. 4f) were identified so far; inclusions of magnetite are frequent; inclusions of pentlandite are rare; one semi-included zircon was found. It is not unusual that a single chromite grain hosts inclusions of almost all the cited minerals (Fig. 4f).

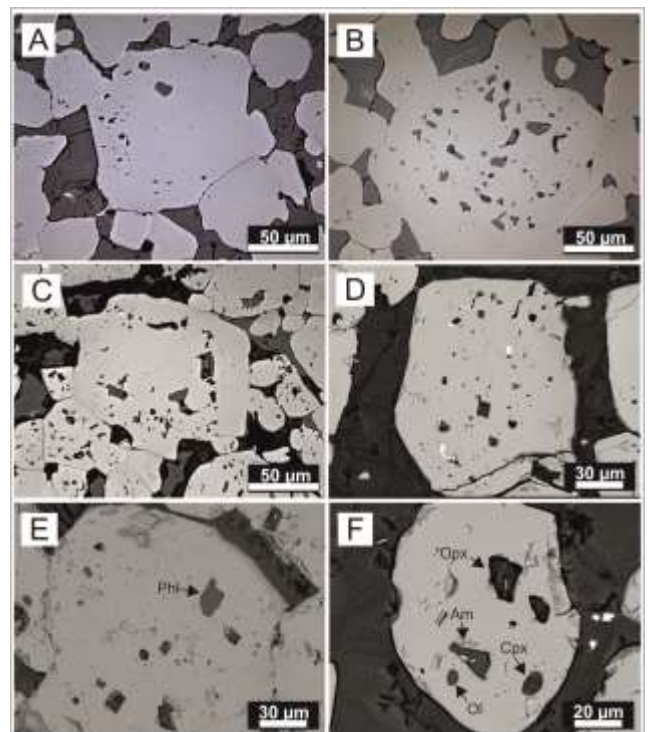


**Figure 4.** **a-c** Photomicrographs with reflected light and **d-f** back-scattered SEM images of mineral inclusions within chromite grains. Phi: phlogopite; Opx: orthopyroxene; Cpx: clinopyroxene; Am: amphibole; Ol: olivine. See main text for explanations.

#### 5 Discussion

The subhedral and euhedral inclusions, along with the single phase character point to entrapment of early crystallized minerals by chromite rather than entrapment of melt in which chromite was forming. Even anhedral and spherical inclusions are composed of one homogeneous phase and do not resemble trapped melt.

The observed internal coronas formed by the mineral inclusions seem to indicate (1) a period of interruption in chromite crystallization allowing precipitation of other minerals around chromite grain boundary followed by a new chromite grow event or (2) that some moments in the chromite formation history are more suitable for mineral entrapment. If the second hypothesis is true and the bulk of chromite is inclusion-bearing, the factors controlling chromite

crystallization can be related to those favouring mineral entrapment.

One important feature regarding inclusions composition is the hydrated nature of some of them (phlogopite and amphibole). These minerals indicate that the primitive magma from which chromite crystallized was initially hydrous or that it became hydrated by the time of chromite crystallization. The presence of hydrous minerals as inclusions in chromite has been reported from various important stratiform chromitite deposits – Bushveld Complex (McDonald 1965; Li et al. 2005), Stillwater Complex (Page 1971; Spandler et al. 2005), Muskox Intrusion (Irvine 1975), Bird River Sill (Talkington et al. 1983) – as well as in ophiolitic chromitites – Oman Ophiolite (Lorand & Ceuleneer 1989; Borisova et al. 2012), Hongguleleng Ophiolite (Peng et al. 1995) and many other minor ophiolites (Talkington et al. 1984). Several authors interpret the presence of these hydrous silicate inclusions as a result of reaction between primitive magmas and fluids, either in a magma chamber context (Peng et al. 1995; Borisova et al. 2012) or in a localized context within inclusions (Li et al. 2005).

Previous workers from the Jacurici Complex have recorded important changes in the magmatic system occurring exactly in the MCL interval. Marques et al. (2003) performed Os and Nd isotopic studies on the Ipueira and Medrado segments and suggest that crustal contamination occurred in MCL interval. Ferreira Filho & Araujo (2009) assumed crustal contamination as a trigger for the MCL formation in the Ipueira and Medrado areas; they suggest increase in oxygen fugacity of the magma, caused by assimilation of carbonate-rich wall rocks. Marques and Ferreira Filho (2003) and Marques et al. (2017, in press) propose that the Jacurici Complex represents remnants of a feeder dike of a large igneous continental province; they consider that huge volumes of primitive magma would be required to explain the anomalously thick chromitite layer in thin mafic-ultramafic intrusions.

In a combined model of chromite formation inside a conduit emplaced in metasedimentary rocks (Marques et al. 2003, Ferreira Filho e Araujo 2009, Marques et al. 2017, in press) argue that primitive magma-wall rock interaction could be expected and crustal contamination involving hydration becomes a possible scenario. The presence of water in the magmatic system is known to widen the stability field of chromite (Ford et al. 2002; Feig et al. 2006), thus favoring extensive chromite crystallization. Fast growth rate is assumed to be required for entrapment of large amounts of small melt inclusion in chromite of komatiites (Barnes 1985; Godel et al. 2013). Considering wall rock assimilation, crustal fluids released into the magma could contribute to fast chromite growth rate, explaining the abundance of trapped minerals.

Chromite-hosted mineral inclusions were already observed in chromitites of other segments in the Jacurici Complex. Detailed work should thus be extended to tentatively map possible stratigraphic and/or geographic variations in the textures and compositions of these inclusions.

## 6 Conclusions

The presence of hydrous silicate mineral inclusions in chromite suggests that the parental magma was initially hydrous or became hydrated during formation of the Jacurici Complex massive chromitite. Although magma hydration and even the role of hydrated fluids remains debatable, it is believed that magma-wall rock interaction accompanied by addition of fluids could have played an important role in chromitite formation. Furthermore, hydrated primitive magmas seem to be a significant feature in chromitite deposits worldwide, so an interaction between fluids and primitive magmas appears to contribute to chromitite formation.

## Acknowledgements

The authors acknowledge the FERBASA Group for allowing access and sampling of the drill core, and for providing support for the fieldwork. We also acknowledge CNPq for the scholarships related to this project. We are also grateful to Michele Santos, who kindly revised the language.

## References

- Barnes SJ (1985) The petrography and geochemistry of Komatiite flows from the Abitibi greenstone-belt and a model for their formation. *Lithos* 18:241-270
- Borisova AY, Ceuleneer G, Kamenetsky VS, Arai S, Béjina F, Abily B, Bindeman IN, Polvé M, Parseval P, Aigouy T, Pokrovski G (2012) A NewView on the Petrogenesis of the Oman Ophiolite Chromitites from Microanalyses of Chromite-hosted Inclusions. *J Petrol* 33: 2411-2440.
- Feig ST, Koepke J, Snow JE (2006) Effect of water on tholeiitic basalt phase equilibria: an experimental study under oxidizing conditions. *Contrib Mineral Petrol* 152: 611-638.
- Ferreira Filho CF, Araujo SM (2009) Review of Brazilian chromite deposits associated with layered intrusions: geological and petrological constraints for the origin of stratiform chromitites. *Applied Earth Sciences (Trans. Inst. Min. Metall. B)* 118, 86-100.
- Ford CE, Biggar GM, Humphries DJ, Wilson G, Dixon D, O'Hara MJ (1972) Role of water in the evolution of the lunar crust; an experimental study of sample 14310; an indication of lunar calc-alkaline volcanism. *Proceedings of 3rd Lunar Scientific Conference. Geochim Cosmochim Acta Supplement* 3:207-229.
- Godel BM, Barnes SJ, Gurer D, Austin P, Fiorentini ML (2013) Chromite in komatiites: 3D morphologies with implications for crystallization mechanisms. *Contrib Mineral Petrol* 165:173-189
- Irvine TN (1975) Crystallization sequences in the Muskox intrusion and other layered intrusions – II. Origin of chromite layers and similar deposits of other magmatic ores. *Geochim Cosmochim Acta* 39: 991-1020.
- Kosin M, Angelim LAA, Souza JD et al (2004) Carta Geológica do Brasil ao Milionésimo, Sistema de Informações Geográficas Programa Geologia do Brasil, CPRM, Brasília, CD-ROM.
- Li C, Ripley EM, Sarkar A, Shin D, Maier WD (2005) Origin of phlogopite-orthopyroxene inclusions in chromites from the Merensky Reef of the Bushveld Complex, South Africa. *Contrib Mineral Petrol* 150: 119-130
- Lorand JP, Ceuleneer G (1989) Silicate and base-metal sulfide inclusions in chromites from the Maqsad area (Oman ophiolite, Gulf of Oman): A model for entrapment. *Lithos* 22:173-190.

- McDonald JA (1965) Liquid immiscibility as one factor in chromite seam formation in the bushveld igneous complex. Econ Geol 60: 1674-1685.
- Marinho MM, Rocha GF, Deus PB, Viana JS (1986) Geologia e potencial cromítifero do Vale do Jacurici-Bahia. 34th Congr Bras Geol, Goiânia, Anais 5, 2074-2088.
- Marques JC, Ferreira Filho CF (2003) The Chromite Deposit of the Ipueira-Medrado Sill, São Francisco Craton, Bahia State, Brazil. Econ Geol 98: 87-108.
- Marques JC, Ferreira Filho CF, Carlson RW, Pimentel MM (2003) Re-Os and Sm-Nd isotope and trace element constraints on the origin of the chromite deposit of the Ipueira-Medrado Sill, Bahia, Brazil. J Petrol 44:659-678.
- Page NJ (1971) Sulfide Minerals in the G and H Chromitite Zones of the Stillwater Complex, Montana. Geol Surv Prof Paper 694: 1-20.
- Peng G, Lewis J, Lipin B, McGee J, Bao P, Wang X (1995) Inclusions of phlogopite and phlogopite hydrates in chromites from the Hongguleleng ophiolite in Xinjiang, northwest China. Amer Miner 80: 1307-1316.
- Silveira CJS, Frantz JC, Marques JC, Queiroz WJA, Roos S, Peixoto VM (2015) Geocronologia U-Pb em zircão de rochas intrusivas e de embasamento na região do Vale do Jacurici, Cráton do São Francisco, Bahia. Braz J Geol 45:453-474.
- Spandler C, Mavrogenes J, Arculus R (2005) Origin of chromitites in layered intrusions: Evidence from chromite-hosted melt inclusions from the Stillwater Complex. Geology 33(11):893-896.
- Talkington W, Watkinson DH, Whittaker PJ, Jones PC (1983) Platinum-Group-Mineral Inclusions in Chromite from the Bird River Sill, Manitoba. Miner Depos 18:245-255.
- Talkington W, Watkinson DH, Whittaker PJ, Jones PC (1984) Platinum-Group Minerals and Other Solid Inclusions in Chromite of Ophiolitic Complexes: Occurrence and Petrological Significance. Tscher Mineral Petrogr Mitt 32:285-301.

## 4.1.4 48º Congresso Brasileiro de Geologia (CBG)

**ESTUDO PETROGRÁFICO E VARIAÇÃO CRÍPTICA DO CROMITITO DE MONTE ALEGRE SUL, COMPLEXO JACURICI – BA***Friedrich, B.M.<sup>1</sup>; Marques, J.C.<sup>1</sup>, Dias, J.R.V.P.<sup>1</sup>, Roos, S.<sup>1</sup>, Botelho, N.F.<sup>2</sup>, Frantz, J.C.<sup>1</sup>*<sup>1</sup>Universidade Federal do Rio Grande do Sul; <sup>2</sup>Universidade de Brasília

**RESUMO:** O Complexo Jacurici é composto por diversos corpos maficos-ultramáficos, mineralizados a cromita, com orientação N-S, que se estendem ao longo de uma faixa de aproximadamente 100 km de extensão, na porção NE do Cráton São Francisco. O corpo Monte Alegre Sul (MAS) ocorre na região central do complexo e está localizado no município de Monte Santo – BA. A sul e a norte, respectivamente, ocorrem os corpos Ipueira-Medrado e Várzea do Macaco já previamente estudados. Todos estes corpos apresentam uma espessa camada maciça de cromita que está sendo investigada para avaliar uma possível correlação. O objetivo deste estudo é investigar as variações petrográficas e químicas ao longo do cromitito do corpo MAS, comparar resultados com os obtidos nos outros corpos e interpretar o significado das semelhanças e diferenças observadas. Para atendimento do objetivo, foi selecionado o furo de sondagem MAS-105-65º que intercepta 8 m de cromitito maciço correspondente à Camada de Cromitito Principal e 1 m de uma camada subordinada de cromitito que ocorre estratigraficamente acima. O teor de cromita nas amostras de cromitito variam de 70 a 95%. Nesta etapa, foram selecionadas cinco amostras do Cromitito Principal para petrografia e química mineral de cromoespínélio, sendo as análises de microssonda realizadas na UnB. A maior parte do Cromitito Principal é representada por cromitito maciço, com teores de cromita iguais ou superiores a 90%. O Cromitito Principal apresenta dois intervalos, um próximo à base e um no centro da camada, com teores mais baixos de cromita, entre 70 e 80%, caracterizados pela presença de grandes cristais (até 1 cm) de olivina e piroxênio poiquiliticos, envolvendo os grãos de cromita. Os grãos de cromita são subédricos, bem preservados, apresentando granulometria fina, até 0,25 mm. A razão de Cr varia de 55,4 a 66,0; a razão de Al varia de 29,8 a 36,5; a razão de Fe<sup>3</sup> varia de 0,7 a 12,6; a razão de Mg varia de 52,4 a 72,3. Al apresenta tendência de empobrecimento enquanto que Fe<sup>3</sup> e Mg tendem a enriquecer para o centro da camada. Tais tendências não são observadas para a razão de Cr. As faixas de cromitito com textura poiquilitica também ocorrem em Ipueira-Medrado e Várzea do Macaco e, à exceção de Fe<sup>3</sup>, as tendências de variação nas razões dos elementos são similares. As amostras do cromitito principal dos três corpos ocupam a mesma região no diagrama Cr-Al-Fe<sup>3</sup> para cromoespínélios. As observações petrográficas e químicas tem mostrado grande similaridade entre o corpo Monte Alegre Sul e os demais corpos do Jacurici, indicando que eles possam constituir um único corpo, fragmentado tectonicamente. Será ainda investigada a camada de cromitito subordinada e realizado estudos de variação críptica em minerais silicáticos ao longo de todo o corpo.

**PALAVRAS-CHAVE:** COMPLEXO ESTRATIFORME; QUÍMICA MINERAL; CROMITA.

## 4.2 Artigo científico de coautoria da pós-graduanda publicado durante o período de Mestrado



### Thick chromitite of the Jacurici Complex (NE Craton São Francisco, Brazil): Cumulate chromite slurry in a conduit



Juliana Charão Marques<sup>a,\*</sup>, João Rodrigo Vargas Pilla Dias<sup>a</sup>, Betina Maria Friedrich<sup>a</sup>, José Carlos Frantz<sup>a</sup>, Waldemir José Alves Queiroz<sup>b</sup>, Nilson Francisquini Botelho<sup>c</sup>

<sup>a</sup> Instituto de Geociências, Universidade Federal do Rio Grande do Sul, Av. Bento Gonçalves 9500 Prédio 43129, Porto Alegre, RS CEP 91501-970, Brazil

<sup>b</sup> Companhia de Ferro Ligeira da Bahia – FERBALA, Pojuca, BA, Brazil

<sup>c</sup> Instituto de Geociências – Universidade de Brasília, Brazil

#### ARTICLE INFO

##### Article history:

Received 31 July 2016

Received in revised form 26 April 2017

Accepted 30 April 2017

Available online 3 May 2017

##### Keywords:

Chromite deposit

Mafic-ultramafic layered complex

Chromite slurry

Conduit

#### ABSTRACT

The Jacurici Complex, located in the NE part of the São Francisco Craton, hosts the largest chromite deposit in Brazil. The mineralized intrusion is considered to be a single N-S elongated layered body, disrupted into many segments by subsequent deformation. The ore is hosted in a thick, massive layer. Two segments, Ipueira and Medrado, have been previously studied. We provide new geological information and chromite composition results from the Monte Alegre Sul and Várzea do Macaco segments located farther north, and integrate these with previous results. The aim of this study is to determine and discuss the magma chamber process that could explain the formation of the thick chromitite layer. All segments exhibit similar stratigraphic successions with an ultramafic zone (250 m thick) hosting a 5–8 m thick main chromitite layer (MCL), and a mafic zone (40 m thick). The chromite composition of the MCL, Mg-numbers (0.48–0.72) and Cr-numbers (0.59–0.68), is similar to chromites from layered intrusions and other thick chromitites. Previous work concluded that the parental magma of the mineralized intrusion was very primitive based on olivine composition (up to Fo<sub>91</sub>) and orthopyroxene composition (up to En<sub>94</sub>) from harzburgite samples, and that it originated from an old subcontinental lithospheric mantle. We estimate that the melt from which the massive chromitite layer crystallized was similar to a boninite, or low siliceous high-Mg basalt, with a higher Fe/Mg ratio. The petrologic evidence from the mafic-ultramafic rocks suggests that a high volume of magma flowed through the sill, which acted as a dynamic conduit. Crustal contamination has previously been considered as the trigger for the chromite crystallization, based on isotope studies, as the more radiogenic signatures correlate with an increase in the volumetric percentage of amphibole (up to 20%). The abundant inclusions of hydrous silicate phases in the chromites from the massive ore suggest that the magma was hydrated during chromite crystallization. Fluids may have played an important role in the chromite formation and/or accumulation. However, the trigger for chromite crystallization remains debatable. The anomalous thickness of the chromitite is a difficult feature to explain. We suggest a combined model where chromite crystallized along the margins of the magma conduit, producing a semi-consolidated chromite slurry that slumped through the conduit forming a thick chromitite layer in the magma chamber where layered ultramafic rocks were previously formed. Subsequently, the conduit was obstructed and the resident magma fractionated to produce a more evolved composition.

© 2017 Elsevier B.V. All rights reserved.

## 4.3 Histórico Escolar

**UFRGS**  
UNIVERSIDADE FEDERAL  
DO RIO GRANDE DO SUL

**Informações Acadêmicas do Aluno**

**Histórico Escolar**

Emissão: 26/12/2018 às 19:48

<b>Aluno</b>		<b>BETINA MARIA FRIEDRICH</b>							
		181327							
									
<b>Atividades Desenvolvidas UFRGS</b>									
<b>Atividades de Ensino</b>									
Período Letivo	Atividade de Ensino	Turma	Créditos	Conceito	Nome Professor	Situação	Orgão		
2016/2	Cristaloquímica Aplicada	A	4	A	<ul style="list-style-type: none"> <li>• ARTUR CEZAR BASTOS NETO</li> <li>• JOSE CARLOS FRANTZ</li> </ul>	Aprovado	Programa de Pós-Graduação em Geociências		
2016/2	Depósitos minerais em ambientes hidrotermais	A	5	A	<ul style="list-style-type: none"> <li>• JULIANA CHARAO MARQUES</li> </ul>	Aprovado	Programa de Pós-Graduação em Geociências		
2016/2	Petrologia e metalogenia de rochas máficas-ultramáficas	A	4	A	<ul style="list-style-type: none"> <li>• MARIA DE FATIMA APARECIDA SARAIVA BITENCOURT</li> </ul>	Aprovado	Programa de Pós-Graduação em Geociências		
2016/2	T. E. Geoquímica: MECANISMOS da deformação dútil: do cristal à litosfera	A	2	A	<ul style="list-style-type: none"> <li>• MARIA DE FATIMA APARECIDA SARAIVA BITENCOURT</li> </ul>	Aprovado	Programa de Pós-Graduação em Geociências		
2016/1	Geologia Estrutural de rochas intrusivas - estrut. magnáticas e subsolid	A	5	A	<ul style="list-style-type: none"> <li>• MARIA DE FATIMA APARECIDA SARAIVA BITENCOURT</li> </ul>	Aprovado	Programa de Pós-Graduação em Geociências		
2016/1	Geoquímica das rochas graníticas	A	5	A	<ul style="list-style-type: none"> <li>• ROMMULO VIEIRA CONCEIÇÃO</li> </ul>	Aprovado	Programa de Pós-Graduação em Geociências		
2016/1	Téc. anal. de espec. de massa e geoq. iso. aplic. a evol. manto-crosta	A	5	A	<ul style="list-style-type: none"> <li>• ROMMULO VIEIRA CONCEIÇÃO</li> </ul>	Aprovado	Programa de Pós-Graduação em Geociências		

4.4 Pareceres da Banca Examinadora

Parecer de Rommulo Vieira Conceição

Parecer de César Fonseca Ferreira Filho

Parecer de Nilson Francisquini Botelho

## ATA Nº 846

A comissão abaixo assinada tendo examinado a Dissertação de Mestrado da aluna **Betina Maria Friedrich**, intitulada "**PETROGÊNESE DA CAMADA DE CROMITITO MACIÇO DO COMPLEXO JACURICI, BAHIA, BRASIL: EVIDÊNCIAS DE INCLUSÕES EM CROMITA**", atribuem os seguintes conceitos:

Prof. Dr. Rommulo Vieira Conceição (PPGGeo/UFRGS)  
**CONCEITO: "A" (EXCELENTE)**

Prof. Dr. César Fonseca Ferreira Filho (UnB)  
**CONCEITO: "A" (EXCELENTE)**

Prof. Dr. Nilson Francisquini Botelho (UnB)  
**CONCEITO: "A" (EXCELENTE)**

de de 2019.

Homologação pela Comissão de Pós-Graduação,
Ata nº _____ Data: _____
<b>Conceito Final:</b>
<b>Rubrica:</b>

**ANEXO I**

Título da Dissertação/Tese:

**"PETROGÊNESE DA CAMADA DE CROMITITO MACIÇO DO COMPLEXO JACURICI, BAHIA, BRASIL: EVIDÊNCIAS DE INCLUSÕES EM CROMITA"**

Área de Concentração: Geoquímica

Autora: **Betina Maria Friedrich**

Orientadora: Profª. Drª. Juliana Charão Marques

Examinador: Prof. Dr. Rommulo Vieira Conceição

Data: 02/02/2019

Conceito: A (Excelente)

**PARECER:**

A geóloga Betina Maria Friedrich apresentou uma dissertação de mestrado consistente e organizada, com dados robustos sobre a petrogênese da camada de cromitito maciço do Complexo Jacurici situado no norte da Bahia, Brasil. A base de seu trabalho é a química mineral de alguns níveis cromitíferos e das inclusões minerais. A dissertação é conduzida de forma a apresentar uma ampla revisão sobre a mineralização de cromo, num contexto geral, e no contexto do Complexo Jacurici. Posteriormente, apresenta dados de petrografia muito detalhados, dados da química mineral obtidos em microscópio eletrônico de varredura que, associados aos dados petrográficos, permitem a Geóloga Friedrich propor discussões e conclusões bem fundamentadas acerca da gênese desses cromititos. A dissertação conta com a submissão de um artigo à revista Mineralium Deposita (Qualis CAPES – A2), que está sob revisão, mas que se apresenta de forma clara e bem escrito, sendo possivelmente aceito com pequenas ou moderadas revisões. Embora o texto seja muito claro, sugiro pequenas revisões, observando-se a falta de algumas palavras em algumas frases. Do ponto de vista científico, talvez a Geóloga Betina Friedrich pudesse também abordar a possibilidade da fonte dos magmas que deram origem ao cromitito e sua encaixante ser um manto metassomatizado. A presença de alguns minerais e as assinaturas isotópicas apresentadas na sua revisão bibliográfica poderiam apontar para essa hipótese, o que justificaria o aumento da atividade de sílica para cristalização dos níveis cromitíferos. Esta metassomatização mantélica também colaboraria para a mudança na fugacidade do magma. Embora essa seja uma ideia possível, a abordagem escolhida pela geóloga Betina Friedrich é clara, possível e absolutamente bem conduzida. Dessa forma, considero a Geóloga Betina Maria Friedrich apta a receber o título de Mestre, cuja dissertação merece o conceito "A" (excelente).

Assinatura:

Data: 02/02/2019

Ciente do Orientador:

Ciente do Aluno:

## **ANEXO I**

**Título da Dissertação/Tese:**

**"PETROGÊNESE DA CAMADA DE CROMITITO MACIÇO DO COMPLEXO JACURICI, BAHIA, BRASIL: EVIDÊNCIAS DE INCLUSÕES EM CROMITA"**

**Área de Concentração: Geoquímica**

**Autora: Betina Maria Friedrich**

**Orientadora: Profa. Dra. Juliana Charão Marques**

**Examinador: Prof. Dr. César Fonseca Ferreira Filho**

**Data: 24 de janeiro de 2019**

**Conceito: Excelente**

### **PARECER:**

#### **Avaliação Geral**

A dissertação de mestrado de Betina Maria Friedrich é uma contribuição inédita e relevante para o entendimento da petrogênese do depósito de cromita do Complexo Jacurici, Bahia. O tema escolhido pela autora é atual e tem sido abordado em diversos trabalhos recentes (i.e., últimos 10 anos) que marcaram um avanço significativo na metalogênese dos depósitos estratiformes de cromita. Em particular, o tema abordado tem aderência com os modelos metalogenéticos envolvendo processos físicos e assimilação crustal como fatores importantes na formação dos cromititos. A autora utilizou métodos apropriados para avaliar a importância da assimilação de mármores e rochas calcisilicáticas pelo magma parental na gênese da camada principal de cromitito do depósito. Os resultados analíticos são de excelente qualidade, foram apresentados e tratados de forma apropriada e corroboram as sugestões e interpretações discutidas na dissertação. Destaco a integração entre as informações geológicas e petrográficas com os dados de química mineral. As discussões e conclusões estão bem inseridas no conhecimento científico atual do tema, permitindo que esta pesquisa seja uma referência adicional para trabalhos futuros abordando a metalogênese de depósitos estratiformes de cromita.

#### **Capítulos 1 e 2**

Estes capítulos apresentam de forma sucinta e adequada a pesquisa desenvolvida no programa de mestrado. A apresentação do contexto geológico regional e a revisão dos modelos de formação de cromita em complexos acamadados representa o estado da arte no tema. A revisão, com destaque para os estudos focados em inclusões em cromita, está embasada em referências atualizadas e representativas do conhecimento atual.

#### **Capítulo 3**

Este capítulo, apresentado no formato da publicação submetida pela autora ao periódico Mineralium Deposita, sintetiza a contribuição científica da dissertação de mestrado. A redação, o tema abordado, a estrutura, as figuras, as tabelas, as discussões e as conclusões, estão apropriadas para um trabalho científico submetido à um periódico de circulação internacional focado em geologia econômica. A minha avaliação é que o trabalho representa uma contribuição relevante e que será atrativa para o corpo editorial do periódico que foi submetido.

#### Capítulo 4

Neste capítulo estão incluídas as publicações com participação da autora desenvolvidas durante o período do Mestrado. As publicações, que incluem um *paper* publicado (*Ore Geology Reviews*, 2017), quatro resumos ou resumos expandidos apresentados em eventos nacionais e internacionais, estão todas relacionadas ao tema principal da dissertação de mestrado (i.e., cromititos), indicando o comprometimento da autora com o tema da pesquisa.

Assinatura:



Data: 24/01/2019

Ciente da Orientadora:

Ciente da Aluna:

ANEXO I	
Título da Dissertação/Tese:	
<b>“PETROGÊNESE DA CAMADA DE CROMITITO MACIÇO DO COMPLEXO JACURICI, BAHIA, BRASIL: EVIDÊNCIAS DE INCLUSÕES EM CROMITA”</b>	
Área de Concentração: Geoquímica	
Autora: Betina Maria Friedrich	
Orientadora: Profa. Dra. Juliana Charão Marques	
Examinador: Prof. Dr. Nilson Francisquini Botelho	
Data: 30/01/2019	
Conceito: Excelente	
<p style="text-align: center;"><b>PARECER:</b></p> <p>Betina Maria Friedrich apresenta uma Dissertação de Mestrado elaborada por meio de métodos analíticos adequados ao tema de pesquisa. O trabalho tem como base uma petrografia bem detalhada, com identificação de minerais ao microscópio petrográfico e microscópio eletrônico, e dados robustos de química mineral, que associados ao estudo petrográfico, constituíram suporte para as interpretações sobre a gênese da camada de cromitito maciço do Complexo Jacurici. As discussões e conclusões são bem fundamentadas e coerentes com os resultados obtidos. Os resultados da Dissertação foram apresentados na forma de artigo científico submetido a periódico internacional A2 do Qualis CAPES. Esse artigo tem redação clara e objetiva e, na minha opinião, necessita apenas de revisões menores e muito pontuais para ser publicado. As sugestões de revisão encontram-se em arquivo encaminhado à interessada e estão centradas em pequenas questões de forma no item sobre métodos analíticos, nas figuras e nas tabelas. Como consideração geral e final, minha avaliação é de que o trabalho de Betina Friedrich atende todos os requisitos de uma Dissertação de Mestrado e sou de parecer pela sua aprovação com conceito excelente.</p>	
<p><i>Nilson Francisquini Botelho</i></p> <p>Assinatura:</p>	
Data: 30/01/2019	
Ciente da Orientadora:	
Ciente da Aluna:	